EXPERIMENTAL EVALUATION OF NOVEL PROPPANTS FOR USE IN HYDRAULIC FRACTURING OF UNCONVENTIONAL RESERVOIRS

A Thesis

by

KEVIN THOMAS WYLIE

Submitted to the Office of Graduate and Professional Studies of
Texas A&M University
in partial fulfillment of the requirements for the degree of

MASTER OF SCIENCE

Chair of Committee,	A. Daniel Hill
Co-Chair of Committee,	Ding Zhu
Committee Member,	Yuefeng Sun
Head of Department,	Duane A. McVay

May 2018

Major Subject: Petroleum Engineering

ABSTRACT

To effectively produce from resource shale, a stimulation method is required. Typically, hydraulic fracturing is utilized for stimulation. Hydraulic fracturing methods range in size, cost, and effectiveness. Once a hydraulic fracture network has been generated, the fractures must be propped open using proppant to allow flow through the fractures. Sand is currently the most commonly used proppant in fracture treatments. Large quantities of sand are required to effectively prop the generated and natural fractures. Sand can be a costly expense in the completion stage of a well. With low oil and gas prices, cutting costs, but not jeopardizing the success of the well is critical. The goal of this study is to find a cheap and abundant material which can act as a sand substitute to provide equal or superior fracture conductivity to that of sand proppant, and serve as an adequate proppant material.

Glass, taconite tailings, coal, and various proppant mixtures' geometry, conductivity, and strength were all evaluated and compared to conventional sand proppants currently being used in industry to evaluate the novel proppant's potential to serve as a sand substitute in hydraulic fracturing treatments. The proppant's geometry was evaluated qualitatively under a microscope. The most favorable proppant geometry was seen in sand proppant followed by taconite, and the least favorable particle geometry was observed in the glass proppant.

Fracture conductivity is an effective means of measuring a fracture treatment's effectiveness. For that reason, the API RP 61 procedure was followed using the modified API cell available in the Texas A&M University Fracture Conductivity Laboratory to evaluate the conductivity of the various proppant packs. API RP 61 is a well-established procedure set forth by the American Petroleum Institute for measuring conductivity of proppant packs. For a given

proppant size, sand had the largest conductivity, followed by taconite, then glass, and finally coal which did not result in any measurable conductivity.

Proppant strength was measured by evaluating proppant crushing. Each conductivity test was conducted at the same six closure stresses starting at 1,000 psi and ending at a maximum closure stress of 6,000 psi. Before the proppant conductivity was tested, a sieve test was conducted to determine the particle distribution of each proppant type and size. Upon conclusion of each conductivity test, after the proppant pack had been exposed to 6,000 psi closure stress, the proppant was sieve tested once again. The particle distributions of the crushed and uncrushed samples were compared side by side to determine how severely the proppant had crushed. For a given proppant size, the glass proppant had the most severe crushing followed by the taconite and sand proppants.

The proppant geometry and strength evaluations were used to support the large variation in conductivity results observed in this study. A dimensionless conductivity evaluation was conducted to determine the potential for each proppant to serve as a sand substitute in hydraulic fracture treatments based on the proppant pack conductivity tested in this study. The dimensionless conductivity values calculated for each proppant based on ideal lab testing conditions for short term conductivity evaluation using a dry gas test fluid revealed that glass, taconite, and the three proppant mixtures tested all have the potential to replace sand in fracture treatments.

DEDICATION

I would like to dedicate my work to my parents, Lynn and Brian, my sister Erin, and my brother Steven who have never stopped encouraging me and pushing me to succeed. I love you, and cannot thank you all enough for the support you have given me since day one.

ACKNOWLEDGEMENTS

I would like to thank my advisor and committee co-chair, Dr. Zhu, for accepting me into her research group and giving me the opportunity to work on such an interesting project. Dr. Zhu has truly been an advisor in every sense of the word, always pushing me to produce quality and timely results and think critically about my research. I would also like to thank Dr. Hill for his guidance, suggestions, and recommendations every week throughout this project in our weekly meetings. Finally I would like to thank Dr. Sun for serving as my out of department committee member.

I also want to thank the professors I had the privilege to learn from at Texas A&M. I have learned more than I could have imagined during my time here at A&M. They made the difficult transition from mechanical engineering to petroleum engineering a very education experience.

I would also like to thank my project sponsor, Marathon Oil, for not only giving me the opportunity to work on this project, but providing the necessary funding and resources to make it possible. I hope that the results of this thesis will be of benefit to Marathon and eventually the entire industry.

I also want to thank my research groupmates Ryan Winner and James Fernandez. Ryan helped me trouble shoot various lab issues and provided test data for a scaled down test. James helped me run the final portion of my conductivity tests. It was a pleasure working with you both.

CONTRIBUTORS AND FUNDING SOURCES

Contributors

This study was supervised by a thesis committee consisting of Dr. A. Daniel Hill and Dr. Ding Zhu of the Harold Vance Department of Petroleum Engineering and Dr. Yuefeng Sun of the Department of Geology and Geophysics.

The laboratory experiments were performed with the assistance of James Fernandez of the Harold Vance Department of Petroleum Engineering.

All other work conducted for the thesis was completed by the student independently.

Funding Sources

This work was supported by an industry partner, Marathon Oil. The contents of the study are solely the responsibility of the author and do not represent the official views of the Marathon Oil.

NOMENCLATURE

q	flow rate
A	cross sectional area perpendicular to flow path
u	flow rate per area
k	permeability
dP/dL	pressure gradient across the proppant pack
P	pressure
L	length pressure drop occurs over
ρ	density
w	proppant pack thickness
h	flow surface width
M	molecular weight of test fluid
z	compressibility factor of test fluid
R	ideal gas constant
T	temperature
C_f	Fracture Conductivity

TABLE OF CONTENTS

Page

LIST OF FIGURES

Page

LIST OF TABLES

Page

1. INTRODUCTION

1.1 Problem Statement

As oil and gas production has evolved throughout the years, efficient production has become more difficult and costly. Conventional reservoirs dominated the industry for decades until high quality reservoirs became more scarce. These reservoirs were easy to produce from compared to modern day unconventional reservoirs. Fortunately, behind every conventional resource is the source rock where the hydrocarbons originated. These source rocks, or shales, are abundant, but pose many difficulties in effectively producing hydrocarbons. Resource shales lack the permeability and porosity that make conventional reservoirs so appealing. Due to the lower level of reservoir quality, shales require extensive stimulation to produce effectively.

Conventional resources have a reservoir that is ready for production, with high reservoir quality that allows flow from the formation into the wellbore during production. Unconventional resources require a reservoir to be created, which allows oil and gas to flow to the wellbore. Some type of stimulation to connect the natural fracture network and small pores in resource shales is necessary for economic production in resource shales. One of the most common means of reservoir generation is hydraulic fracturing. Hydraulic fracturing consists of pumping a fluid-proppant slurry into the shale at high enough pressures to generate fractures. These fractures will act as a man-made reservoir to be utilized for production. Generating fractures alone is not an effective means of reservoir generation for the fractures will close under the formation pressure. To ensure that these fractures can serve as an effective means of fluid transportation, proppant must be used to hold the fracture open once the fracture treatment has concluded. Ideally, these propped fractures will provide highly conductive pathways for fluid production.

1.2 Literature Review

Proppant pack conductivity has been studied thoroughly since Cooke's work in the early 1970's. One method of measuring a fracture treatment's performance is by the conductivity of the fractures. Cooke, a pioneer in conductivity research, defined fracture conductivity as the fracture width multiplied by the apparent permeability of the proppant pack (Cooke, 1973). Conductivity quantifies the fracture's ability to allow fluids to flow through the fracture. In all successful fracture treatments, proppant is pumped along with fracture fluid to keep the fractures propped open, allowing the fractures to establish and maintain conductivity. Many fracture treatments have been used and studied throughout the history of resource shale development. The proppant size, shape, distribution, physical properties, and quantity all play a role in the effectiveness of a treatment.

The first commercial fracture treatment was performed by Haliburton in 1949 (Montgomery and Smith, 2010). This treatment was very small compared to modern day treatments, consisting of 150 pounds of sand from a nearby river. Soon after hydraulic fracturing was introduced to the industry it was observed that the treatment enhanced well performance. In the early 1970's, C.E. Cooke published several papers on his work regarding fracture conductivity through proppant packs. Cooke's work helped identify the mechanics behind hydraulic fracture treatments, and understanding of how the treatments aided production. Cooke observed that an increase in fracture conductivity by a factor of ten can lead to a fracture treatment that is up to six times as effective of a treatment (Cooke, 1973). This observation drives home the importance of fracture conductivity, and is the motivation in understanding fracture conductivity in resource shales, and how best to maximize conductivity through a propped fracture.

Early in the development of hydraulic fracturing, sand was the predominant type of proppant used for stimulation, and remains the most widely used proppant today. Cooke observed that in deep formations with high closure stress the silica sand was not strong enough to effectively prop the generated fractures. Under high closure stress, weak sand often crushes, producing fine particles and fragments that can drastically reduce the conductivity of a propped fracture (Cooke, 1977). The negative effect that proppant crushing has on fracture conductivity is more pronounced when large diameter proppant is used, and proppant embedment becomes a significant means of conductivity reduction at low concentrations (Cooke, 1977).

In the early 2000's Lehman et al. described the benefits of proppants coated in a sticky material, particularly with regards to fine particle reduction of conductivity. As observed by Cooke, fines, either from crushed proppant, or smaller proppant used earlier in treatment pumping, can severely reduce the conductivity of a propped fracture. Lehman et al. observed that the use of sticky surface modification agents on proppant particles can extend conductivity life by reducing the negative impact fines migration has on a proppant pack's conductivity (Lehman et al., 2003). If fine particles are a concern in a given treatment, sticky surface modification agents can be used to maintain a high level of conductivity. There will still be fines production, but the fine particles will not migrate due to the sticky nature of the proppant surfaces, and thus cannot accumulate in conductive pathways.

The idea of connecting to and utilizing the natural fracture network in shales is a new idea which requires a different treatment style. Large proppants result in the largest fracture conductivity, but can easily crush and reduce conductivity over time as the crushed particles block flow pathways. Large particles also pose the issue of proppant transport. Large proppants cannot be carried to the fracture tip or throughout the natural fracture network. Small proppants

such as 100 mesh or 40/70 mesh are thought to be capable of propping the natural fracture network (Zhu and Hill, 2013), thus maximizing the conductive fracture contact with the reservoir. More recent work suggests that less viscous fluid is also advantageous when attempting to contact the natural fracture network.

In 1977 Novotny thoroughly studied proppant transport as part of an Exxon project. Novotny found that the amount of production increase or stimulation from a fracture treatment depends on the conductivity of the proppant in the fracture (Novotny, 1977). The final distribution of proppant in the fracture can have a significant impact on the conductivity of the proppant pack. To ensure a good proppant distribution, the proppant should be evenly spread throughout the fracture, and not settled at the bottom of the fracture. When the fracture treatment is over and the injected fluid is lost to the formation, the fracture begins to close, which can take over two hours (Novotny, 1977). During this stage, the proppant will settle toward the bottom of the fracture. Unless the settling time of the proppant can be increased, there will likely be a decrease in production caused by the reduced fracture permeability in a poorly distributed propped fracture.

There are many factors that contribute to an acceptable hydraulic fracture treatment. Various types of proppant and fracture techniques have been studied, all with the goal of maximizing production, by increasing fracture conductivity. Many fracture treatments have been used, and no single treatment has had universal success in all formations or applications, but there are solutions to common hydraulic fracture issues.

The purpose of the proppant is to provide a conductive pathway from the reservoir to the wellbore by keeping the fracture from closing once the high pressure applied to create the fracture is relieved (Economides et al. 2013). Factors that contribute to a highly conductive

proppant pack are the particle roundness, particle size, and particle size range or sorting. The more round proppant is, the larger the voids between particles will be. If the particles are more angular, and less round, then the jagged edges can fill the void between particles, reducing the available space for flow. As well, the larger the proppant particles are, the larger the voids between particles will be. If the particles are a uniform size, then there will not be smaller particles to fill the void space, which would lead to a reduction in possible flow paths.

One critical attribute of proppant is its ability to withstand crushing. When proppant particles crush under fracture closure stress they produce smaller particles, which will fill the voids between uncrushed proppant particles, and ultimately reduce the conductivity through the proppant pack.

Sand is the most commonly used proppant in shale formations. In general, sand has a high resistance to crushing relative to other natural sand substitutes. Millions of years of weathering have given sand particles relatively spherical and smooth shapes, which is advantageous to enhancing proppant pack conductivity. However, there are several more expensive man-made proppants that can far out perform the crush strength of sand, and exhibit even more desirable roundness and sphericity.

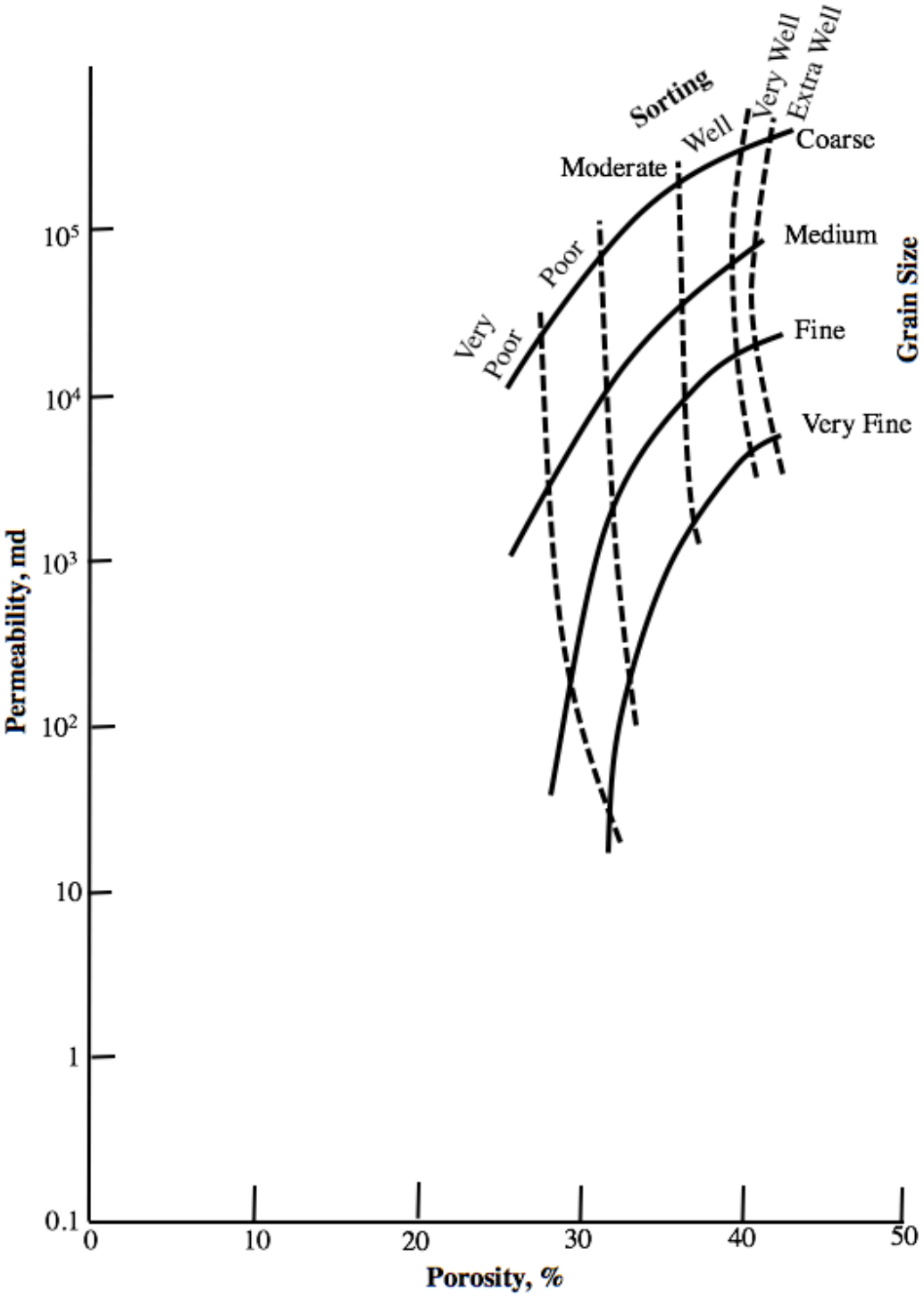

Figure 1.1. Porosity, permeability, sorting, and grain size (adapted from Selley, 1998).

Recall that fracture conductivity is defined as the product of permeability and fracture width, so as permeability increases, conductivity increases proportionally. Figure 1.1 shows the relationship between porosity, permeability, sorting, and grain size. In general, as the porosity increases, the permeability also increases, but this is not always the case. Grain size has a major impact on particle pack permeability. Permeability can vary by three orders of magnitude depending on the particle size. Figure 1.1 also shows that sorting, or range of particle size, has a large effect on particle pack permeability. Depending on the grain size of the proppant, the level of sorting can cause a variation in permeability of about two orders of magnitude in some cases. Clearly the type of proppant, particle size, and particle size range or sorting have a major impact on permeability, and ultimately fracture conductivity of a given treatment.

High-strength sintered bauxite proppant has been used since the late 70's and has been shown to improve fracture conductivity at high closure stresses (Atteberry et al., 1979). Sintered bauxite proppant was not tested in this study, for the aim was to find a substitute that is more cost effective and abundant than sand. Sintered bauxite performs well at high closure stresses because of its superior crush strength. At high stresses when most conventional proppant would crush and generate fines leading to conductivity decreases, the sintered bauxite proppant is resistant to crushing and maintains a high level of conductivity. Also, sintered bauxite proppant can be made to be highly spherical, even more so than sand.

Larson discussed the importance of sphericity and roundness in a proppant pack with regards to conductivity. He defined roundness as the smoothness of a grain's surface or the lack of rough edges, and sphericity as the degree a sand grain resembles a sphere (Larsen and Smith, 1985). Both values can be quantified and compared between proppants. As previously discussed, a highly conductive proppant pack should have large voids between particles which will act as

flow pathways for fluid through the fracture. Sintered bauxite is such a superior proppant to conventional sands because of its high sphericity, roundness, and crush strength. These properties not only generate a highly conductive pack, but also maintain that high level of conductivity by reducing fine migration and pathway blockage. However, sintered bauxite proppant is often prohibitively costly, and is not commonly used in US onshore unconventional plays.

Crush strength can also be improved by coating normal sand proppant with a higher strength material (Cutler et al., 1985). This can solve the problem or fines migration allowing conductivity to be maintained. Some coated sands have crush strengths higher than 20,000 psi which is much higher closure stress than most proppant would encounter in US onshore unconventional plays. Any alteration to the sand increases cost of the proppant, so coating sand proppant can lead to large increases in proppant cost for a fracture treatment, but is a more cost-effective approach than pumping sintered bauxite proppant.

Ideally a fracture treatment would consist of large, spherical, uniformly sized proppant particles that have a high crush strength that can reach deep into the fracture network.

1.3 Objectives of Study

The objective of this study is to evaluate potential sand substitutes for proppant in fracture treatments. The conductivity for several materials and material mixtures have been tested in the lab to evaluate the effectiveness of each proppant pack's ability to allow flow. There may exist a cheaper and more abundant particle that can replace sand in future fracture treatments. However, this study has been limited to three novel proppant materials, coal, glass, and taconite tailings, and does not consider the extent of potential sand substitutes. This study is not focused on the economics of completion design, but rather the evaluation of the potential for novel proppants to provide conductive pathways in a fracture treatment. This study could benefit the industry if a cheaper, more abundant proppant sand substitute is deemed an adequate material for creating conductive pathways.

2. EXPERIMENTAL DESIGN AND METHODOLOGY

This chapter discusses the laboratory methodology used to assess proppant pack conductivity.

2.1 Testing Proppant Pack Conductivity

This section outlines the conductivity test procedure.

2.1.1 Experiment Setup

The main components of the experimental setup are listed below:

1. Test Fluid Source (Nitrogen gas)
2. Gas Flow Meter
3. GCTS hydraulic press
4. Modified API Test Cell
5. Pressure Sensors
6. Back Pressure Regulator Valve

Figure 2.1 shows a schematic of the test setup used to measure conductivity of various proppant packs. Figure 2.2 shows the fully assembled modified API conductivity cell.

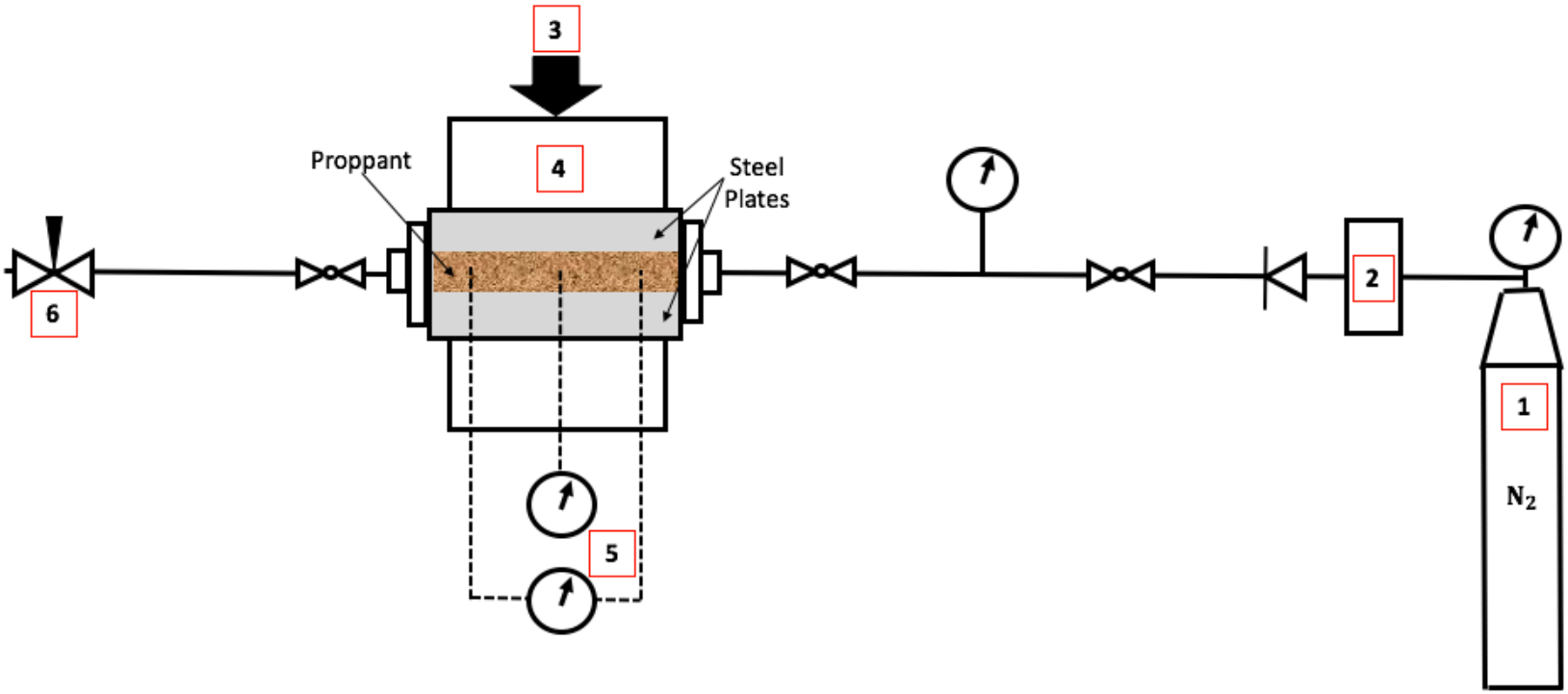

Figure 2.1. Test setup schematic.

Figure 2.2. Fully assembled test setup.

2.1.2 Experiment Procedure

Once the sample has been properly loaded into the modified API cell, the test procedure can begin. The test procedure is listed below.

1. Check that back pressure regulator is open to allow any air to escape while increasing load to desired closure stress.
2. Increase GCTS press load to desired closure stress.
3. Zero pressure sensors.
4. Close back pressure regulator.

5. Slowly open gas valve, ensuring that the gas flow rate never exceeds 0.2 L/min.
6. Continue opening gas valve until cell pressure reaches 30 psi.
7. Check for leaks in the system.
    a. Cell pressure should maintain 30 psi.
    b. There should be no pressure drop across the sample.
    c. Gas flow meter should read 0 L/min.
    d. If one or more of these conditions is not met, spray soap solution on fitting and cell openings to find leak.
    e. If leak is detected, tighten necessary fittings until conditions a, b, and c are satisfied.
8. Slowly open back pressure regulator, make sure the gas flow rate does not increase too quickly. Introducing a large increase in flow rate may rearrange the proppant and create a conductive channel in or around the proppant pack.
    a. Ensure that the cell pressure does not reach less than 26 psi, and the differential pressure does not exceed 1.2 psi.
9. Once the desired pressure drop has been reached, allow the system to reach steady state with a constant gas flow rate, cell pressure, and differential pressure.
10. Record gas flow rate, cell pressure, and differential pressure.
11. Slowly close the back-pressure regulator until the pressure drop reaches three-quarters of the original pressure drop.
12. Once the desired pressure drop has been reached, allow the system to reach steady state with a constant gas flow rate, cell pressure, and differential pressure.
13. Record gas flow rate, cell pressure, and differential pressure.

14. Slowly close the back-pressure regulator until the pressure drop reaches one-half of the original pressure drop.
15. Once the desired pressure drop has been reached, allow the system to reach steady state with a constant gas flow rate, cell pressure, and differential pressure.
16. Record gas flow rate, cell pressure, and differential pressure.
17. Slowly close the back-pressure regulator until the pressure drop reaches one-quarter of the original pressure drop.
18. Once the desired pressure drop has been reached, allow the system to reach steady state with a constant gas flow rate, cell pressure, and differential pressure.
19. Record gas flow rate, cell pressure, and differential pressure.
20. Slowly close the gas valve.
21. Slowly open the back-pressure regulator until it is fully open and the gas flow rate, cell pressure, and differential pressure all reach a value of zero.
22. Increase GCTS press to next desired closure stress.
23. Repeat steps 4-22 for each desired closure stress.
24. After final closure stress, unload the GCTS press to 500 psi.
25. Disconnect all fittings.
26. Return GCTS press to relative zero displacement.
27. Remove test cell from hydraulic press.
28. Disassemble test setup, remove sample, and collect proppant for post-conductivity sieve test to evaluate proppant crushing.

2.2 Sample Preparation

This section discusses the procedure to prepare for a conductivity test.

2.2.1 Steel Plate Design

Steel plates were used to confine the proppant in the modified API test cell. The plates were designed specifically to fit the modified API cell using SolidWorks, and were manufactured by CNC milling at the Texas A&M University Mechanical Engineering Machine Shop. The Steel plates were designed to be 1 inch thick, and stacked three plates on top of each other for ease of manufacturing. In total, six steel plates were manufactured to fit the cell. Figure 2.3 shows the engineering drawing, and dimensions used for the steel plates.

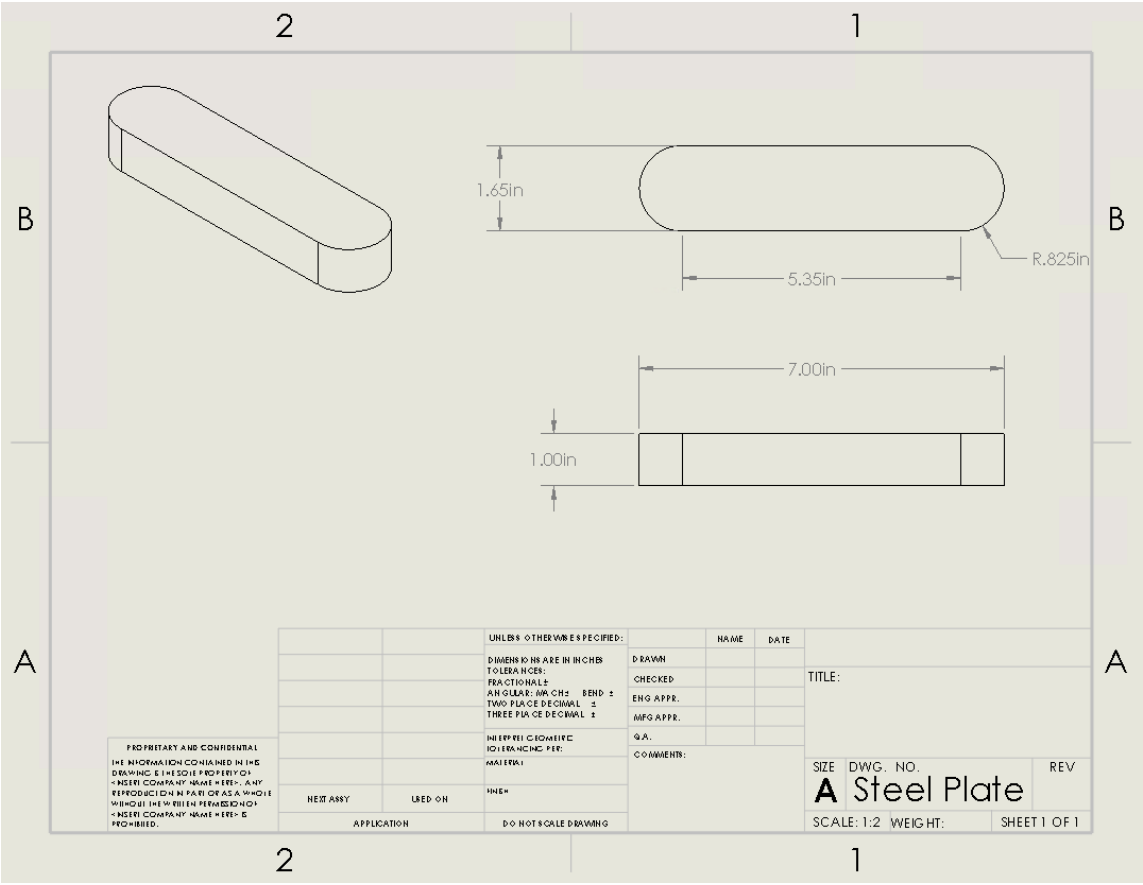

Figure 2.3. Steel plate engineering drawing and dimensions.

2.2.2 Steel Plate Assembly

Six steel plates make up the sample assembly. Three plates are stacked on top of each other to confine the proppant from below, and the remaining three plates are stacked on top of each other to confine the proppant from above. The plate assemblies act as pistons which apply stress to the proppant pack to simulate various closure stresses.

For both the top and bottom portion of the sample, the plates were stacked ensuring a smooth alignment, and adhered together. Each set of plates was then covered in blue painter's tape to allow the epoxy to adhere to the sample as seen in Figure 2.4.

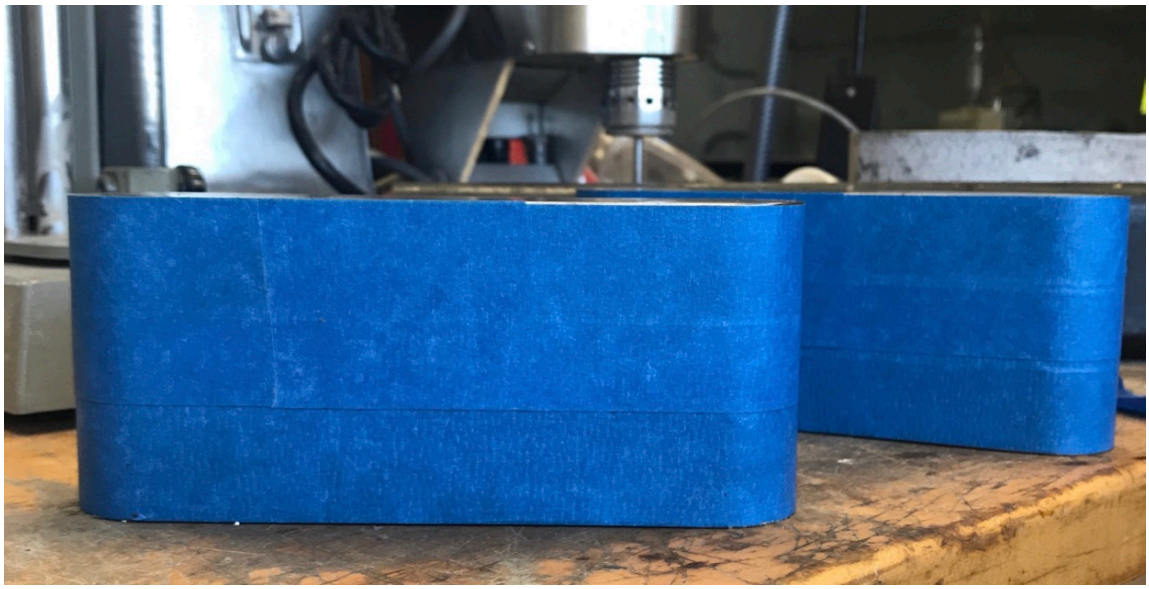

Figure 2.4. Steel plate assemblies covered in blue painter's tape.

Steel wool was used to roughen the surface of the tape to better allow binding with the epoxy. Momentive SS4155 Primer for use with RTV silicone rubber adhesive was applied to each set of plates three times, allowing 15 minutes to dry between each application. The sample assemblies were loaded into separate three-inch-tall molds, designed to be slightly larger than the modified API cell to ensure no leakage between the internal walls of the test cell and the sample. The assemblies were arranged in the molds so that it is equidistant from all edges of the mold so

that an even rubber epoxy layer is formed. Momentive RTV627 gray two-part potting and an encapsulating compound was mixed in equal weight ratios, and then poured into the void between the mold and sample. The epoxy mixture should only be poured from one point of entry to avoid trapping air bubbles. The molds were then placed in an oven at 120°C for four hours to cure. The steel plate assembly is most effectively removed by removing all fittings and using a manual hydraulic press to release the sample from them mold. Figure 2.5 shows the bottom sample assembly, covered in rubber epoxy and ready for testing.

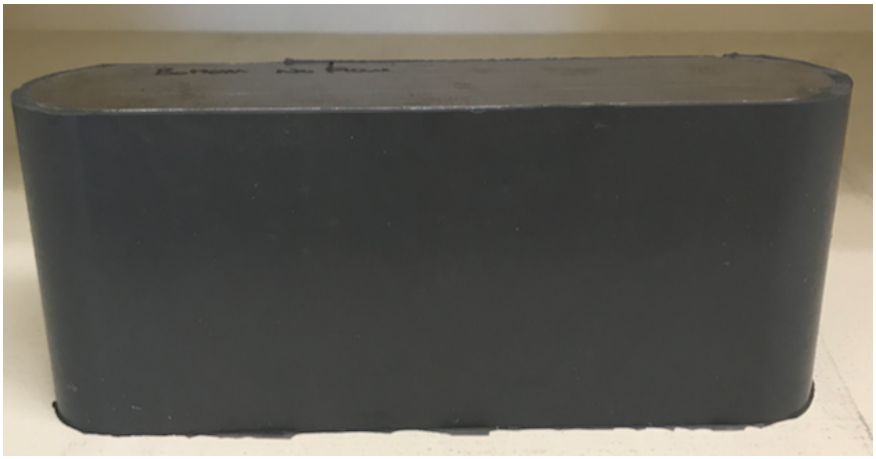

Figure 2.5. Steel plate sample assembly covered in rubber epoxy and ready for testing.

2.2.3 Sieve Test

Before any proppant conductivity was tested, the proppant was sieve tested to confirm the proppant size range, or to create a desired proppant size range from a randomly distributed sample. To determine the particle distribution of a proppant 30, 40, 50, 70, 80, and 100 mesh sieves were typically used. However, any desired sieve assortment can be used.

Before testing the proppant, the mass of each empty sieve was measured. After measuring the sieve masses, they were stacked with the largest mesh sieve (30 mesh) on top, and

the smallest mesh sieve (100 mesh) on bottom. A proppant sample of known mass was placed in the top sieve. The sieve assembly was secured in the sieve shaker and run for ten minutes.

The mass of each sieve and contents were measured once the sieve test was completed. The particle distribution was expressed in weight percent as shown in Figure 2.6. The particle distributions for each proppant can be found in Appendix A.

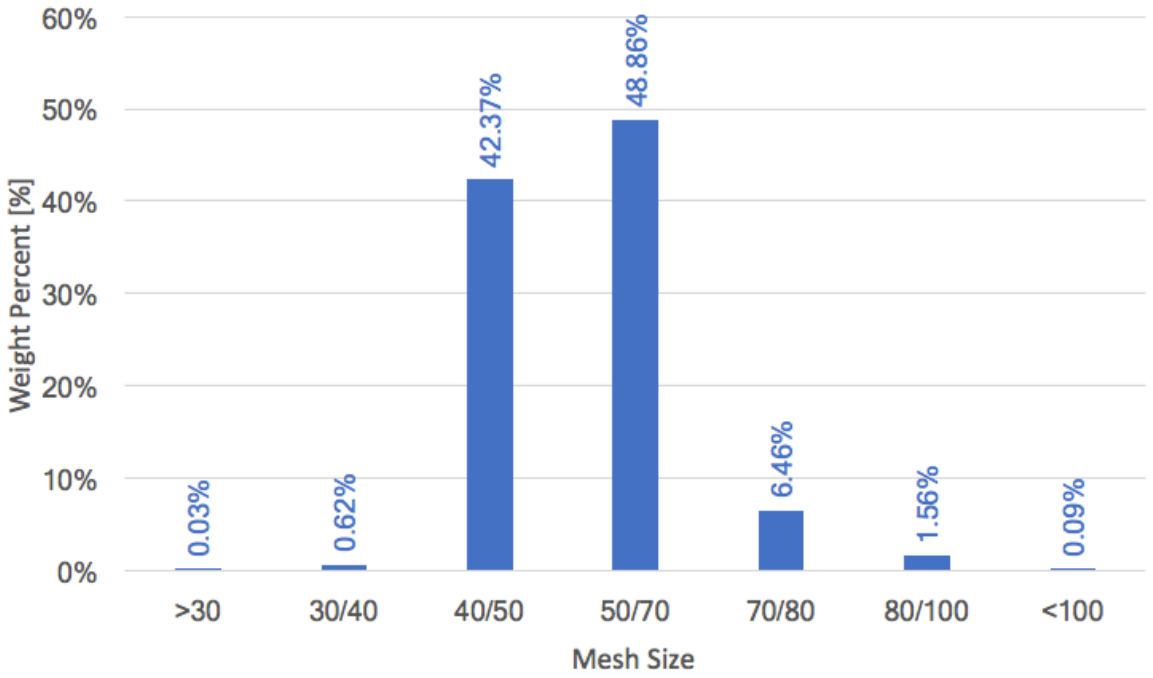

Figure 2.6. Example of 40/70 particle distribution obtained from sieve test

Following a conductivity test, the proppant was analyzed using a sieve test and compared to the particle distribution to the untested sample. This comparison shows how much proppant crushing occurred during the conductivity test. However, the comparison will not reveal at what closure stress the proppant crushing occurred. Nor will it show which particles in a given mesh range are the result of larger particle crushing, and which are smaller particles that have remained uncrushed. Figure 2.7 shows an example of the aforementioned comparison.

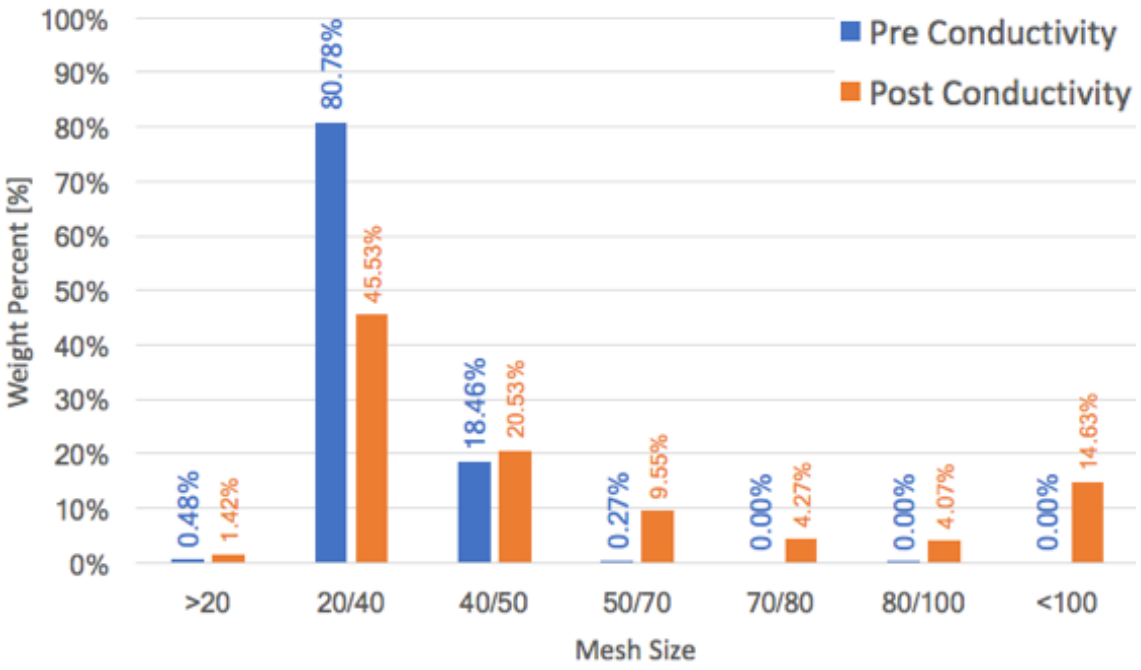

Figure 2.7. Comparison of particle distribution for a sample of 20/40 glass proppant.

2.2.4 Proppant Placement

Each test was run on a volume equivalent basis (45 cm^3) as recommended by API RP 61 when comparing different proppants. This volume corresponds to a proppant loading between 1.65 – 2.16 lb/ft^2 (PPF). Before the proppant was placed in the test cell it was measured to the correct volume. The bulk density of each proppant was measured using a balance and graduated cylinder. Once the bulk density was established, a mass corresponding to 45 cm^3 was calculated. It was found to be more consistent to measure the mas equivalent to 45 cm^3 for each test rather than measure the volume.

The bottom steel plate assembly was loaded through the bottom opening of the modified API test cell. The lower piston was then loaded through the bottom of the cell until the top of the steel plate assembly was visible through the inlet, outlet, and pressure ports. 170 mesh screens were placed in the inlet, outlet, and pressure ports, then all fittings are attached to confine the

proppant, prevent it from spilling over the edge of the steel plate assembly, and to prevent sensor interference.

45 cm^3 of proppant, which will result in a ¼ inch thick layer of proppant, is measured. The proppant was then poured down a funnel onto the surface of the steel plates. Proppant was evenly distributed across the entire plate, smoothed with a straight edge, and measured at multiple points to ensure an even proppant distribution. Figure 2.8 shows an aerial view of the evenly distributed proppant pack.

Figure 2.8. Aerial view of the evenly distributed proppant pack of 40/70 sand proppant.

After the proppant had been placed evenly across the bottom steel plate assembly, the top steel plate sample assembly was inserted through the top opening of the modified API test cell followed by the top piston. Figure 2.9 shows a schematic of what the fully assembled test sample should look like. The full assembly includes the top and bottom steel plate assemblies as well as the evenly distributed proppant layer.

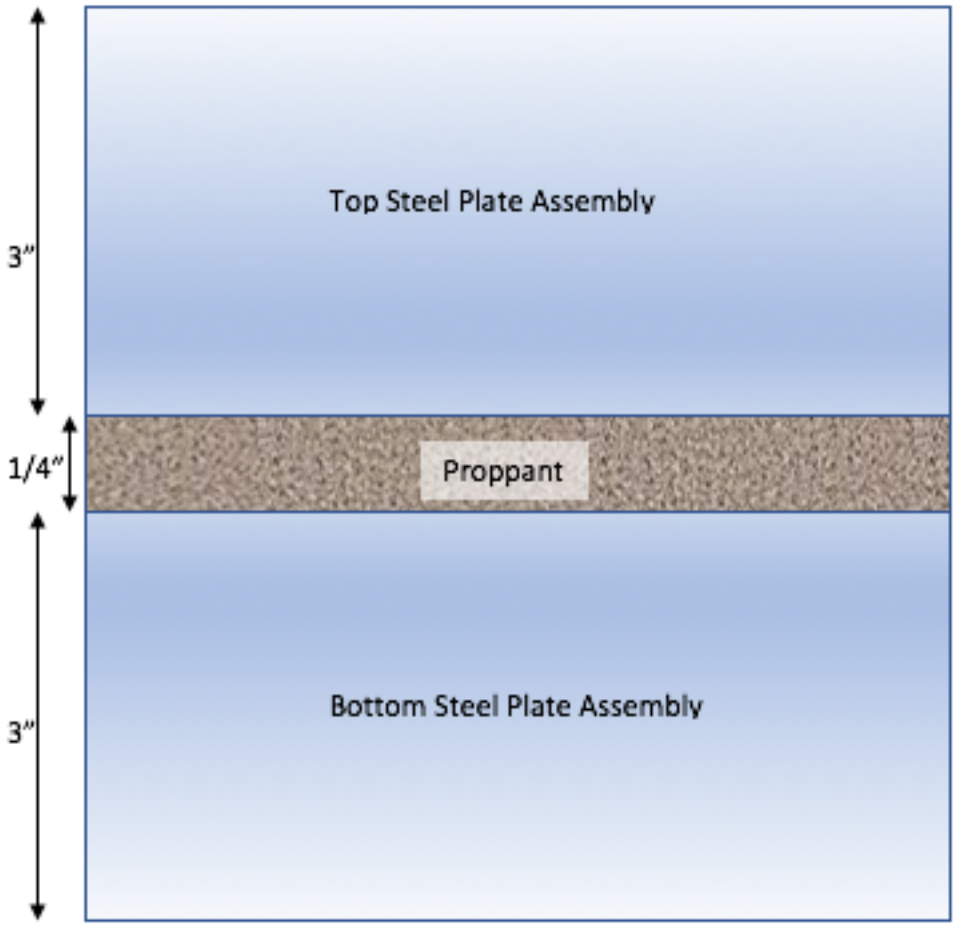

Figure 2.9. Full sample assembly.

2.3 Data Collection

At each closure stress tested, four separate gas flow rates and corresponding cell pressure and differential pressure combinations were recorded. These values were used to evaluate the conductivity of the proppant pack at a given closure stress. The derivation in section 2.3.1 shows the relationship between known values and the unknown values measured in the laboratory (gas flow rate, cell pressure, and differential pressure).

Measurements for novel proppant were conducted under room temperature, between two metal plates, using dry nitrogen gas, in short term, and high proppant loading conditions. Testing under these conditions allows for quick, comparable, and easily reproducible results.

2.3.1 Relation Between Known and Unknown Variables (Derivation)

The theory behind laboratory evaluation of conductivity begins with Darcy's law. By making some general assumptions and rearranging Darcy's law, unknown values were measured experimentally and conductivity for a sample was calculated.

Darcy's Law:

$$\frac{q}{A} = u = -\frac{k}{\mu}\frac{dP}{dL} \tag{2.1}$$

Rearranging and separation of variables leads to the form:

$$dP = -\frac{\mu u}{k}dL \tag{2.2}$$

Definition of cross sectional area:

$$A = wh \tag{2.3}$$

Both sides of equation 2.2 are multiplied by density.

$$\rho dP = -\frac{\mu u}{k}\rho dL \tag{2.4}$$

Using the ideal gas law, density can be expressed in known variables.

$$Pv = znRT \tag{2.5}$$

$$PM = zRT\frac{m}{v} = zRT\rho \tag{2.6}$$

$$\rho = \frac{PM}{zRT} \tag{2.7}$$

Equation 2.7 is substituted into the left hand side of Darcy's Law equation (2.4):

$$\frac{PM}{zRT}dP = -\frac{\mu u}{k}\rho dL \tag{2.8}$$

Integrate and multiply each side by -1:

$$\frac{M}{zRT}\int_{P_1}^{P_2} PdP = -\frac{\mu u}{k}\rho\int_0^L dL \tag{2.9}$$

$$\frac{M}{zRT}\frac{[P_1{}^2 - P_2{}^2]}{2} = \frac{\mu u}{k}\rho(L-0) \tag{2.10}$$

By definition of flow rate per area (2.1) and area (2.3):

$$\frac{M}{zRT}\frac{[P_1{}^2 - P_2{}^2]}{2} = \frac{\mu}{kwh}q\rho L \tag{2.11}$$

Assumptions about test cell and pressure measurement locations:

$$\Delta P = P_1 - P_2 \tag{2.12}$$

P_{cell} is located half way between P1 and P2:

$$P_1 - P_{cell} = P_{cell} - P_2 = \frac{1}{2}\Delta P \tag{2.13}$$

Using the above assumptions (2.12 and 2.13):

$$P_1 = \frac{1}{2}\Delta P + P_{cell} \tag{2.14}$$

$$P_2 = P_{cell} - \frac{1}{2}\Delta P \tag{2.15}$$

After substitution of equation 2.14 and 2.15 into equation 2.11, the altered Darcy's Law equation becomes:

$$\frac{M}{zRT}\frac{\left[\left(\frac{1}{2}\Delta P + P_{cell}\right)^2 - \left(P_{cell} - \frac{1}{2}\Delta P\right)^2\right]}{2} = \frac{\mu}{kwh}q\rho L \tag{2.16}$$

Equation 2.16 simplifies to:

$$\frac{M}{zRT}\frac{2P_{cell}\Delta P}{2} = \frac{\mu}{kwh}q\rho L \tag{2.17}$$

Equation 2.17 can be rearranged in a useful linear format.

$$\frac{P_{cell}\Delta PM}{LzRT} = \frac{\mu q \rho}{h}\frac{1}{kw} \tag{2.18}$$

Definition of fracture conductivity:

$$C_f = kw \tag{2.19}$$

The final form of the equation relating known and unknown variables used to calculate proppant pack conductivity is formed by the final step of substituting equation 2.19 into equation 2.18:

$$\frac{P_{cell}\Delta PM}{LzRT} = \frac{\mu q \rho}{h}\frac{1}{C_f} \tag{2.20}$$

Above is the final form of the equation used (2.20) to determine conductivity in a lab setup. The unknowns which were measured in the lab are the cell pressure (P_{cell}), differential pressure across the length L (ΔP), and the fluid flow rate (q). At any given fracture closure stress the conductivity of the fracture and proppant pack were determined by flowing fluid at several different rates, and using the corresponding cell pressure and differential pressure in order to plot the left-hand side of the equation vs. the right-hand side of the above equation which will have a slope that is inverse of conductivity at that closure stress.

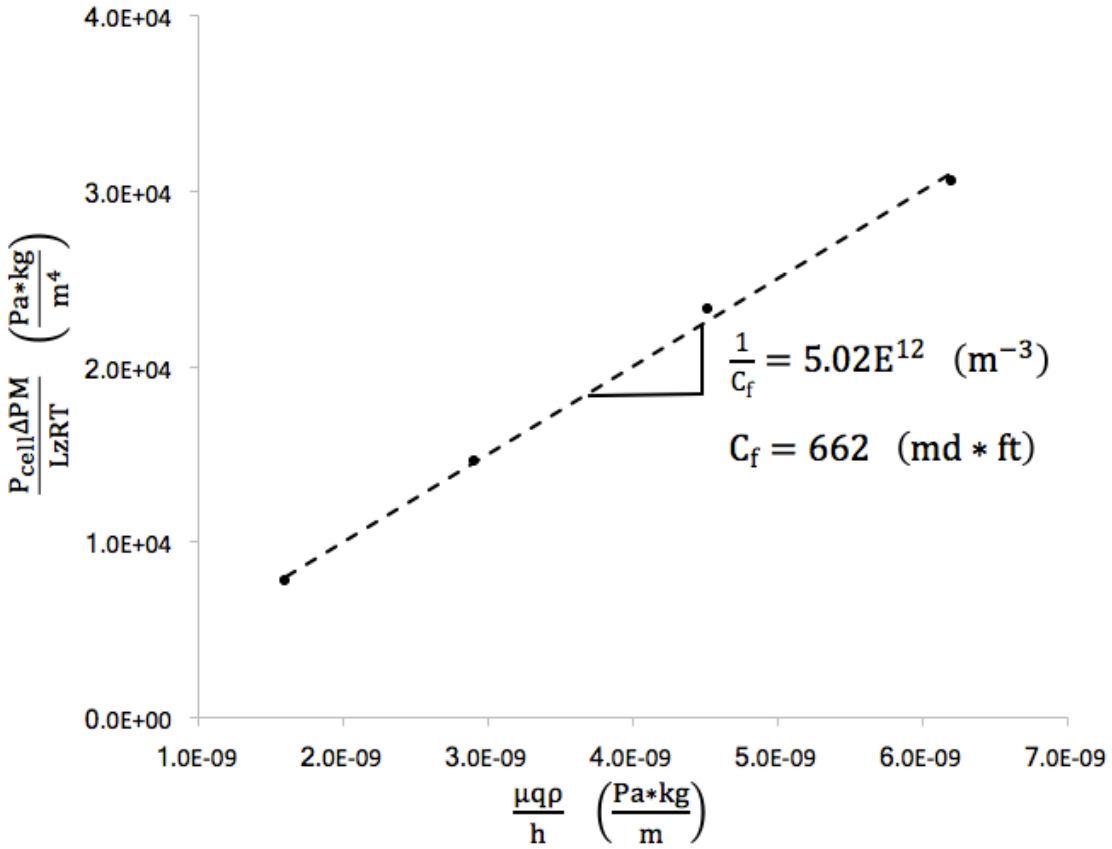

Figure 2.10. Experimental results used to determine the conductivity of a proppant pack.

It is important to note that the conductivity values measured in the lab are higher than the actual fracture conductivity observed downhole. However, the lab conductivity measurements serve as a means of comparison between proppant types, concentration, flow fluid, and many other variable testing factors. Even though the conductivity downhole will be less than that determined in the lab, multiple lab tests can be used to determine which treatments will perform better than others.

3. RESULTS

This chapter discusses the results of 35 conductivity tests conducted on 13 different proppant types, size, and mixtures. Table 3.1 shows the testing matrix used. Figure 3.1 shows the conductivity test results for all proppants and proppant combinations tested in this study. Each proppant was tested at six different closure stresses: 1,000, 2,000, 3,000, 4,000, 5,000, and 6,000 psi. There are only error bars included on the conductivity curve for 40/70 glass due to the wide variation in conductivity results for this proppant. All other conductivity curves shown in figure 3.1 were able to be reproduced within a reasonable range, and the error bars were excluded for figure clarity. The conductivity test results for each individual test can be found in Appendix B with error bars for each proppant which was tested three or more times.

Proppant Type			Number of Tests Completed
1	Sand	20/40	2
2		30/50	3
3		40/70	7
4		100	1
5	Glass	20/40	3
6		40/70	3
7	Taconite	20/40	2
8		30/50	2
9		40/70	3
10	Coal	80/100	4
11	Mixtures 50%:50%	20/40 Sand & Glass	2
12		40/70 Sand & Taconite	2
13		40/70 Sand & Glass	1
Total			35

Table 3.1. Testing matrix.

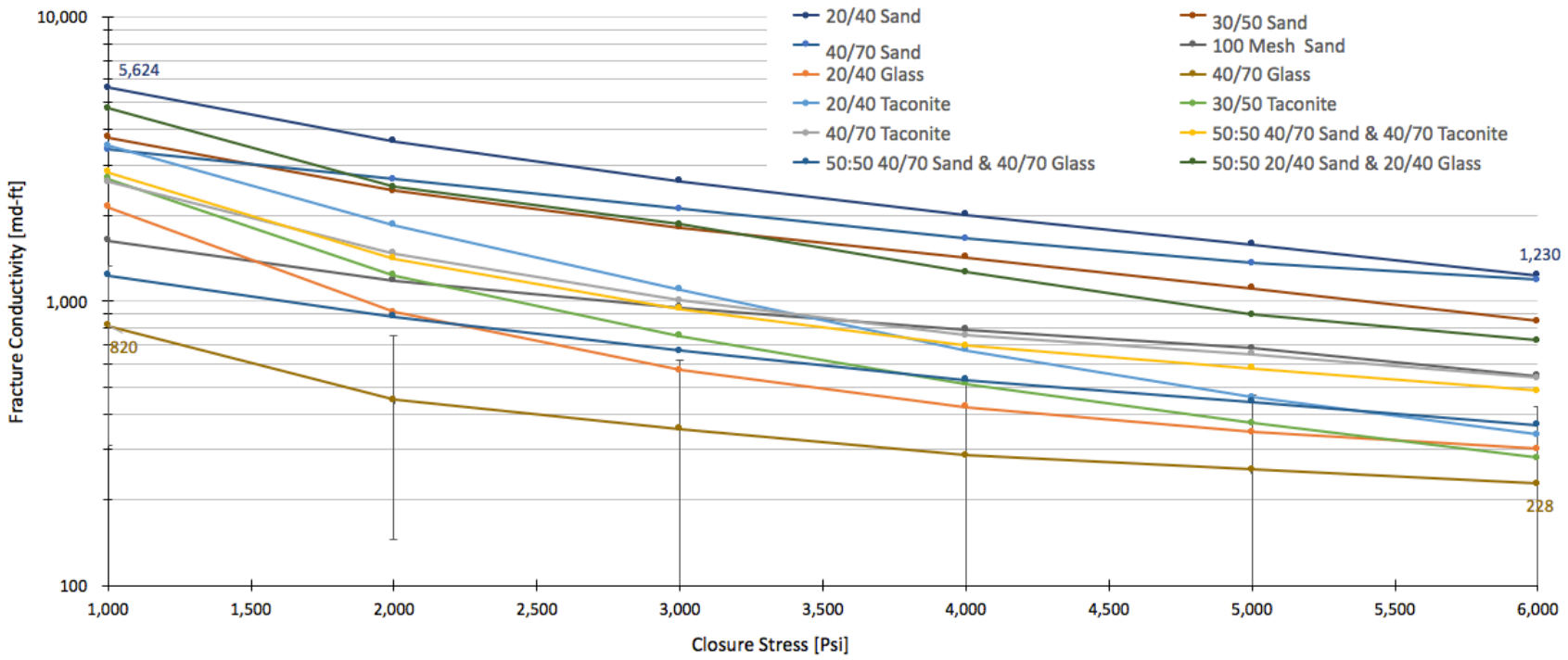

Figure 3.1. Conductivity test results for all proppants tested.

There are several important features of the proppant particles and assortment which dictate a proppant's conductivity. Figure 3.2 shows the relationship between proppant grain size, sorting, permeability, and porosity. Larger grains should result in a more permeable proppant pack, so it is expected that the conductivity of a 20/40 proppant of any type should exceed that of a 40/70 proppant of the same proppant type. As well, sorting is important. For this reason, proppant size is denoted by a mesh range such as 20/40, 30/50, or 40/70 to ensure that all of the particles are within a given particle diameter range, resulting in good sorting and higher proppant pack permeability than an unsorted particle distribution.

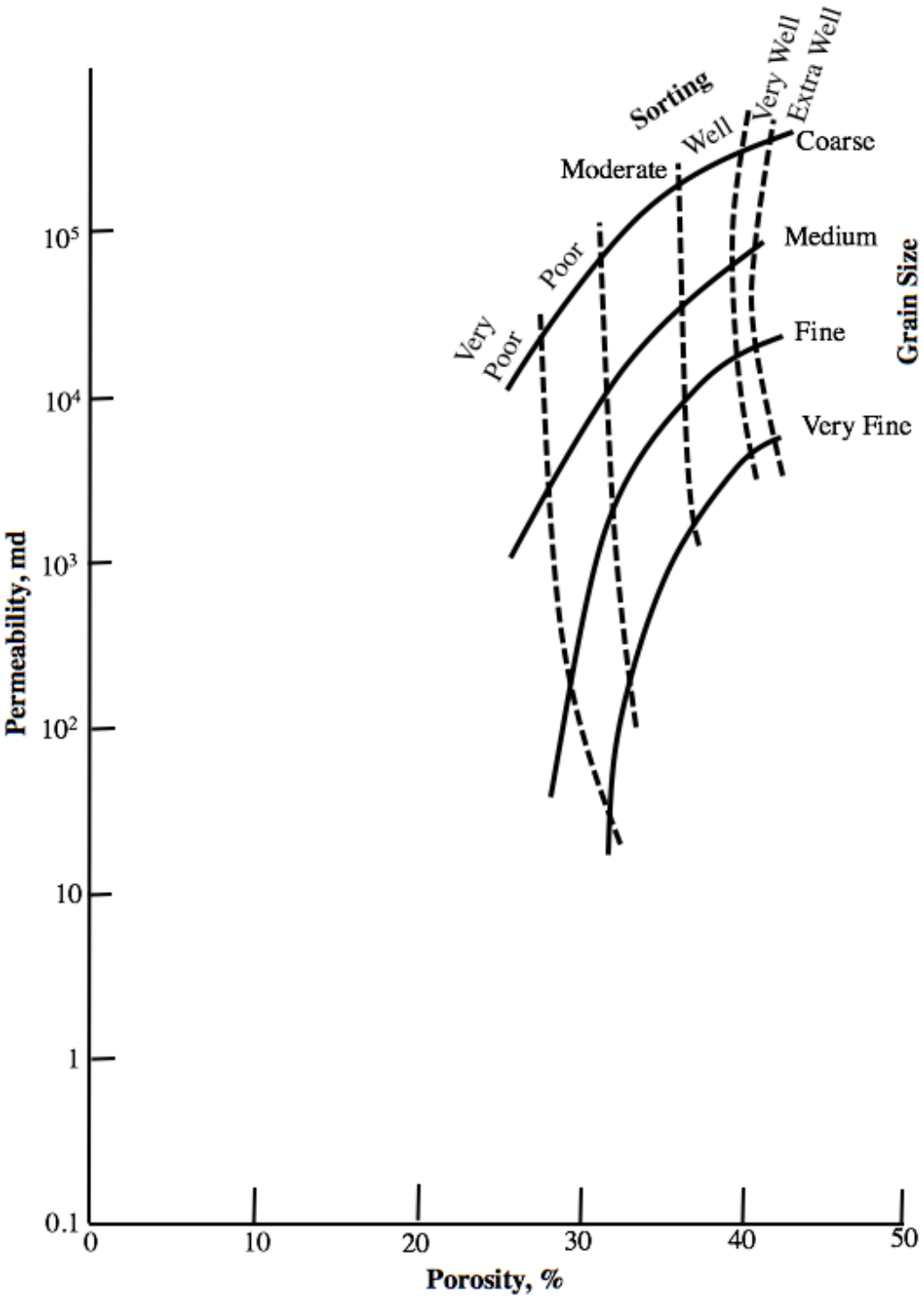

Figure 3.2. Porosity, permeability, sorting, and grain size (adapted from Selley, 1998).

Sphericity and roundness also play an important role in a proppant pack's conductivity. Ideally all proppant particles should be both round and spherical. Roundness refers to how smooth the corners of a particle are. Sphericity refers to how well that particle resembles a sphere. The more round and spherical the particles are, the larger voids they will leave between them when they pack together. The larger the voids, the more opportunity for flow paths to be present. If a particle is not round, and has sharp edges those edges can fill the voids between particles and reduce opportunities for flow pathways. Figure 3.3 shows a Krumbein and Sloss chart which shows examples of various levels of particle sphericity and roundness.

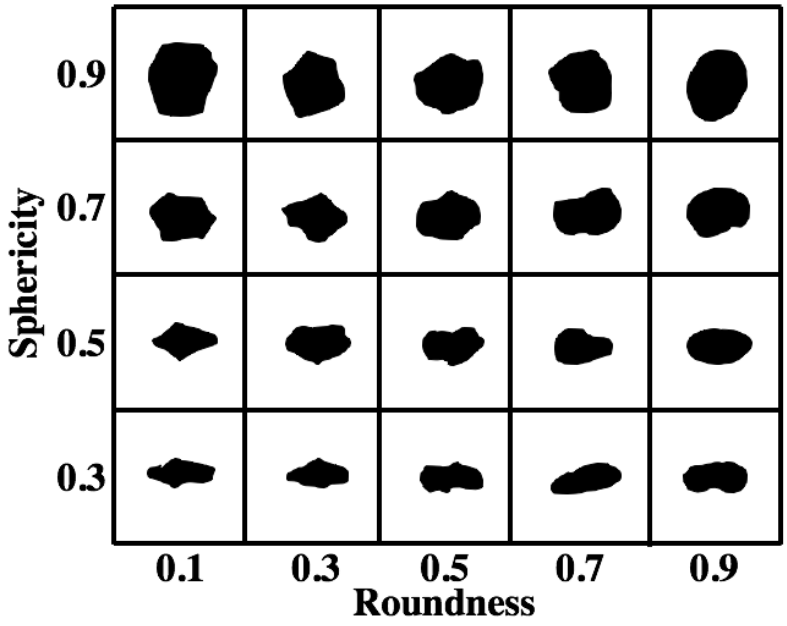

Figure 3.3. Krumbein and Sloss chart (adapted from Larsen and Smith, 1985).

Sorting is not an issue initially, but as closure stress increases, proppant can crush and generate smaller particles, decreasing the sorting, particle roundness, and particle sphericity, ultimately reducing the porosity, permeability, and most importantly conductivity of the proppant pack.

Before every conductivity test, the proppant was sieve tested to establish a particle distribution for the proppant mesh range. Additionally, a sieve test was conducted once again after a conductivity test was run to 6,000 psi closure stress. The results of the sieve tests will be presented in the "Proppant Crushing" section for sand, glass, and taconite proppants.

3.1 Conventional Sand Baseline

Four different mesh sizes of sand were measured to establish a baseline, check results, and compare novel proppant effectiveness. The sand proppant sizes measured were 20/40, 30/50, 40/70, and 100 mesh proppant distributions. The sand proppant conductivity results from testing in the Texas A&M conductivity lab were deemed comparable to long term conductivity results found in literature. This established validity of the testing procedure and ability to produce reasonable results.

3.1.1 Proppant Geometry

The sand proppant was the most well rounded and spherical proppant tested. Figure 3.4 shows a microscopic image of 20/40 sand proppant. In this image, it is clear that the sand particles are all well rounded and some are very spherical. Based on the geometry of these particles the conductivity should be expected to be high.

Figure 3.4. Microscopic image of 20/40 sand particles.

3.1.2 Conductivity

Sand proppants were some of the most conductive proppants tested in this study. Figure 3.5 shows the conductivity results for all proppants and proppant mixtures tested, the sand proppant results are highlighted in red. Figure 3.6 shows the results for sand proppants only.

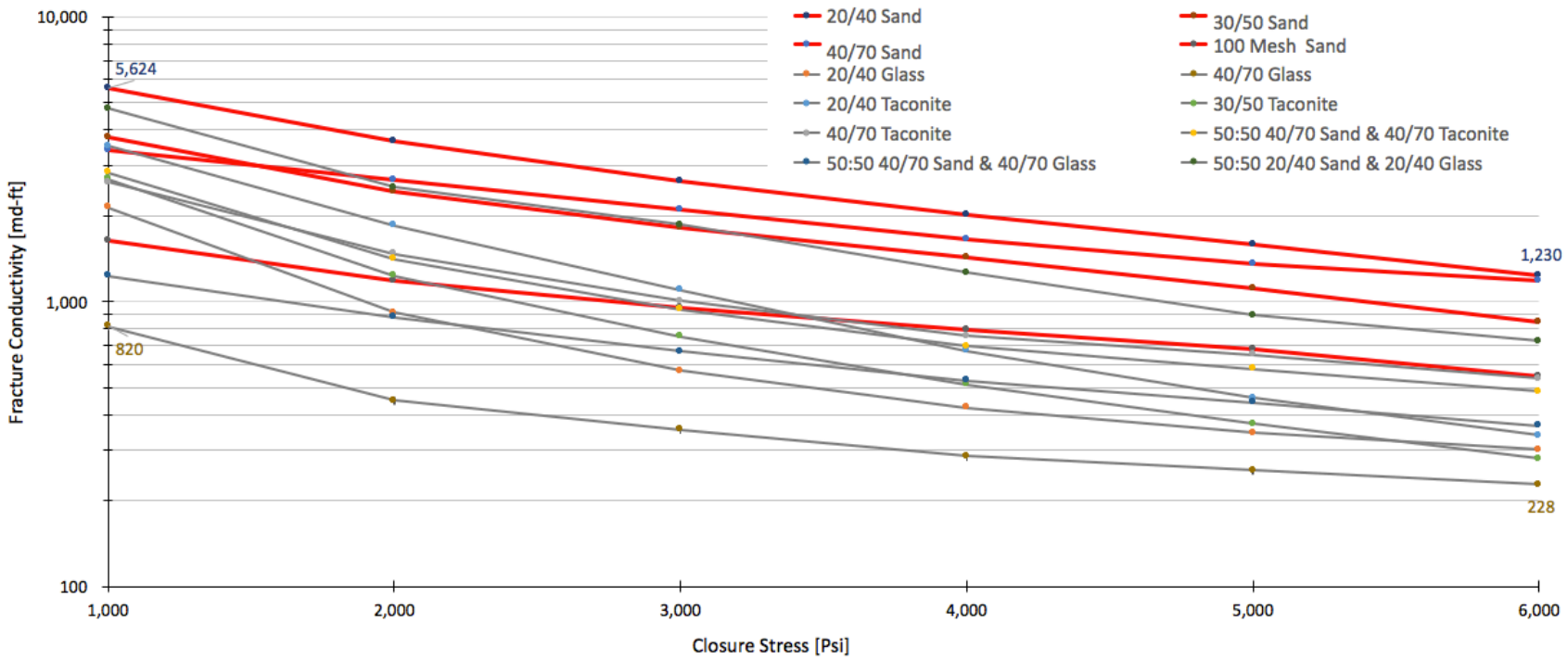

Figure 3.5. Comparison of sand proppant conductivity to other tested proppants.

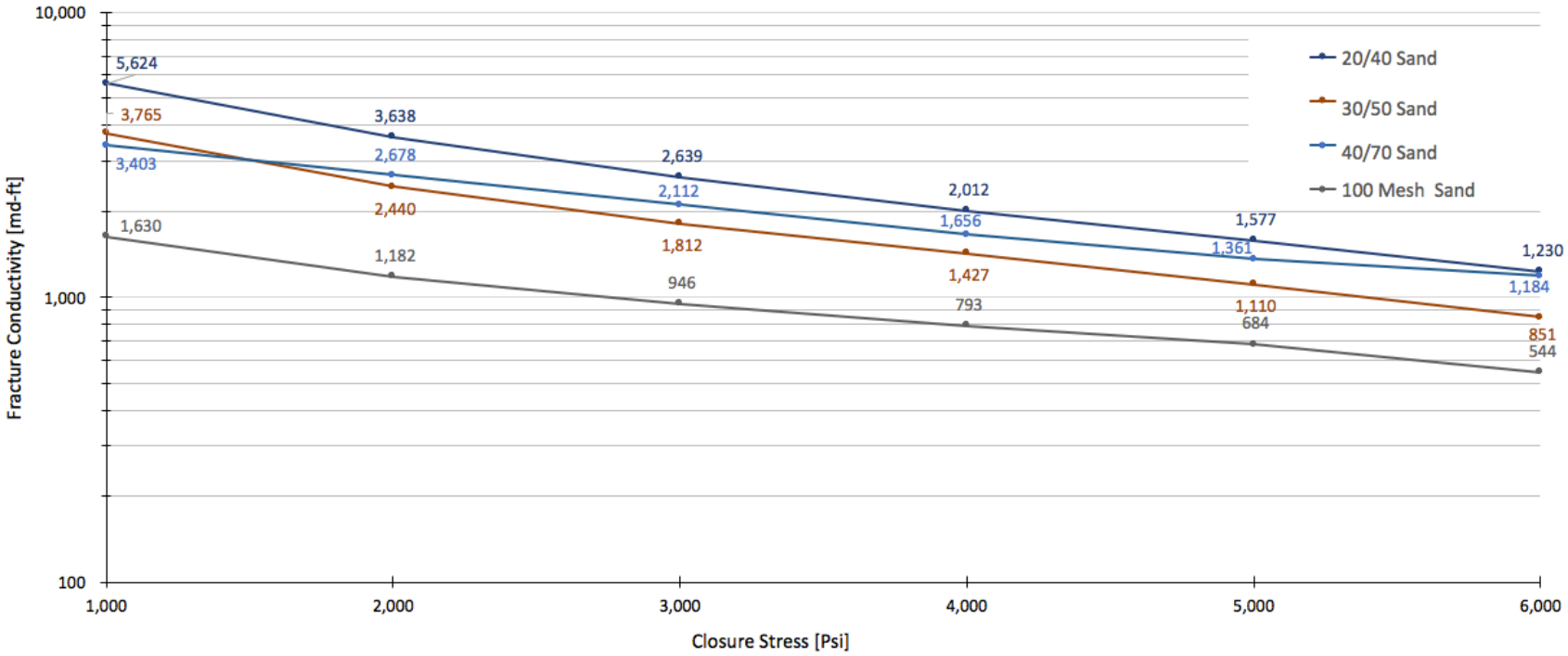

Figure 3.6. Sand proppant conductivity Results.

The conductivity results for sand proppants reflect what is to be expected based on grain size and particle geometry. At low closure stress the largest mesh proppant (20/40) results in the highest conductivity followed by 30/50, 40/70, and finally 100 mesh sand proppant. However, between 1,000 and 2,000 psi closure stress, the 30/50 sand proppant's conductivity decreases to below the 40/70 sand proppant. This is likely due to the larger 30 mesh range particles crushing during the closure stress increase. Larger particles have lower crush strength than smaller particles. For every closure stress increase the larger mesh sand proppant experienced a greater reduction in conductivity than the smaller mesh proppants. The only exception to this for sand proppant occurs between 3,000 and 4,000 psi where 40/70 mesh sand experiences a conductivity decrease of 546 md-ft, but the larger 30/50 mesh sand only experiences a conductivity decrease of 385 md-ft.

3.1.3 Proppant Crushing

Sand proppant experienced the least amount of particle crushing during the conductivity test up to 6,000 psi closure stress. Figure 3.7 shows the particle distribution for 20/40 sand proppant both before and after completion of a conductivity test.

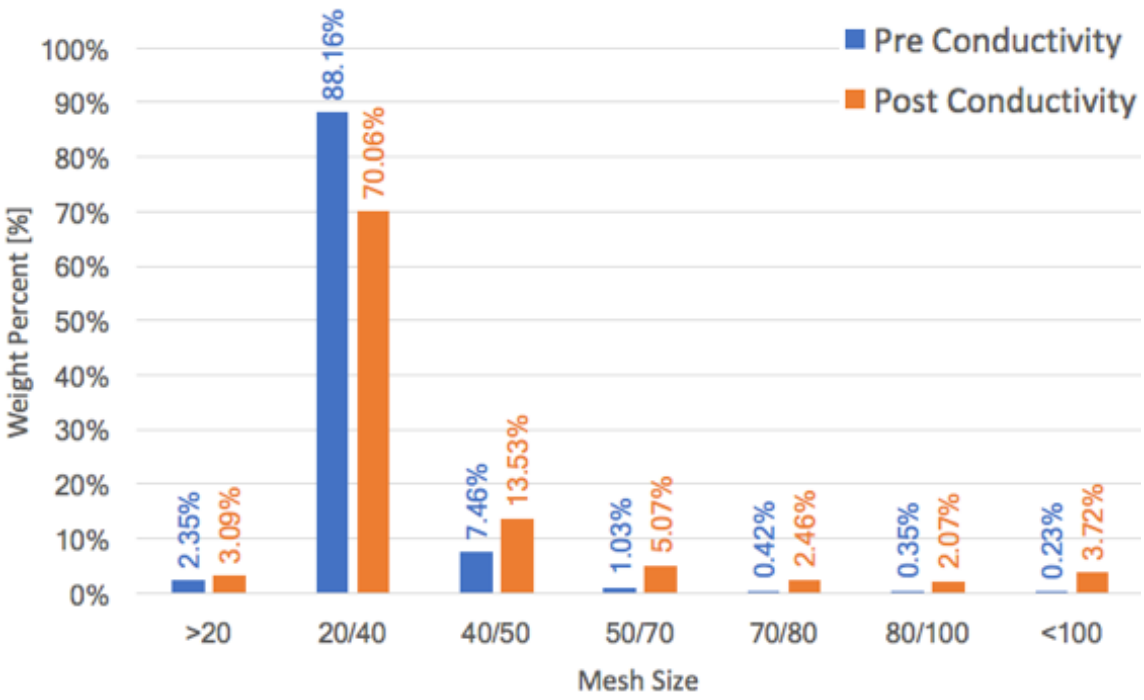

Figure 3.7. 20/40 sand proppant particle distribution.

Figure 3.7 shows that there is not a significant amount of proppant crushing that occurred during the conductivity test for 20/40 sand proppant. The same is true for 30/50, 40/70, and 100 mesh sand proppants. There is however still crushing that occurred. The 20/40 mesh range particles decreased 18% by mass, which means those particles were crushed and contributed to the increase in the amount of more fine particles.

3.1.4 Discussion of Sand Test Results

The sand proppant conductivity test results were some of the highest measured conductivity results in this study. This is not a surprise considering the particle geometry and lack of proppant crushing. The sand particles exhibit round and spherical features which contribute to quality proppant pack conductivity. There is also a small amount of proppant

crushing which allows for the proppant sorting to be maintained throughout the conductivity test, sustaining high permeability.

The most unexpected aspect of the sand proppant results is that the 40/70 proppant resulted in higher conductivity than the 30/50 proppant at high closure stress. I believe this is due to the larger 30 mesh range particles crushing at lower closure stress than the smaller 40 mesh particles. The 40/70 proppant experienced less crushing than the 30/50 mesh proppant throughout the conductivity test.

The decline rate for the two larger sand proppants, 20/40 and 30/50, appear to be similar, and the decline rate for the two smaller sand proppants, 40/70 and 100 mesh, appear to be similar. There may be a proppant size threshold where the decline rate begins to decrease from what is seen in the larger proppants to what is seen in the smaller proppants. That threshold appears to be between the 30/50 and 40/70 mesh proppants. Perhaps the largest particles in a 40/70 mesh proppant have a significantly greater crush strength than the largest particles in a 30/50 mesh proppant, resulting in a shallower conductivity decline.

3.2 Glass

Two mesh sizes of glass proppant were tested, 20/40 and 40/70 mesh sizes. The conductivity for these two sizes of glass proppants were two of the lower conductivity curves for any of the tested proppants. This section will present the results and possible reasons the glass proppant did not exhibit conductivity as high as the sand proppant.

3.2.1 Proppant Geometry

The glass proppant was the least well rounded and spherical proppant tested. Figure 3.8 shows a microscopic image of 20/40 glass proppant. In this image, it is clear that the glass

particles are neither round nor spherical. Based on the geometry of these particles the conductivity should be expected to be lower than that of equal sized sand proppant.

Figure 3.8. Microscopic image of 20/40 glass particles.

3.2.2 Conductivity

The conductivity for glass proppants were two of the least conductive proppants tested in this study. Figure 3.9 shows the conductivity results for all proppants and proppant mixtures tested, the glass proppant results are highlighted in red. Figure 3.10 shows the results for glass proppants and equivalent sized sand proppants.

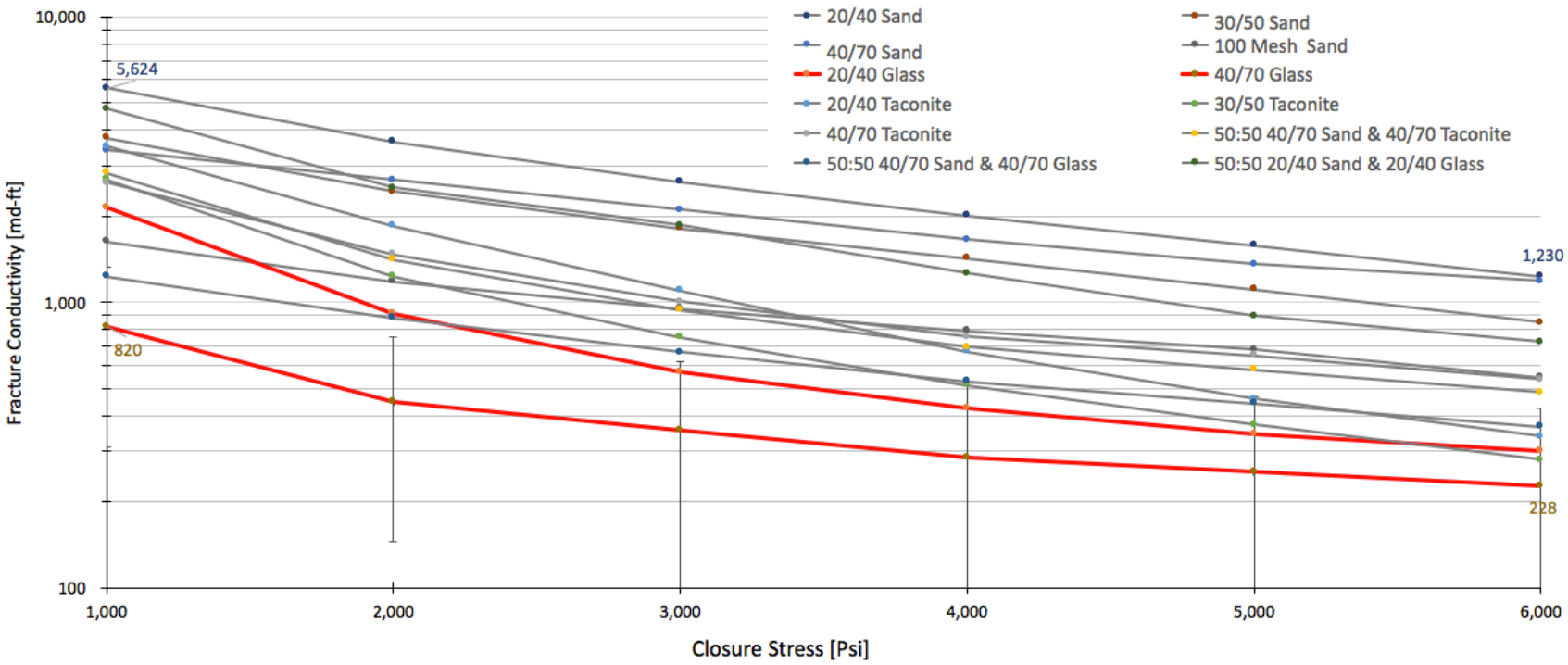

Figure 3.9. Comparison of glass proppant conductivity to other tested proppants.

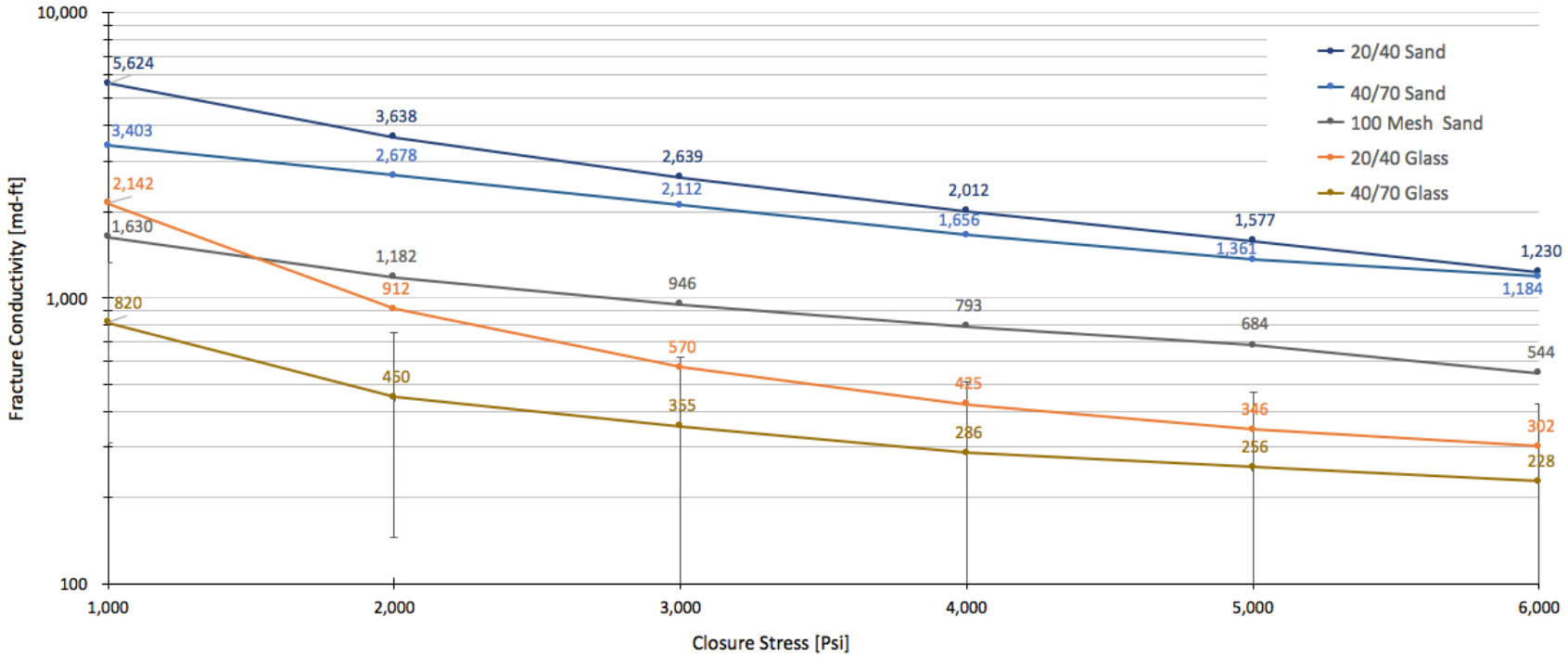

Figure 3.10. Glass proppant conductivity results compared to sand.

The conductivity results for glass proppants reflect what is to be expected based on grain size and particle geometry. At low closure stress the glass proppants conductivity is well below the conductivity values for equal sized sand proppants. This is likely due to the glass proppant's lack of roundness and sphericity. The voids that sand proppant is able to leave open when packing together, could possibly be filled by the jagged edges of the rough glass particles. This is likely amplified as closure stress increases and the proppant is forced closer together causing the proppant to re-arrange and fill more of the void space, or even proppant crushing that creates smaller particles which fill the gaps between proppant particles and reduce the potential for flow paths through the proppant pack.

For every closure stress increase the larger mesh glass proppant experienced a greater reduction in conductivity than the smaller mesh proppants. This is due to the fact that larger particles have lower crush strength and are more easily crushed.

Error bars were included on the 40/70 glass proppant conductivity curve. The 40/70 glass and 80/100 coal proppants had the widest range on conductivity results. The error bars represent one standard deviation of the three conductivity tests that were run. There is a wide range in conductivity results, but even the highest conductivity values found for 40/70 glass in the laboratory were still at the lower end of conductivity for all tested proppants.

3.2.3 Proppant Crushing

Glass proppant experienced the most severe amount of particle crushing during the conductivity test up to 6,000 psi closure stress. Figure 3.11 shows the particle distribution for 20/40 glass proppant both before and after completion of a conductivity test.

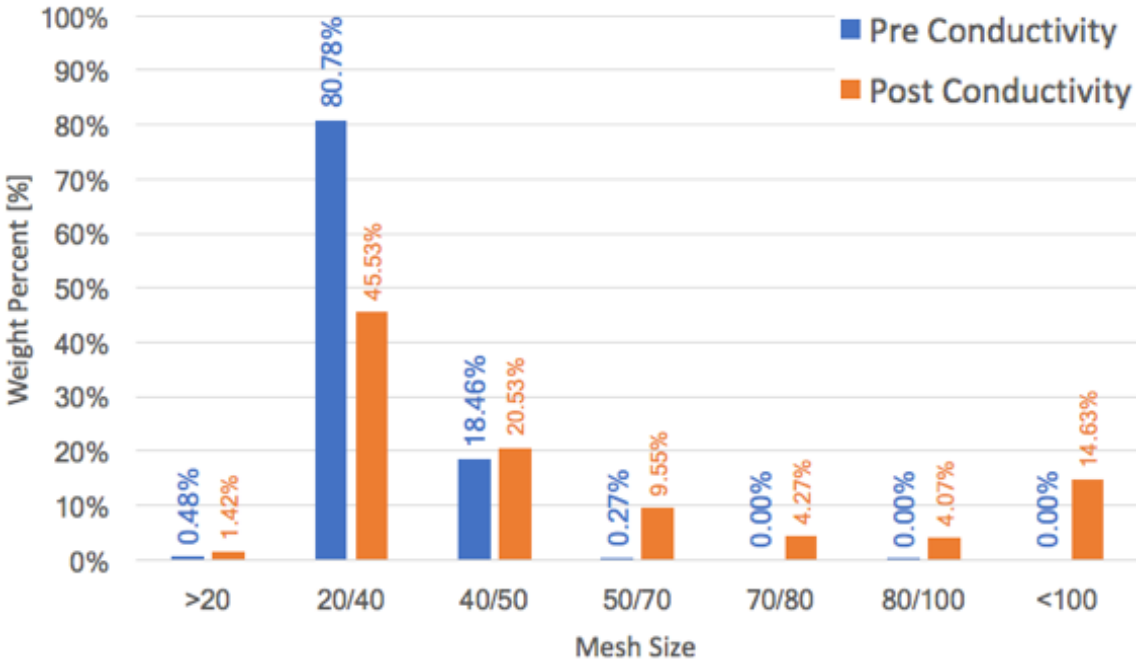

Figure 3.11. 20/40 glass proppant particle distribution.

Figure 3.11 shows that there is a significant amount of proppant crushing that occurred during the conductivity test for 20/40 glass proppant. The same is true for 40/70 mesh glass proppants. This large amount of proppant crushing is likely a contributing factor to the relatively poor conductivity exhibited by both glass proppant samples. The proppant particle size distribution comparisons for all tested proppants are shown in Appendix A.

3.2.4 Discussion of Glass Test Results

The glass proppant conductivity test results were some of the lowest measured conductivity results in this study. This is not a surprise considering the particle geometry and large amount of proppant crushing. The glass particles do not exhibit round or spherical features which reduces the amount of void space between proppant particles, and causes a lower conductivity in the proppant pack. There is also a large amount of proppant crushing which reduces the amount of sorting in the proppant pack, lowering the permeability and conductivity.

There was difficulty in reproducing the 40/70 glass proppant conductivity curves. This may be due to the wide range of particle shapes. Although each sample of 40/70 glass that was tested consisted of the same proppant volume, the variety in particle shape could have varied greatly from test to test.

3.3 Taconite

Taconite is an iron-bearing sedimentary rock, which is often mined for iron ore. The crushed waste rock is referred to as taconite tailings. Taconite tailings are composed of primarily quartz (about 60%) and varying levels of iron oxides, carbonate, and silicate.

Three mesh sizes of taconite tailing proppants were tested: 20/40, 30/50, and 40/70 mesh sizes. The conductivity for these three sizes of taconite proppants fell in the middle of the conductivity curves for all other tested proppants. This section will present the results and possible reasons the taconite proppant did not exhibit conductivity as high as the sand proppant, but had higher conductivity than the glass proppant.

3.3.1 Proppant Geometry

The taconite proppant is not as round and spherical as the sand proppant, but it is noticeably more round and spherical than the glass proppant. Figure 3.12 shows a microscopic image of 20/40 taconite proppant. In this image, it is clear that the taconite particles have roundness and sphericity between the high levels of sand and the low levels of glass. Based on the geometry of these particles the conductivity should be expected to be in between that of equal sized sand and glass proppants.

Figure 3.12. Microscopic image of 20/40 taconite particles.

3.3.2 Conductivity

The conductivity curves for taconite proppants fell in the middle of the 13 proppant and proppant mixtures tested in this study. Figure 3.13 shows the conductivity results for all proppants and proppant mixtures tested, and the taconite proppant conductivity curves are highlighted in red. Figure 3.14 shows the results for taconite proppants and equivalent sized sand proppants.

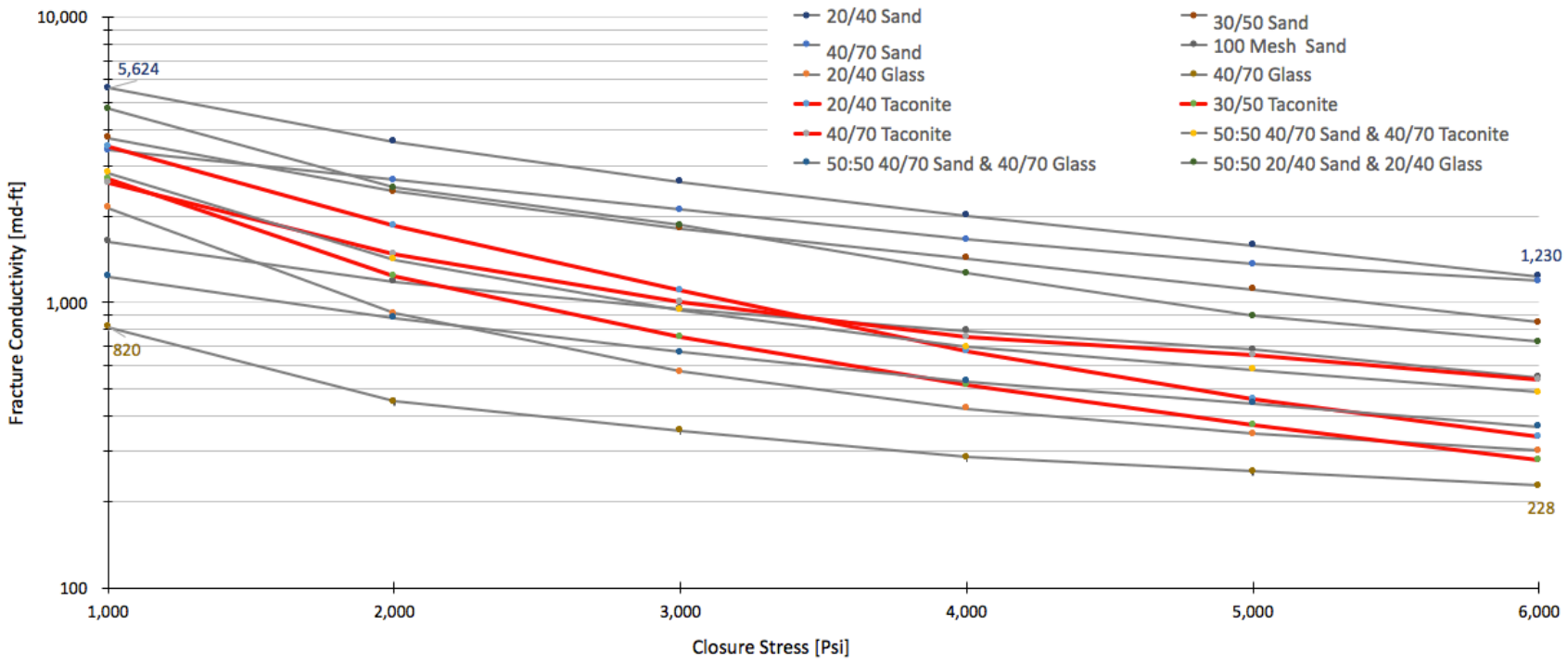

Figure 3.13. Comparison of taconite proppant conductivity to other tested proppants.

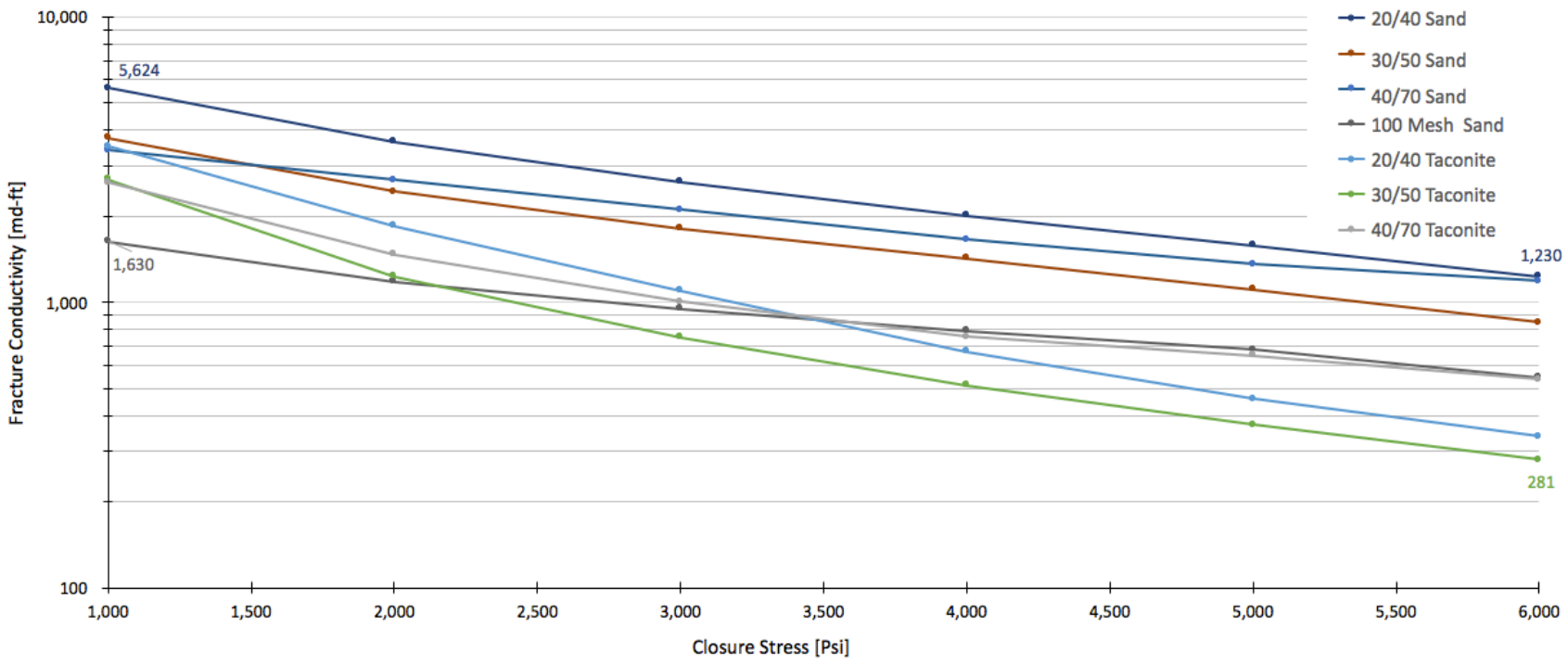

Figure 3.14. Taconite proppant conductivity results compared to sand.

The conductivity results for taconite proppants reflect what is to be expected based on grain size and particle geometry. At low closure stress, the taconite proppant conductivity is near, but slightly below the conductivity values for equal sized sand proppant. As well, the taconite proppant conductivity at low closure stress was higher than the values for equal sized glass proppants. This is likely due to the taconite proppants' roundness and sphericity being lower quality than the sand proppant, but much more well-rounded than the glass proppant. The voids that sand is able to leave open when packing together, could possibly be filled by the more jagged edges of the rougher taconite particles. This is likely amplified as closure stress increases and the proppant is forced closer together causing the proppant to re-arrange and fill more of the void space, or even crushes and creates smaller particles to fill the gaps between proppant particles and reduce the potential for flow paths through the proppant pack. This effect was not nearly as significant in the taconite proppant as it was in the glass proppant.

It is also worth noting the similarity in decline rate of the 20/40 and 30/50 proppant, and the much shallower declining slope exhibited by the 40/70 taconite proppant. This is similar to what was observed with the sand proppants.

3.3.4 Proppant Crushing

Taconite proppant experienced a notable amount of particle crushing during the conductivity test up to 6,000 psi closure stress. Figure 3.15 shows the particle distribution for 20/40 taconite proppant both before and after completion of a conductivity test.

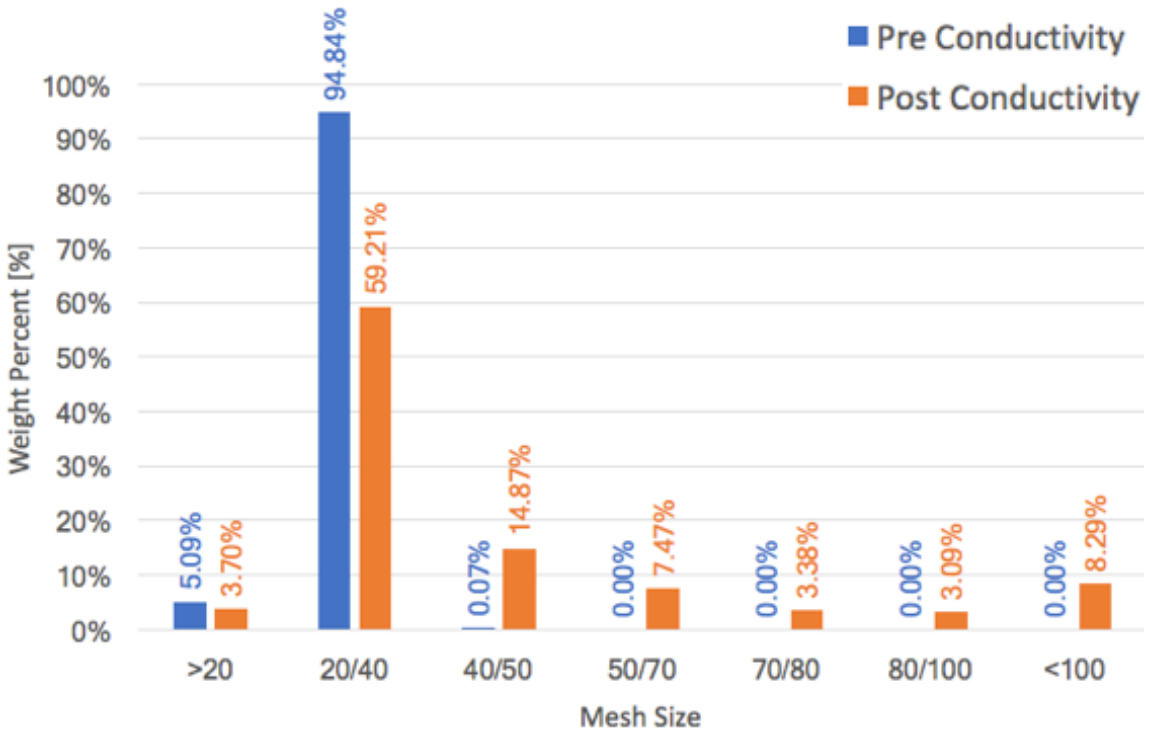

Figure 3.15. 20/40 taconite proppant particle distribution.

Figure 3.15 shows that there is a noticeable amount of proppant crushing that occurred during the conductivity test for 20/40 taconite proppant. The same is true for 30/50 and 40/70 mesh taconite proppants. This noticeable amount of proppant crushing is likely a contributing factor to the relatively poor conductivity exhibited by all three taconite proppant samples compared to equivalent sized sand proppants.

3.3.5 Discussion of Taconite Test Results

The taconite proppant conductivity test results fell in the middle range of conductivity results for all proppants and proppant mixtures tested in this study. This is not a surprise considering the particle geometry and significant proppant crushing. The taconite particles were geometrically between that of sand proppant and glass proppant. The less rounded and spherical

features of taconite cause a reduction in void space between proppant particles when compared to sand, but not to the extreme that is likely to occur in glass proppant packs.

As observed with the sand proppant, there is a noticeably different slope between the large taconite proppant (20/40 and 30/50) conductivity curves and the smaller proppant (40/70) conductivity curve. This slower conductivity decline resulted in 40/70 mesh taconite proppant having the highest taconite conductivity at high closure stresses. The 40/70 taconite proppant pack conductivity was very similar to that of 100 mesh sand. Smaller size taconite proppant had lower initial conductivity which is expected. This is likely due to particle crushing. Larger particles are more prone to crushing than smaller particles. There is likely some crushing that occurs at closure stresses less than 1,000 psi. Conductivity was not tested below 1,000 psi, because such a large quantity of proppant was used during the tests that it was easily moved, potentially creating channels for gas to bypass the proppant pack at larger closure stresses. Had the tests been run at 500 psi, I suspect that there would have been a greater difference in conductivity values between the larger and smaller taconite proppants. The larger size taconite proppant experienced more severe crushing than the 40/70 taconite, which lead to lower conductivity.

3.4 Proppant Mixtures

Three proppant mixture conductivities were tested in the lab. Each mixture was mixed 50% sand and 50% novel proppant on a volume basis. Each mixture was mixed with equivalent sized proppant for both sand and novel proppant to ensure good particle sorting was maintained. For example, only 20/40 sand was mixed with 20/40 novel proppant, and only 40/70 sand was mixed with 40/70 novel proppant. The results of these tests varied widely.

3.4.1 Conductivity

Novel proppant mixtures with sand can improve the proppant pack conductivity results from using novel proppant alone. The three mixtures tested were 20/40 sand and glass, 40/70 sand and taconite, and 40/70 sand and glass. The results for all three mixtures are shown in Figure 3.16. The 20/40 sand and glass mixture had that highest conductivity of all three proppant mixtures tested, followed by the 40/70 sand and taconite mixture, and the 40/70 sand and glass mixture.

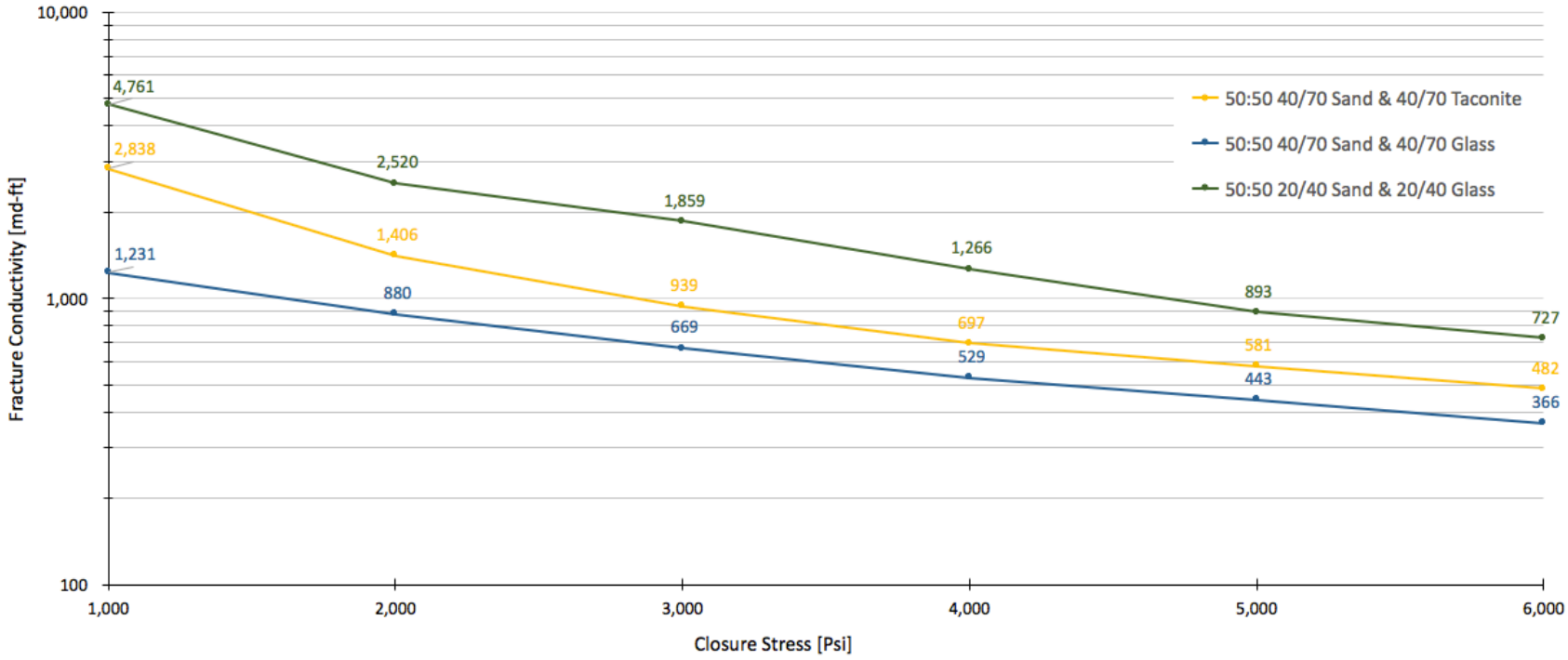

Figure 3.16. Conductivity results for all proppant mixtures tested.

3.4.1.1 20/40 Sand and Glass Mixture

The mixture of 20/40 sand and glass proppants had the largest conductivity of any proppant mixture tested. Figure 3.17 shows the conductivity curves for 20/40 sand, 20/40 glass, and the mixture of the two. The mixture curve falls between the sand and glass curves which is to be expected. The round geometry of the sand should create more porosity and permeability when packing together than using glass proppant alone. However, the angular geometry should reduce the porosity and permeability from using solely sand proppant. The conductivity benefits of sand proppant should not be expected to be totally negated by the inclusion of glass particles, but it is expected there would be a reduction in conductivity by including more angular grains. The mixture of 20/40 sand and glass resulted in a conductivity increase of about 400 md-ft from using 20/40 glass proppant alone.

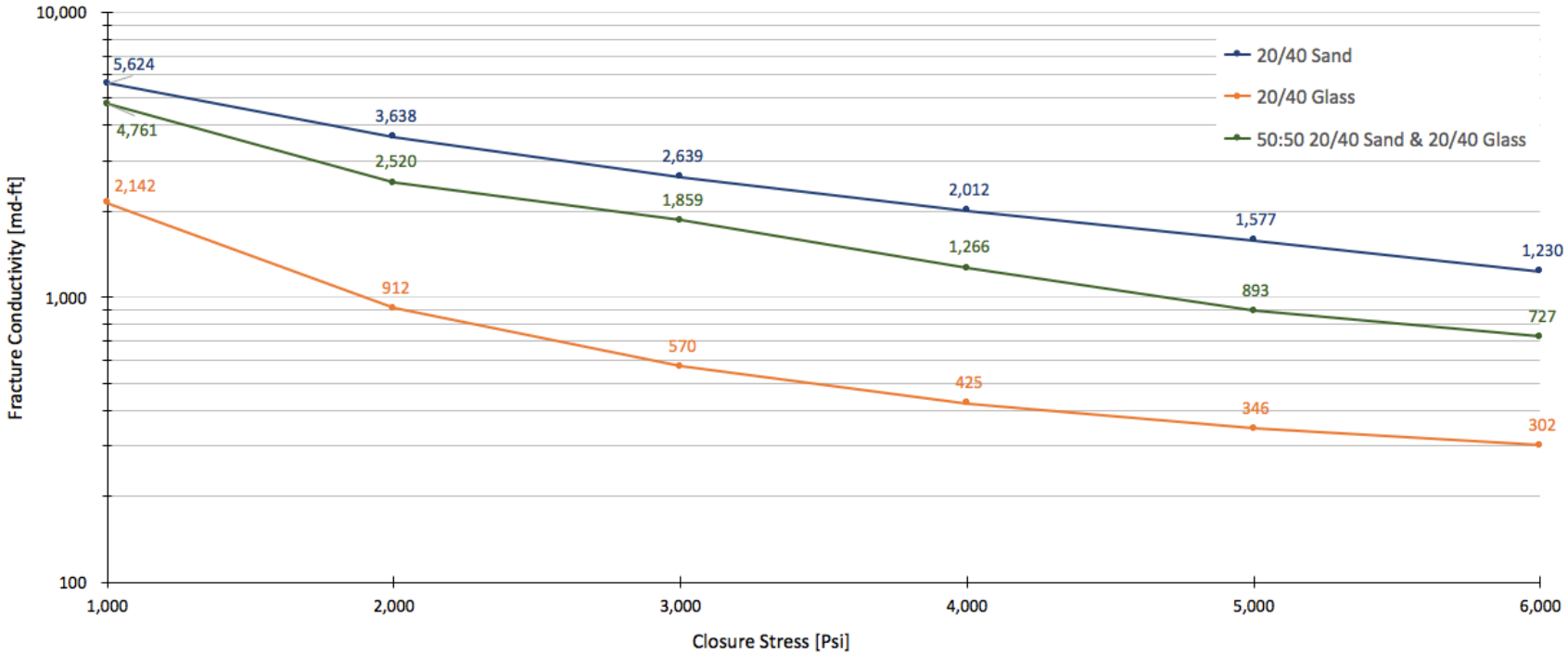

Figure 3.17. Conductivity of 20/40 sand and glass mixture.

3.4.1.2 40/70 Sand and Taconite Mixture

Mixing 40/70 sand with 40/70 taconite proppant did not yield an improvement from using 40/70 taconite on its own. Figure 3.18 shows the conductivity curves for the proppant mixture as well as the component proppants. At low closure stresses the mixture has higher conductivity than the 40/70 taconite proppant, but after 1,000 psi closure stress the conductivity mixture declines to less than the conductivity of only 40/70 taconite proppant. There is only a minor difference in the proppant pack conductivity of the mixture and the 40/70 taconite.

It is not clear why mixing 40/70 sand with 40/70 taconite did not improve the conductivity compared to just 40/70 taconite. I speculate that the difference in grain size from the 20/40 sand and glass mixture is the biggest difference between the 20/40 mixture and 40/70 mixture. In the 20/40 sand and glass mixture the conductivity was likely improved by the round geometry of the sand proppant, and that benefit was amplified by larger grain size particles. Even though the same should be true for 40/70 proppant mixtures, a conductivity increase provided by the sand geometry was not observed in this mixture.

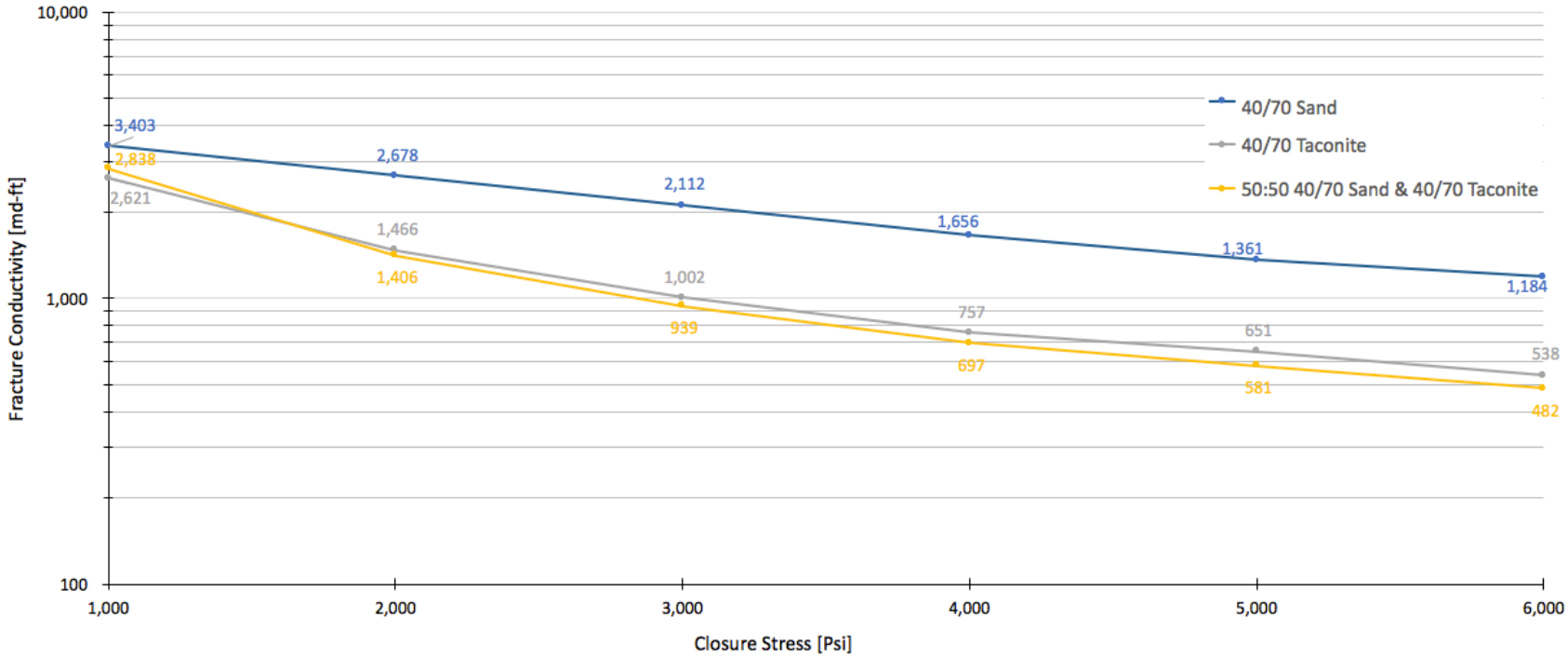

Figure 3.18. Conductivity of 40/70 sand and taconite mixture.

3.4.1.3 40/70 Sand and Glass Mixture

Mixing 40/70 sand with 40/70 glass proppant did not yield much of an improvement from using 40/70 glass on its own. Figure 3.19 shows the conductivity curves for the proppant mixture as well as the component proppants. At every closure stresses the mixture has higher conductivity than the 40/70 glass proppant on its own. There is a measurable difference in the proppant pack conductivity of the mixture and the upper limit of 40/70 glass proppant conductivity results.

Similar to the 40/70 sand and taconite mixture, the small grain size of the proppant mixture minimized the impact of beneficial geometric features of sand proppant. In the 20/40 sand and glass mixture the conductivity was likely propped up by the round geometry of the sand proppant, and that benefit was amplified by larger grain size particles. Even though the same should be true for 40/70 proppant mixtures, the conductivity increase provided by the sand geometry was not as extreme as that of the 20/40 sand and glass mixture. Mixing 40/70 glass with sand increased the conductivity of 40/70 glass alone. However, that increase was near the highest conductivity results from 40/70 glass proppant packs.

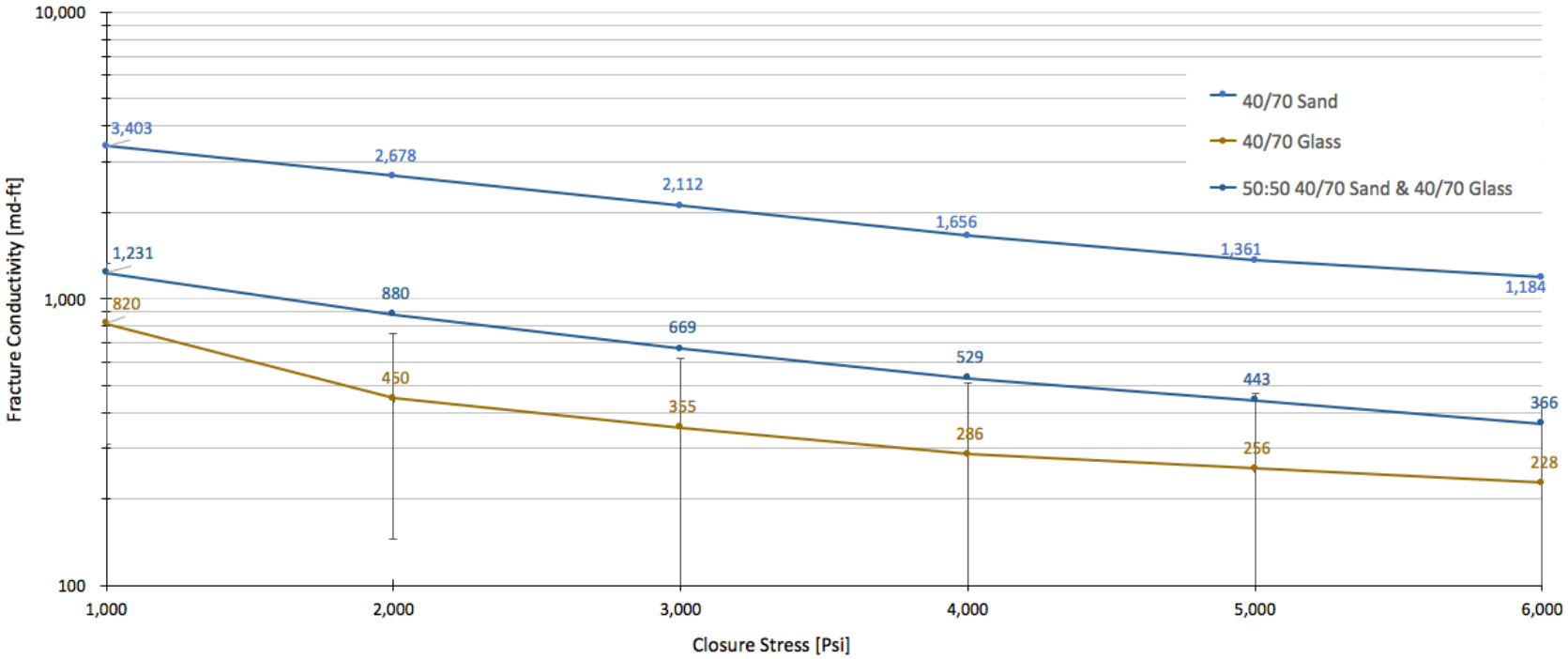

Figure 3.19. Conductivity for 40/70 sand and glass mixture.

3.4.2 Findings of Mixed Proppant Tests

All proppant mixture conductivity values fell between or near the conductivity of the mixture components. That is to be expected; sand geometry should provide and increase in conductivity, and the angular geometry of the novel proppants should cause a decrease in conductivity.

The conductivity improvement of mixing sand into the novel proppant was less significant with smaller mesh proppants. When packing perfectly round and spherical particles together, larger grains will leave larger voids between the particles which increases porosity, permeability, and conductivity. Those voids can be decreased by introducing angular particles that will pack closer together and reduce the void space. These angular particles have a greater effect on proppant pack conductivity when the proppant particles, and resulting voids between them, are smaller. This is why the 40/70 mesh proppant mixtures did not show as much of a conductivity improvement from using only the novel proppant as was seen in the 20/40 sand and glass mixture.

Even though not all proppant mixtures will result in a higher conductivity than the mixture's least conductive component, there are mixtures that can provide a significant conductivity increase from the least conductive component. Not all proppant combinations were tested in this study, and perhaps there is a mixture that will result in conductivity equivalent to the sand component. From the three proppant mixtures tested, it is clear that mixing novel proppant with sand proppant can, but will not always, increase the conductivity of using novel proppant on its own.

3.5 Coal

Coal was the final novel proppant tested. In total, four conductivity tests were attempted for 80/100 mesh coal proppant. Two of the conductivity tests resulted in an inability to flow gas into or through the test cell. Figure 3.20 shows the 80/100 mesh coal proppant after it had been removed from the test cell.

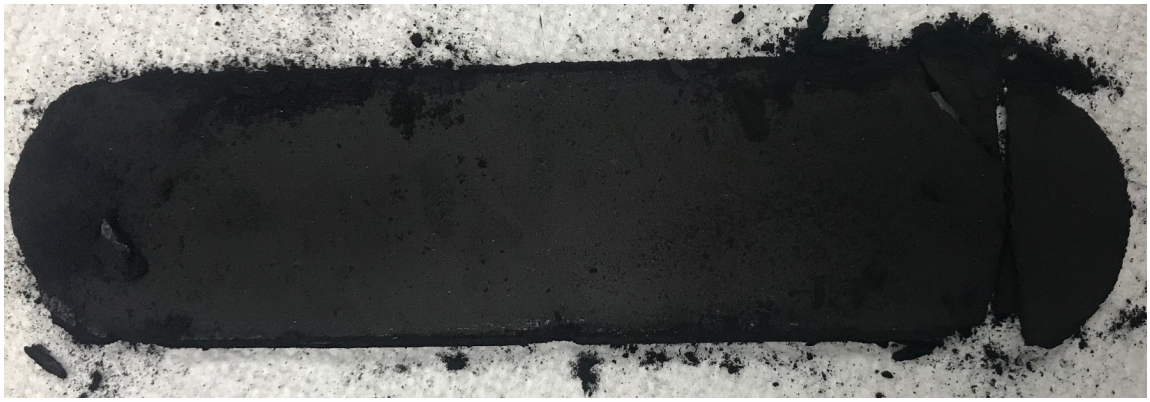

Figure 3.20. 80/100 coal proppant after conductivity test.

In all four conductivity tests, the coal proppant looked the same as seen in Figure 3.20. For all other proppants tested, when the bottom steel plate was removed, the proppant fell out in individual particles which then had to be swept up and collected for post conductivity sieve testing. The coal proppant however came out in one solid piece. The coal proppant was fully compacted into an impermeable coal wafer that did not allow any flow through the proppant pack. Non-digital pressure gauges were attached to the test cell to confirm that no gas flow had entered the cell. Neither pressure gauge registered any pressure, indicating that no gas was able to enter the test cell or flow through the coal proppant pack.

The results of the two tests where flow was able to enter the test cell will be discussed in the next section.

3.5.1 Conductivity

Conductivity was measured for two of the four attempted tests. Figure 3.21 shows the results of the two tests where the necessary values required to calculate conductivity were measured.

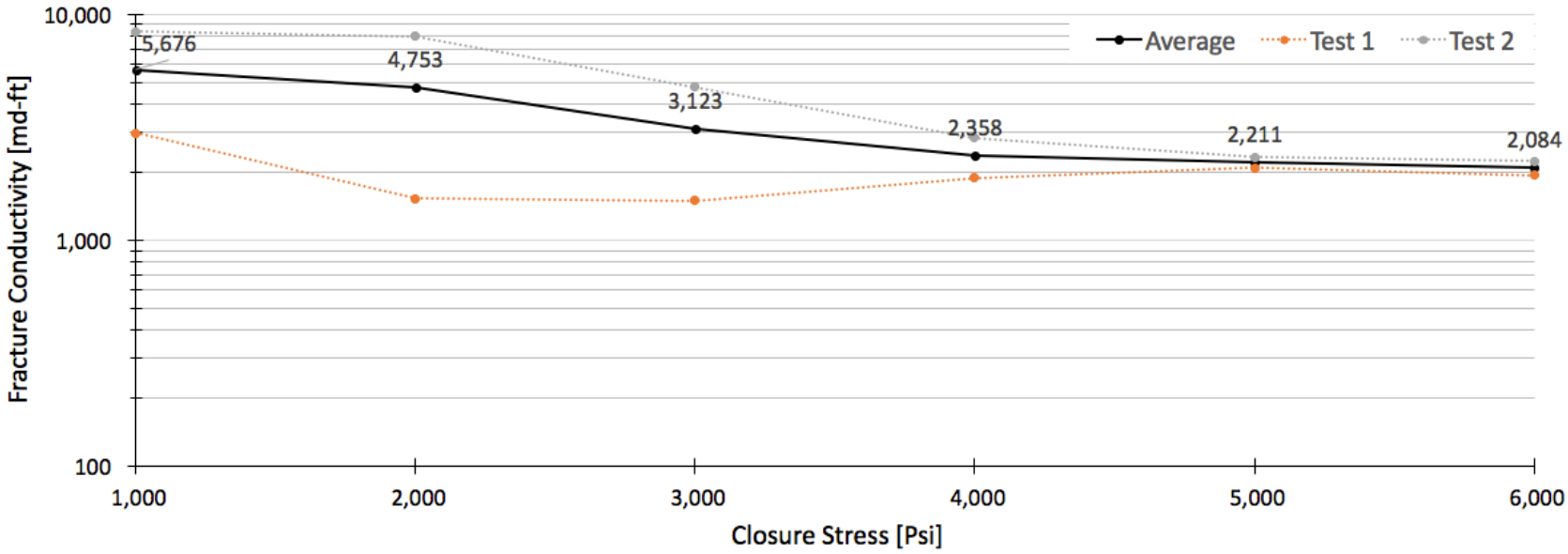

Figure 3.21. Conductivity results for 80/100 coal proppant.

The two dashed curves in Figure 3.21 represent the two individual conductivity test results when gas was able to enter the test cell. The two conductivity tests resulted in drastically different results. Test 1 is the bottom dashed curve in figure 3.21. The behavior between closure stresses 1,000 and 2,000 psi is expected, a decrease in conductivity with an increase in closure stress. However, after 3,000 psi the conductivity for test 1 begins to increase. This trend was not expected, there is no reason for any proppant pack that the conductivity of a proppant should increase as closure stress increases. Due to the fact that tests 1 and 2 converged to a conductivity value around 2,000 md-ft at closure stresses of 5,000 and 6,000 psi, I believe that this conductivity actually reflects the conductivity of the space between the impermeable coal proppant pack and the inside wall of the test cell. This phenomenon is referred to as "race tracking" which refers to flow taking a highly conductive flow path through or around the proppant pack which is not representative of the actual proppant pack conductivity.

There is the potential that test 1 measured the true proppant pack conductivity at 1,000 and 2,000 psi closure stress, but the same could be said about test 2. Neither of these test results were able to be reproduced, and they differ significantly from one another. Regardless of what was being measure in each test below 5,000 psi closure stress, I think that it is evident that the two tests measured the same values above 5,000 psi, which I believe to be a conductivity measurement of gas flow race tracking between the proppant pack and cell wall.

3.5.2 Discussion of Coal Test Results

Coal proppant did not show potential for being able to replace sand as a conductive proppant material. In the four tests conducted, only two tests were able to measure the necessary values required to calculate conductivity. These conductivity measurements are likely not a true reflection of the coal proppant pack conductivity, but were the result of gas flowing between the proppant pack and the test cell wall. As seen in figure 3.20, the coal proppant packed very tightly together and formed what I consider to be an impermeable coal pack. This impermeable coal pack did not allow any flow to enter the test cell for two tests, and forced flow around the coal pack in the two tests where flow was induced across the test cell.

3.6 Proppant Crushing

Proppant crushing was a main cause of conductivity reduction. Larger particles of a given material have a lower crush strength than smaller particles of the same material. This was confirmed for each proppant of a larger mesh size of a given material had a greater decrease in conductivity for every closure stress increase with the exception of three points. Table 3.2 shows the decrease in conductivity per 1,000 psi increase in closure stress for every proppant. The three exceptions to larger proppant experiencing greater conductivity reduction are shown in red. The larger particles crushed more easily, resulting in a greater conductivity decrease between each closure stress increase for larger mesh proppants.

Average Decrease in Conductivity Between Closure Stresses						
Proppant	Sand				Glass	
	20/40 Sand	30/50 Sand	40/70 Sand	100 Mesh Sand	20/40 Glass	40/70 Glass
Closure Stress						
1,000 - 2000	1,986	1,325	725	448	1,230	370
2,000 - 3000	998	628	566	235	342	95
3,000 - 4000	627	385	456	153	145	69
4,000 - 5000	435	317	295	109	79	30
5,000 - 6000	347	259	177	139	44	28
Proppant	Taconite			Mixture		
	20/40 Taconite	30/50 Taconite	40/70 Taconite	50:50 40/70 Sand & Taconite	50:50 40/70 Sand & Glass	50:50 20/40 Sand & Glass
Closure Stress						
1,000 - 2000	1,673	1,465	1,154	1,432	351	2,241
2,000 - 3000	747	479	464	467	211	660
3,000 - 4000	429	241	244	242	140	593
4,000 - 5000	211	141	107	116	86	373
5,000 - 6000	121	90	113	99	77	166

Table 3.2. Decrease in average conductivity per 1,000 psi closure stress.

Sieve tests were conducted before and after each conductivity test. Comparison of particle distributions between before and after each proppant underwent 6,000 psi closure stress revealed how severe crushing was in each proppant type. It was observed that sand had the most resistance to particle crushing, followed by taconite, and finally glass which had the most severe amount of crushing and fines generation.

The large amount of proppant crushing and fines generation appeared to reduce conductivity in the laboratory conductivity tests, but could pose even more issues when implemented in the field. Fines migration is a well-established means of reducing proppant pack conductivity. During flow back and production the large amount of fines generated in the novel proppants may further reduce the conductivity of the generated fracture.

3.7 Particle Shape and Porosity

Particle geometry has a well-established impact of proppant pack permeability and porosity. The effect of particle geometry features discussed in the results section proved to have a significant impact on proppant pack conductivity for all proppants tested. Ideally a well sorted, large grain size, well rounded, and highly spherical proppant should result in a highly conductive proppant pack.

This was confirmed by comparing proppant pack conductivity at low closure stresses for each proppant. All proppants tested were assumed to be very well sorted as designated by the proppant mesh range of 20/40, 30/50, 40/70 and so forth. For each proppant material, before much crushing had likely occurred at 1,000 psi closure stress the largest grain size proppant had the highest conductivity, and the smallest grain size proppant had the lowest conductivity.

Also at low closure stresses for a given mesh sized proppant, the most well rounded and spherical proppant tested (sand) had the largest conductivity. The second most well rounded and spherical proppant tested (taconite) had the second largest conductivity. Finally glass, the least well rounded and spherical proppant had the lowest conductivity for a given mesh range.

The importance of sorting, grain size, roundness, and sphericity were reflected in the conductivity results for all proppants at low closure stress. At higher closure stresses these features remain important, but are all degraded by various levels of proppant crushing. Figure 3.22, 3.23, and 3.24 show the results of all proppants of the same size. In these figures, it is clear that the most well rounded and spherical proppants have higher proppant pack conductivity than the proppants with lesser geometric qualities.

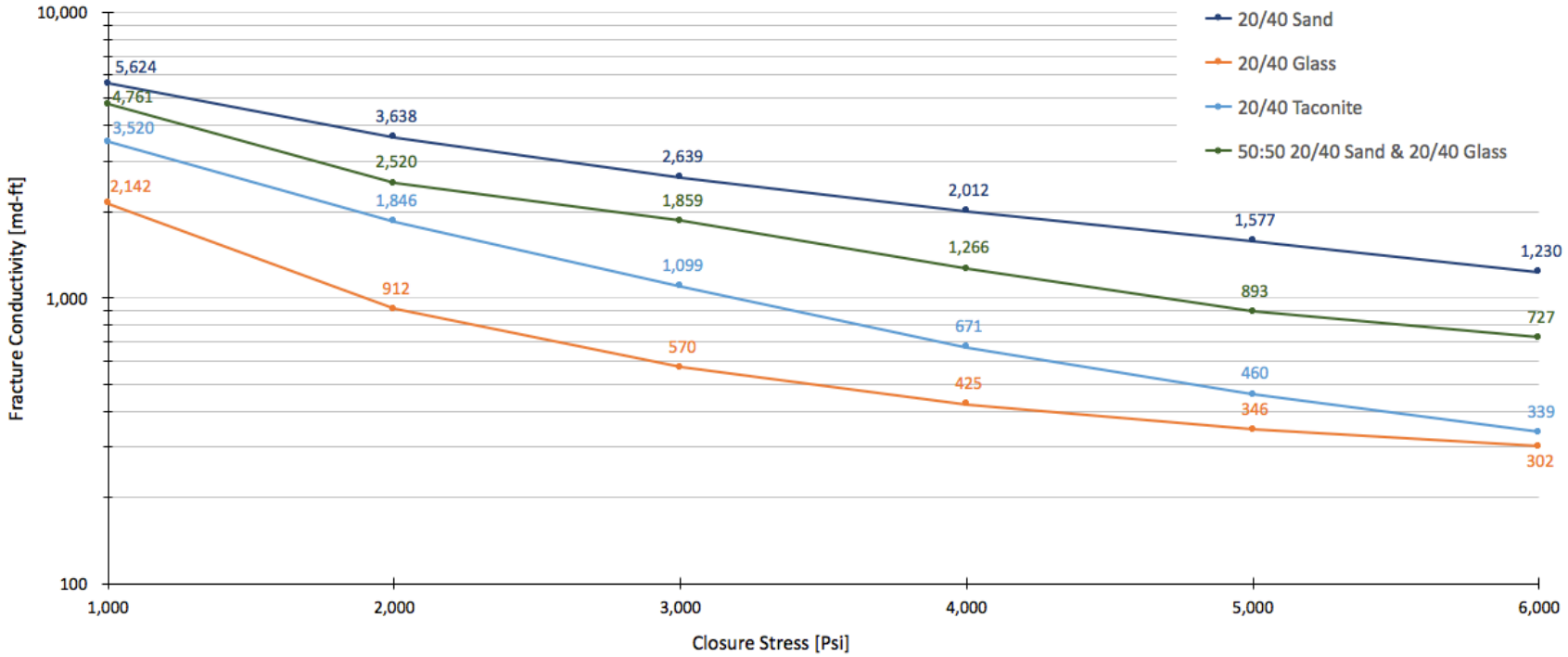

Figure 3.22. Conductivity results for all 20/40 mesh proppants tested.

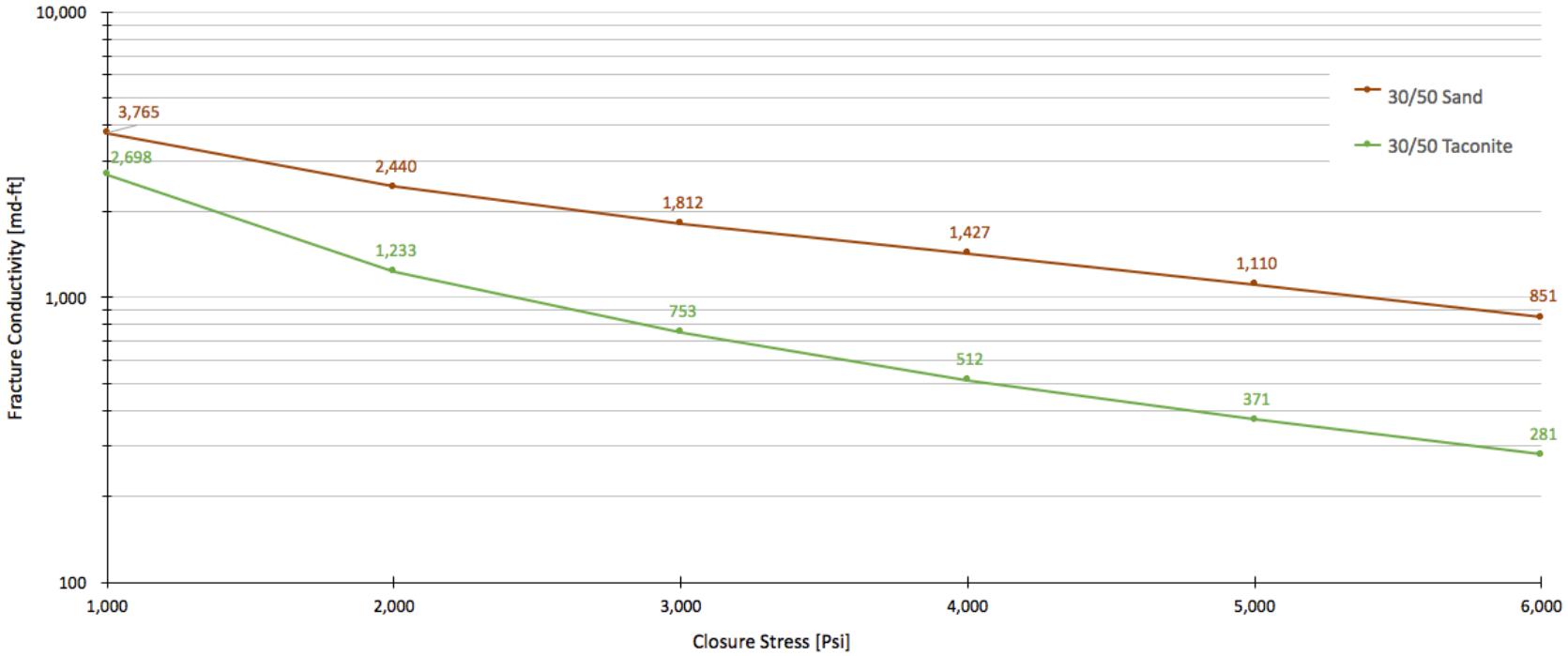

Figure 3.23. Conductivity results for all 30/50 mesh proppants tested.

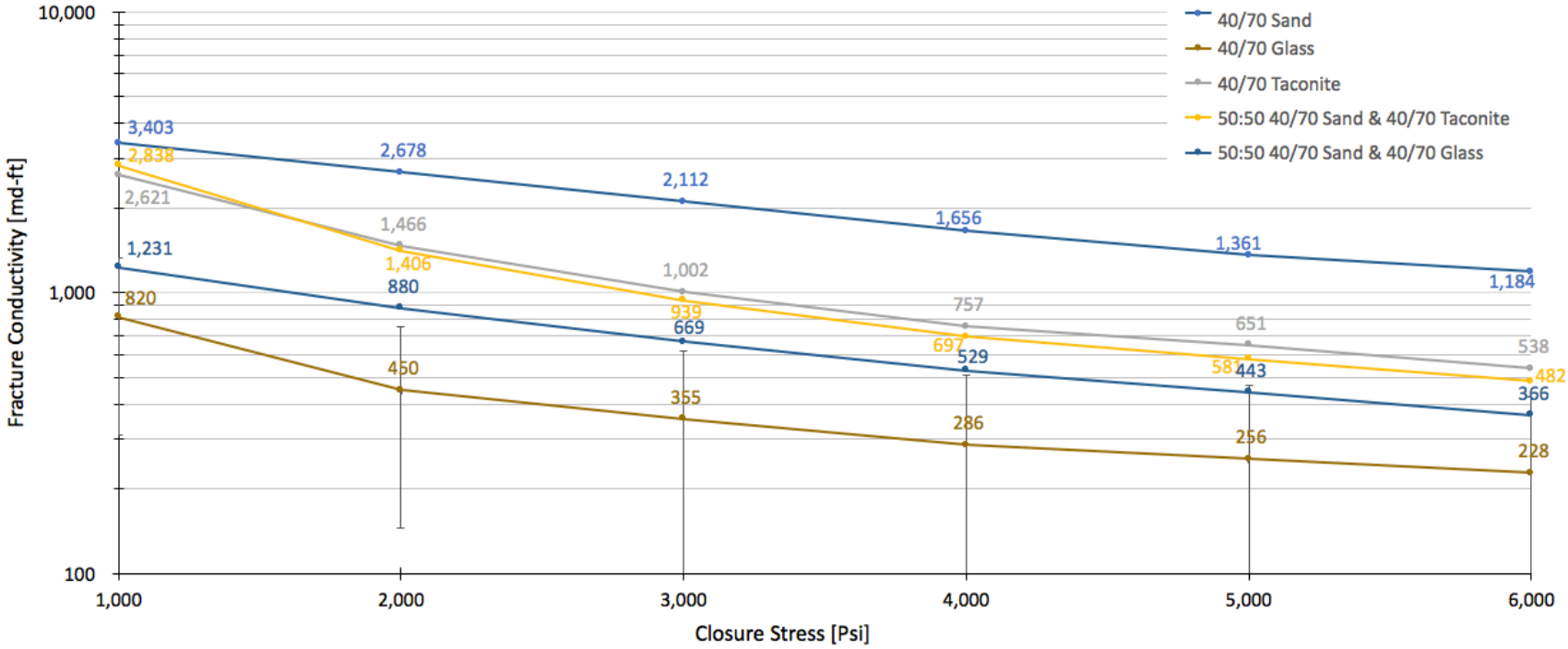

Figure 3.24. Conductivity results for all 40/70 mesh proppants tested.

3.8 Dimensionless Fracture Conductivity

Dimensionless fracture conductivity is defined as the ratio of generated fracture conductivity to the product of matrix permeability and fracture half length. Dimensionless fracture conductivity can be used to estimate the productivity increase resulting from a fracture treatment.

The conductivity results calculated in this study are for proppant loading concentrations equivalent to 2 PPF, however a more realistic proppant loading concentration used in fracture treatments is 0.1-0.4 PPF. The API RP 61 standard for testing proppant conductivity states that 2 PPF proppant loading be used, as this is a proppant evaluation study, that is the loading concentration that was utilized for testing.

In order to calculate dimensionless conductivity, the results from this study were scaled down to 0.2 PPF equivalent proppant loading. Three additional conductivity tests were conducted using Meramec Shale core samples and 0.2 PPF proppant loading concentrations. The three tests were conducted using 20/40 sand, 40/70 taconite, and 20/40 glass proppant. The results from these three tests were used to scale down the 2 PPF conductivity tests to a more realistic 0.2 PPF proppant loading concentration for each type of proppant. Figure 3.25 shows the conductivity results for both 2 PPF between steel plates and 0.2 PPF between fractured Meramec core samples.

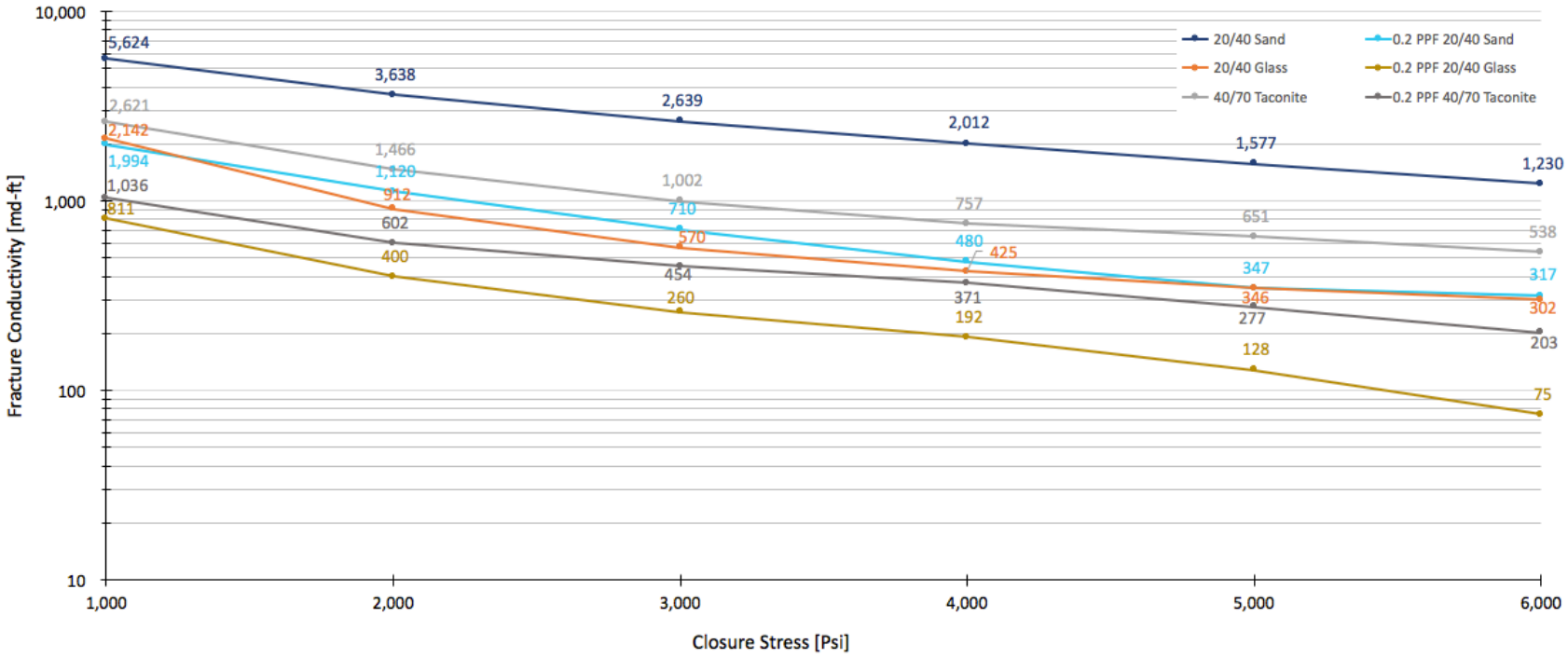

Figure 3.25. Comparison of 2 PPF and 0.2 PPF Conductivity Results

The conductivity for each proppant type was lower at 0.2 PPF than at 2 PPF. This was expected, for conductivity is defined as the product of proppant pack permeability and fracture width. Lower proppant concentration results in a smaller fracture width, and will ultimately lead to a lower conductivity. Since these proppants were also tested between fractured core samples, there is an added component of surface roughness. The 2 PPF samples were tested between smooth steel plates, but the lower concentration tests were conducted between a rough fractured surface. The surface roughness should also be expected to cause a decrease in conductivity.

Using the conductivity results from the 2 PPF and 0.2 PPF tests, a scale factor was determined for each proppant type. The scale factor reflects how much larger the conductivity is for a 2 PPF proppant pack between steel plates than a 0.2 PPF proppant pack between rough fracture surfaces. Table 3.3 shows the average conductivity values for each proppant at 2 PPF loading conditions. Table 3.4 shows the scale factor used to scale down the conductivity results for each proppant type. Table 3.5 shows the scaled down conductivity results after the scale factor has been applied.

Dimensionless Conductivity was calculated with constant values for both fracture half-length and matrix permeability; 150 ft for fracture half-length, and 100 nd (0.0001 md) for matrix permeability. The model used to calculate dimensionless conductivity assumes pseudo-radial flow to a single fracture that is created. In reality a fracture network is generated when hydraulically fracturing shales. For this reason the matrix permeability must be adjusted to account for high permeability fracture network. An adjusted matrix permeability of 0.04 md was used to calculate the dimensionless conductivity of a theoretical fracture treatment using 0.2 PPF proppant concentration for each proppant type. The dimensionless conductivity results are shown in Table 3.6. The dimensionless conductivity results are all large values that correspond to very

similar productivity increase for each proppant type. Depending on wellbore radius and drainage radius, there is minimal productivity increase for dimensionless conductivity values greater than dimensionless conductivity values of 20-40. Small increases in dimensionless conductivity can lead to large productivity increases for low dimensionless conductivity values (less than 10), but the productivity increase is negligible for any additional increase in dimensionless conductivity above 20-40.

Several tested proppants have dimensionless conductivity values less than 20. However, these dimensionless conductivity values will still result in satisfactory productivity increases. For a fracture to effectively drain its contact area, dimensionless conductivity greater than 1 is necessary, and the productivity increase diminishes at dimensionless conductivity values greater than 10 (Al-Tailji et al., 2016). The largest productivity increase occurs between fracture conductivity values of 1 and 10. Only the dimensionless conductivity for 40/70 glass proppant at 6,000 Psi closure stress is less than dimensionless conductivity of 10, at a value of 9. However, 40/70 glass proppant should still be an effective proppant for a fracture treatment.

	Sand				Glass		Taconite			Mixture		
Proppant	20/40 Sand	30/50 Sand	40/70 Sand	100 Mesh Sand	20/40 Glass	40/70 Glass	20/40 Taconite	30/50 Taconite	40/70 Taconite	50:50 40/70 Sand & Taconite	50:50 40/70 Sand & Glass	50:50 20/40 Sand & Glass
Closure Stress												
1,000	5,624	3,765	3,403	1,630	2,142	820	3,520	2,698	2,621	2,838	1,231	4,761
2,000	3,638	2,440	2,678	1,182	912	450	1,846	1,233	1,466	1,406	880	2,520
3,000	2,639	1,812	2,112	946	570	355	1,099	753	1,002	939	669	1,859
4,000	2,012	1,427	1,656	793	425	286	671	512	757	697	529	1,266
5,000	1,577	1,110	1,361	684	346	256	460	371	651	581	443	893
6,000	1,230	851	1,184	544	302	228	339	281	538	482	366	727

Table 3.3. Average conductivity for 2 PPF proppant concentration.

Scale Factor - 0.2 PPF Tests			
Proppant	Sand	Taconite	Glass
Closure Stress			
1,000	2.8	2.5	2.6
2,000	3.2	2.4	2.3
3,000	3.7	2.2	2.2
4,000	4.2	2.0	2.2
5,000	4.5	2.4	2.7
6,000	4.5	2.7	4.1

Table 3.4. Scale factor for each proppant type.

	Sand				Glass		Taconite			Mixture		
Proppant	20/40 Sand	30/50 Sand	40/70 Sand	100 Mesh Sand	20/40 Glass	40/70 Glass	20/40 Taconite	30/50 Taconite	40/70 Taconite	50:50 40/70 Sand & Taconite	50:50 40/70 Sand & Glass	50:50 20/40 Sand & Glass
Closure Stress												
1,000	1,994	1,335	1,207	578	811	311	1,392	1,067	1,036	1,006	436	1,688
2,000	1,120	751	825	364	400	197	757	506	602	433	271	776
3,000	710	487	568	254	260	162	498	341	454	252	180	500
4,000	480	340	395	189	192	129	328	251	371	166	126	302
5,000	347	244	300	151	128	95	195	158	277	128	98	197
6,000	271	187	261	120	75	56	128	106	203	106	81	160

Table 3.5. Conductivity values scaled down to 0.2 PPF proppant concentration.

	Sand				Glass		Taconite			Mixture		
Proppant	20/40 Sand	30/50 Sand	40/70 Sand	100 Mesh Sand	20/40 Glass	40/70 Glass	20/40 Taconite	30/50 Taconite	40/70 Taconite	50:50 40/70 Sand & Taconite	50:50 40/70 Sand & Glass	50:50 20/40 Sand & Glass
Closure Stress												
1,000	329	221	199	95	134	51	230	176	171	166	72	279
2,000	185	124	136	60	66	33	125	84	99	72	45	128
3,000	117	80	94	42	43	27	82	56	75	42	30	83
4,000	79	56	65	31	32	21	54	41	61	27	21	50
5,000	57	40	49	25	21	16	32	26	46	21	16	32
6,000	45	31	43	20	12	9	21	18	34	18	13	26

Table 3.6. Dimensionless conductivity for scaled down proppant concentration of 0.2 PPF.

4. CONCLUSIONS AND RECOMMENDATIONS

4.1 Conclusions

This study presented the results of testing the conductivity of 13 different proppants and proppant combinations. The tests were conducted following the API RP 61 guidelines for proppant evaluation. The results showed for a given particle size, sand had the highest conductivity followed by taconite, glass, and finally coal which did not result in any measurable conductivity.

Not all proppant mixtures will result in a higher conductivity than the mixtures least conductive component, but there are mixtures that can provide a significant conductivity increase from the least conductive mixture component.

Coal proppant did not show potential for replacing sand as a conductive proppant material. The coal proppant packed very tightly together and formed an impermeable coal pack under laboratory conditions. This impermeable coal pack did not allow any flow to enter the test cell for two tests, and forced flow around the coal pack in the two tests where flow was induced across the test cell.

As expected, the conductivity for each proppant type was lower at 0.2 PPF than at 2 PPF. Lower proppant concentration results in a smaller fracture width, and will ultimately lead to a lower conductivity.

The dimensionless conductivity values for all proppants tested show that any of these proppants besides coal could be suitable sand substitutes in hydraulic fracture treatments, and all can be expected to effectively drain the fracture contact area. However, this evaluation is based solely on the conductivity results for large proppant concentrations (2 PPF), between smooth

steel plate surfaces, with a dry nitrogen test fluid. There are other factors that contribute to a successful fracture treatment including proppant transport, fines migration, proppant-reservoir interactions, and proppant flowback fluid interactions which are outside the scope of this project. Although sand, glass, and taconite proppant resulted in satisfactory conductivity values in an ideal laboratory setting, that does not mean that they will perform as well down hole, at high temperatures, in a formation fracture, and in the presence of liquid. The many fines generated by glass proppant may further reduce conductivity with more viscous flowback fluid. The angular geometry of these novel proppants may also result in enhanced proppant embedment downhole in a water swollen shale fracture. I believe that further testing should be conducted in order to test how the novel proppants respond to these additional factors.

4.2 Recommendations and Future Work

I believe it would be beneficial to conduct further conductivity tests at more realistic proppant concentrations between Meramec core samples. Proppant loading of 0.1-0.4 PPF as opposed to 2 PPF tested in this study could yield interesting results that are more directly applicable to downhole conditions. I think that using fractured Meramec Shale samples would be most useful to gain insight on the proppant-reservoir interactions. Testing under these conditions could result in important relations between the Meramec formation of interest and the novel proppants. It would also be of value to see how water effects the novel proppant especially when placed between core samples. The fracture conductivity lab at Texas A&M University is equipped for testing proppant conductivity with water as well as nitrogen gas. These tests could show more clearly how the novel proppants will interact with the formation of interest.

There is also the potential to test more proppant mixtures. Perhaps using cheaper more abundant proppant such as glass would allow for extra money to be spent on sintered bauxite proppant for a mixture. A high strength, very well rounded, and spherical proppant such as sintered bauxite may prevent some of the crushing that occurs in glass and taconite proppants, and may provide a conductive proppant pack at lower cost to the operator.

REFERENCES

Al-Tailji, W. H., Shah, K., & Davidson, B. M. (2016, February 1). The Application and Misapplication of 100-Mesh Sand in Multi-Fractured Horizontal Wells in Low-Permeability Reservoirs. Society of Petroleum Engineers. doi:10.2118/179163-MS

Atteberry, R. D., Tucker, R. L., & Ritz, J. W. (1979, January 1). Application Of Sintered Bauxite Proppants To Stimulation Of Low Permeability South Texas Gas Reservoirs. Society of Petroleum Engineers. doi:10.2118/7924-MS

American Petroleum Institute. Recommended Practices for Evaluating Short Term Proppant Pack Conductivity. 1st ed., RP-61, 1989, Recommended Practices for Evaluating Short Term Proppant Pack Conductivity.

Cooke, C. E. (1973, September 1). Conductivity of Fracture Proppants in Multiple Layers. Society of Petroleum Engineers. doi:10.2118/4117-PA

Cooke, C. E. (1977, October 1). Fracturing With a High-Strength Proppant. Society of Petroleum Engineers. doi:10.2118/6213-PA

Cutler, R. A., Enniss, D. O., Jones, A. H., & Swanson, S. R. (1985, April 1). Fracture Conductivity Comparison of Ceramic Proppants. Society of Petroleum Engineers. doi:10.2118/11634-PA

Economides, M.J., Hill, A.D., Ehlig-Economides, C., Zhu, D. 2013. The Design and Execution of Hydraulic Fracturing Treatments. In Petroleum Production Systems, second edition. 18. Westford, Massachusetts: Pentice Hall.

Kincaid, K. P., Snider, P. M., Herring, M., Mahoney, R. P., & Soane, D. (2013, February 4). Self-Suspending Proppant. Society of Petroleum Engineers. doi:10.2118/163818-MS

Larsen, D. G., & Smith, L. J. (1985, January 1). New Conductivity Found in Angular Blends of Fracturing Sand. Society of Petroleum Engineers. doi:10.2118/13814-MS

Lehman, L. V., Shelley, B., Crumrine, T., Gusdorf, M., & Tiffin, J. (2003, January 1). Conductivity Maintenance: Long-Term Results from the Use of Conductivity Enhancement Material. Society of Petroleum Engineers. doi:10.2118/82241-MS

Montgomery, C. T., & Smith, M. B. (2010, December 1). Hydraulic Fracturing: History of an Enduring Technology. Society of Petroleum Engineers. doi:10.2118/1210-0026-JPT

Novotny, E. J. (1977, January 1). Proppant Transport. Society of Petroleum Engineers. doi:10.2118/6813-MS

Selley, R.C. 1998. The Reservoir. In Elements of Petroleum Geology, second edition. 6., P. 258. San Diego, California: Academic Press.

Wilson, A. (2015, March 1). Unconventional Proppant Combined With Channel Fracturing Increases Effectiveness. Society of Petroleum Engineers. doi:10.2118/0315-0089-JPT

Zhang, J. (2014). *Creation and Impairment of Hydraulic Fracture Conductivity in Shale Formations* (Unpublished doctoral dissertation). Texas A&M University, College Station, TX.

Zhu, D., Hill, A. D. 2013. Conductivity of Complex Fracturing in Unconventional Shale Reservoirs. Technology Status Assessment: 11122-07-TAMU-Zhu.

APPENDIX A

PROPPANT PARTICLE DISTRIBUTION

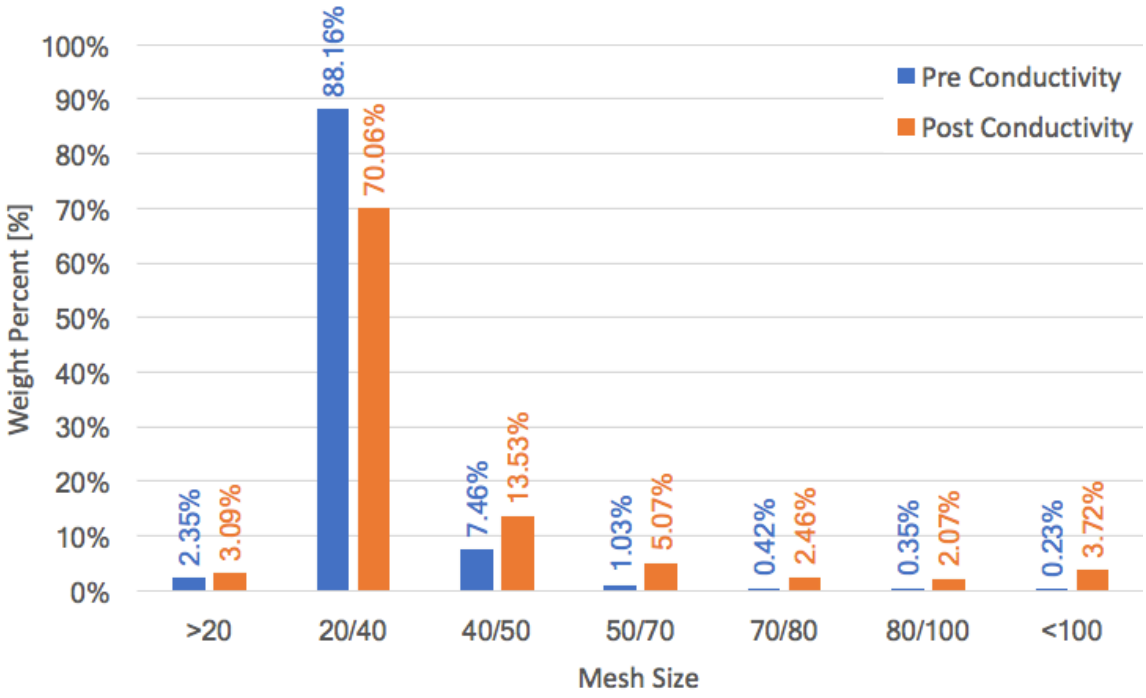

Figure A.1 20/40 sand particle distribution.

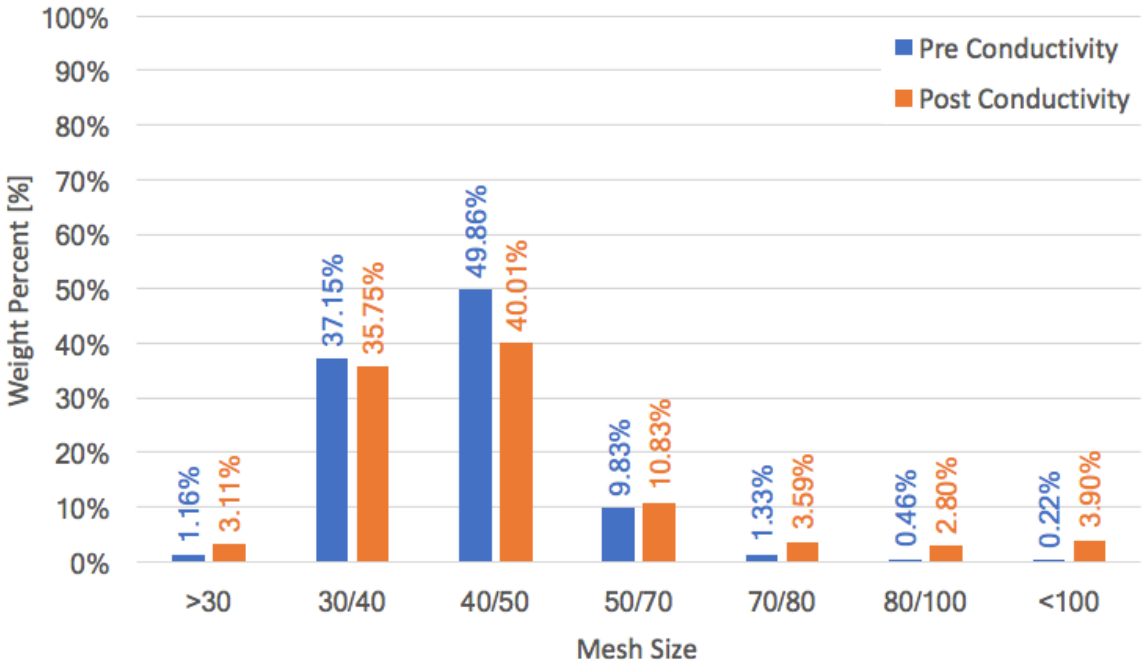

Figure A.2 30/50 sand particle distribution.

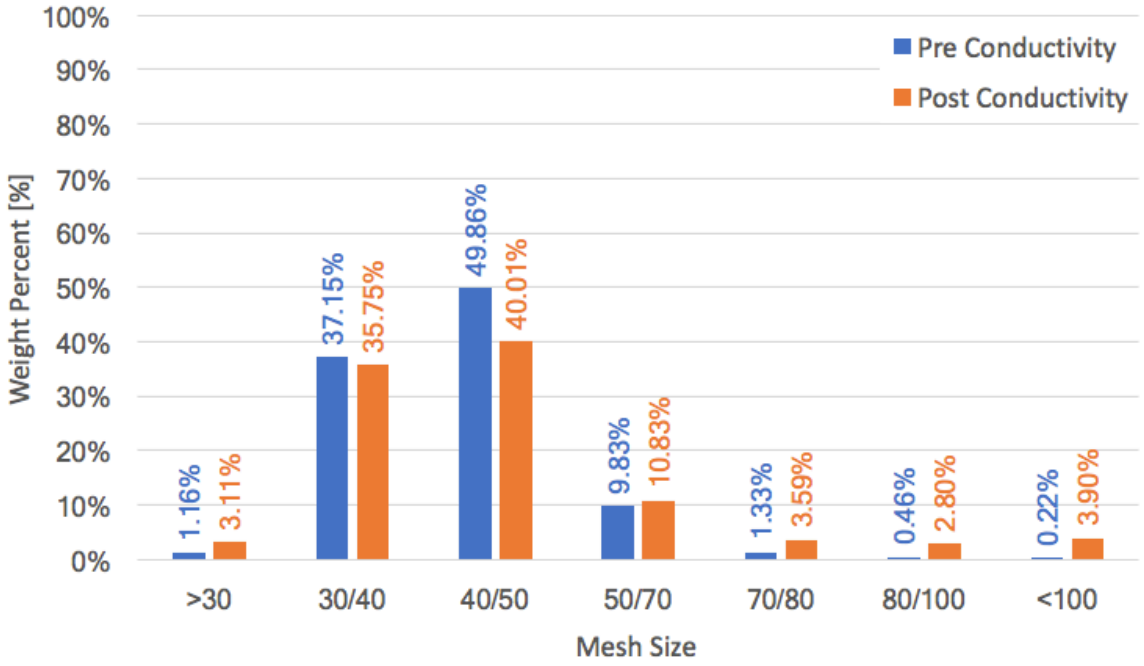

Figure A.3 40/70 sand particle distribution.

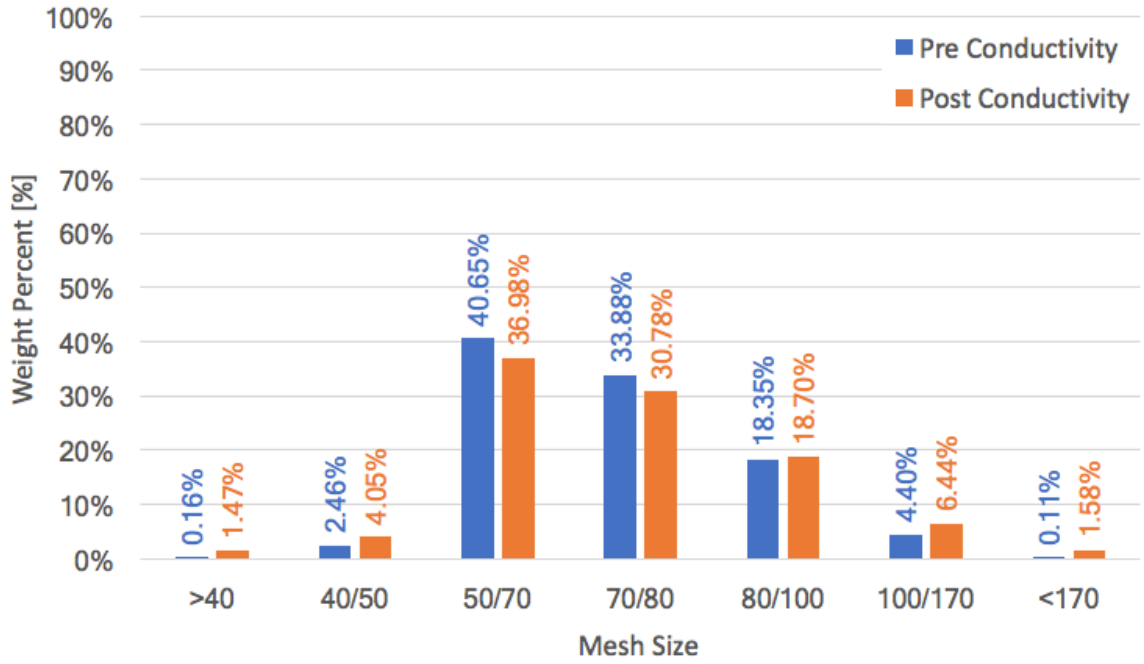

Figure A.4 100 mesh sand particle distribution.

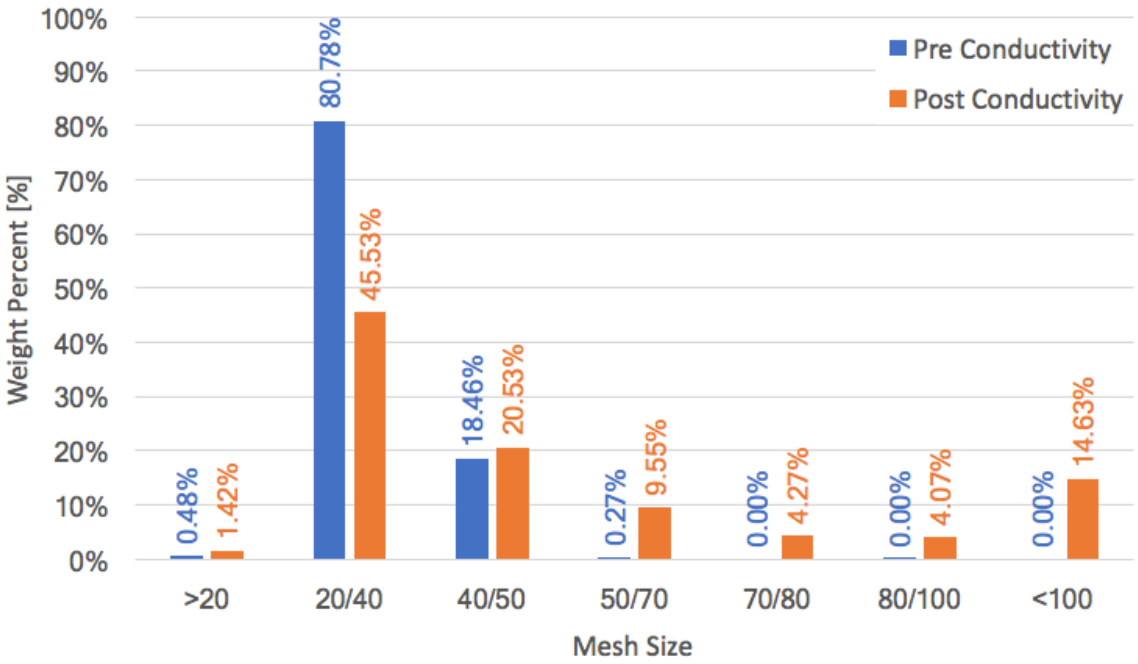

Figure A.5 20/40 glass particle distribution.

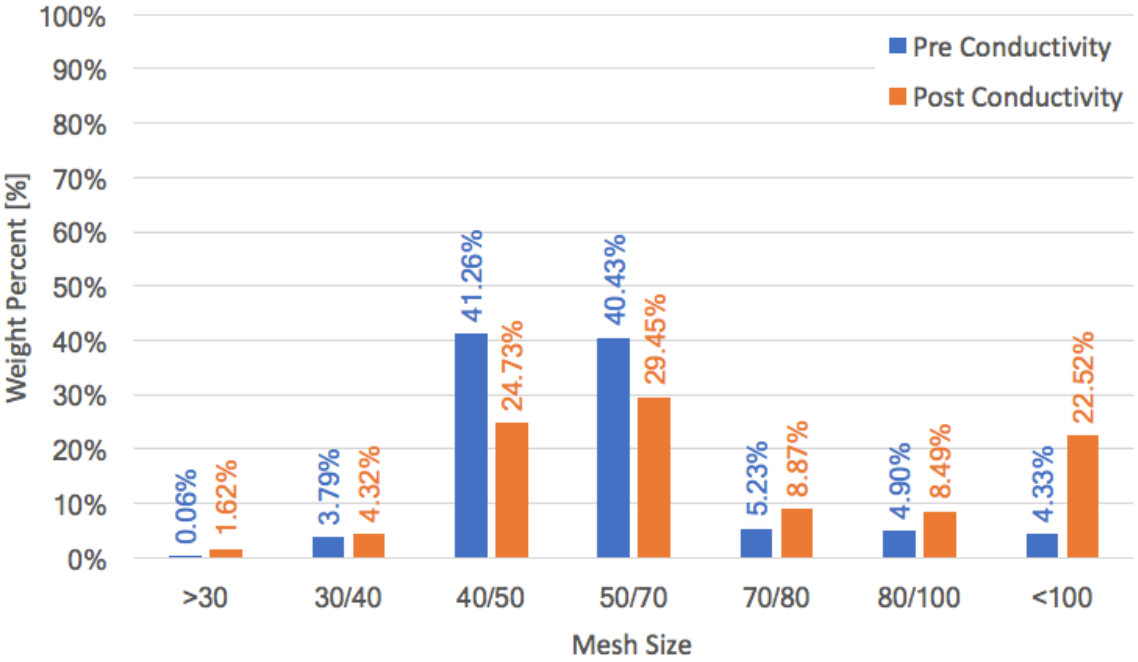

Figure A.6 40/70 glass particle distribution.

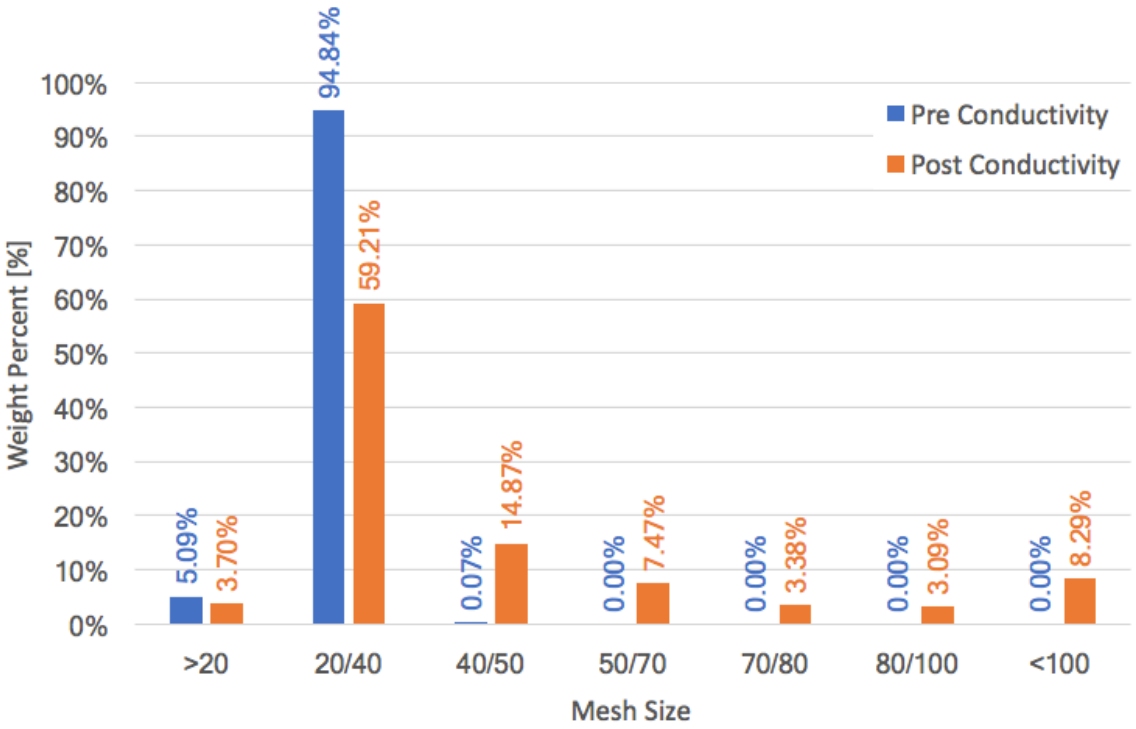

Figure A.7 20/40 taconite particle distribution.

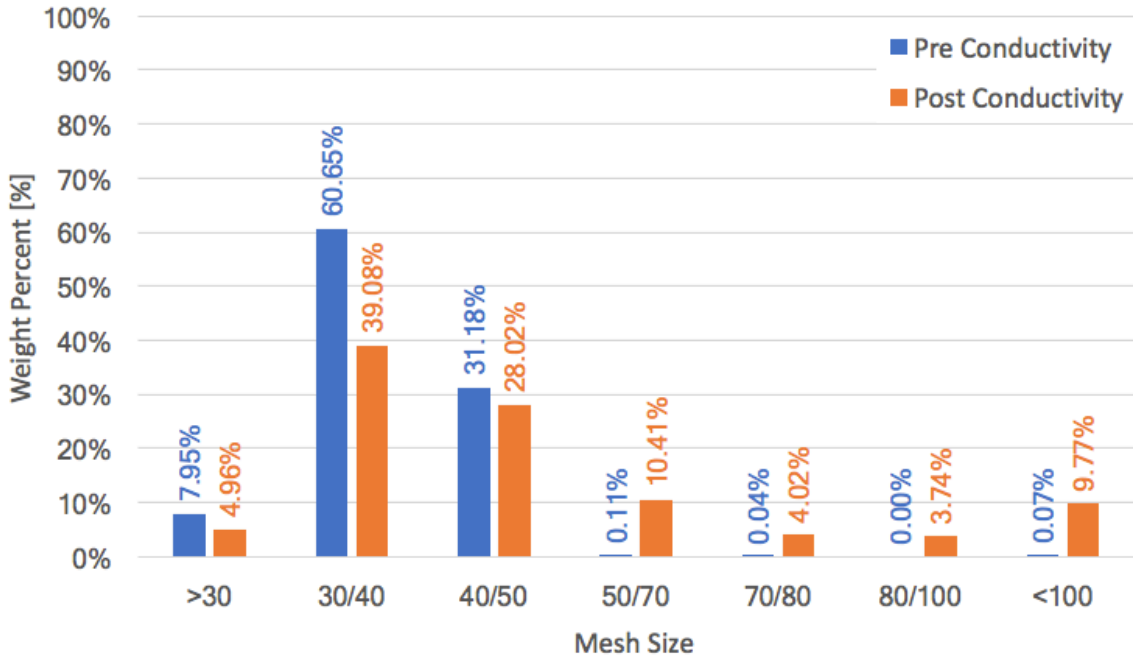

Figure A.8 30/50 taconite particle distribution.

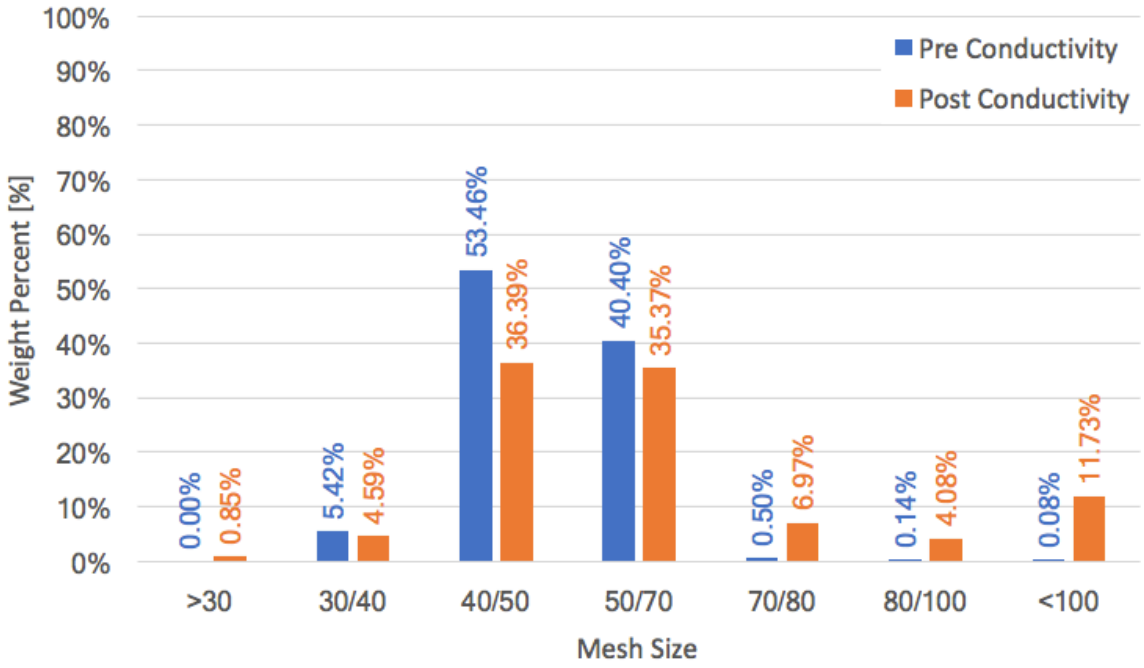

Figure A.9 40/70 taconite particle distribution.

APPENDIX B
INDIVIDUAL CONDUCTIVITY TEST RESULTS

For all figures in this section, the dotted lines represent individual test results, the solid line represents the average conductivity at each closure stress.

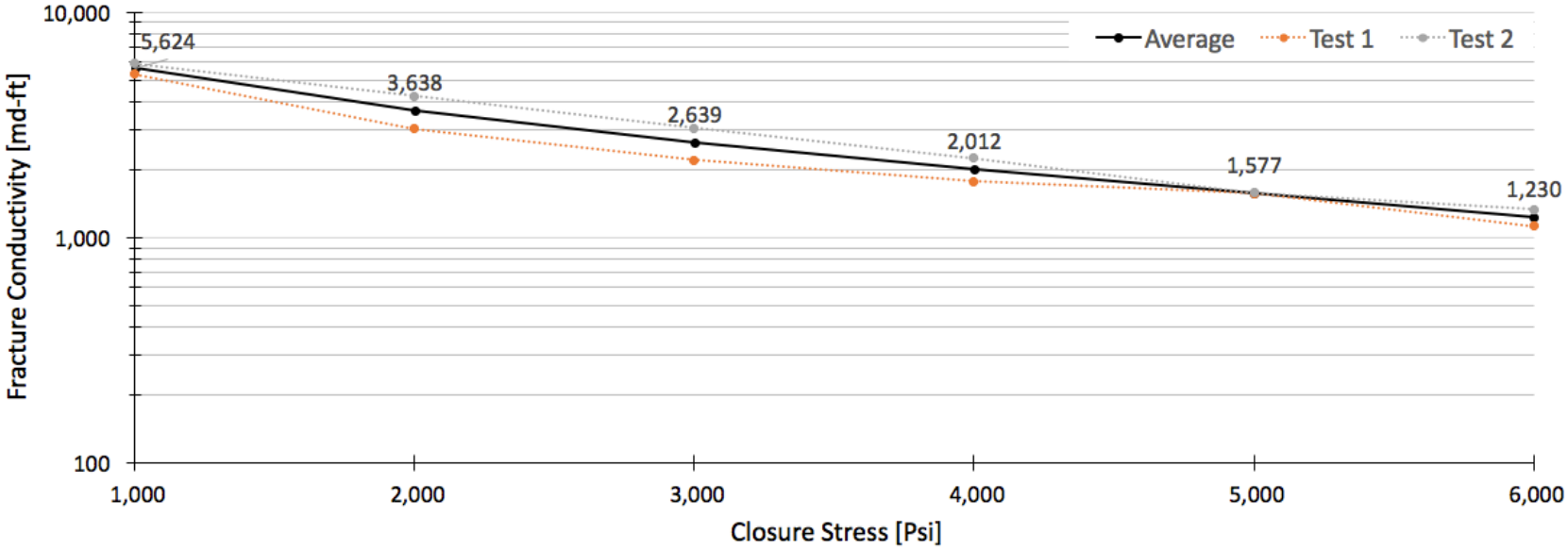

Figure B.1 20/40 sand individual test conductivity results.

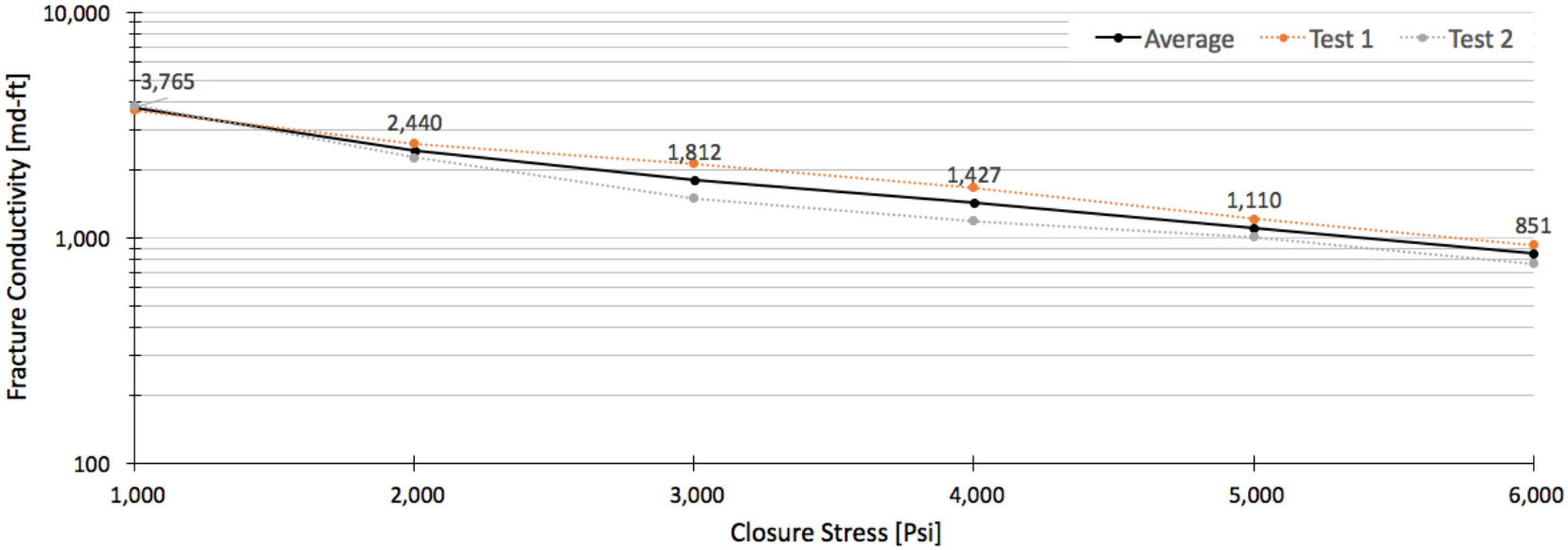

Figure B.2 30/50 sand individual test conductivity results.

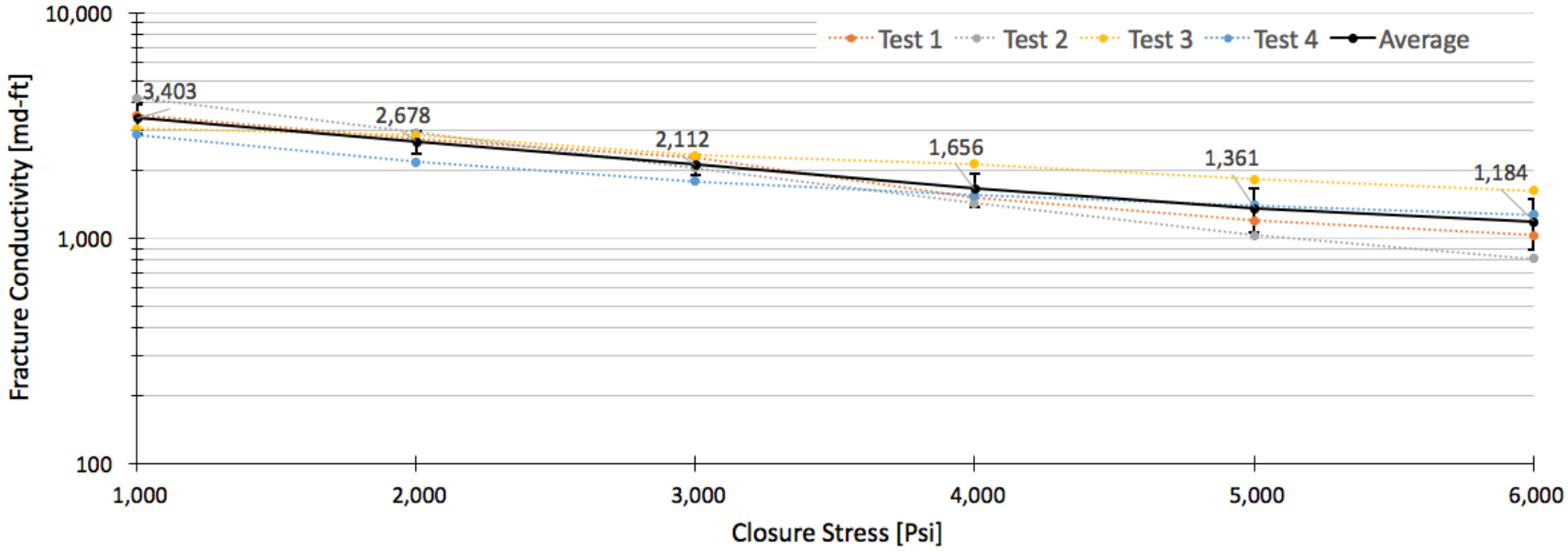

Figure B.3 40/70 sand individual test conductivity results.

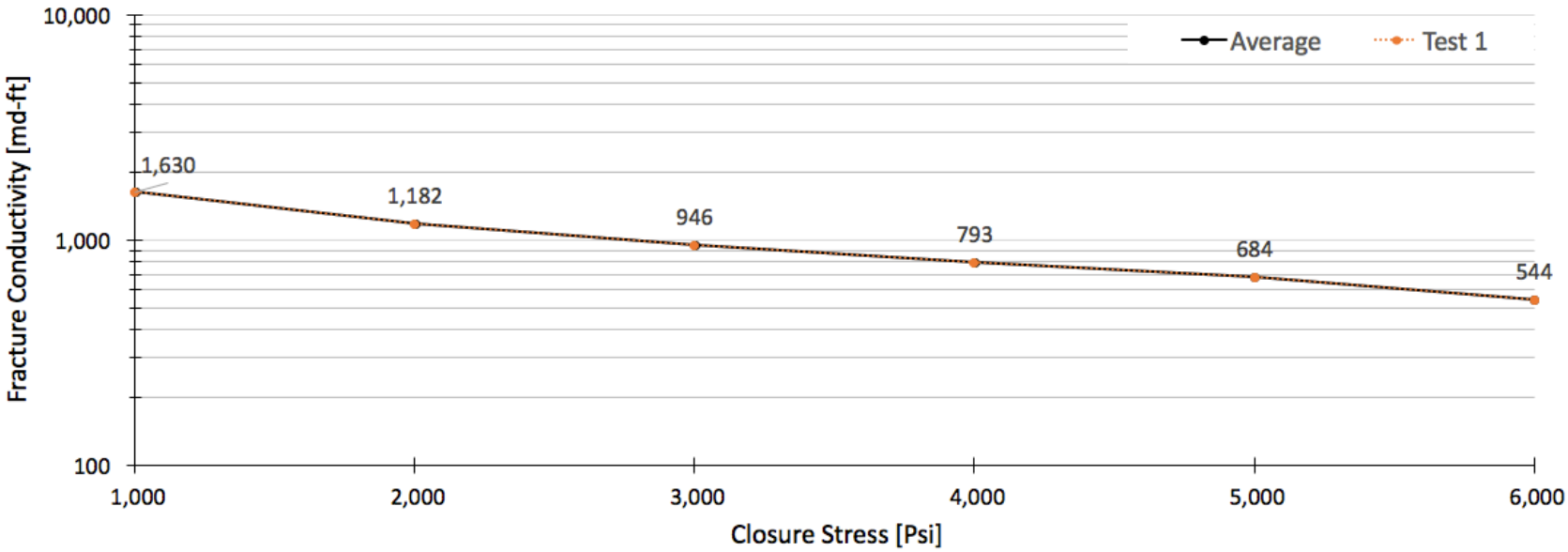

Figure B.4 100 mesh sand individual test conductivity results.

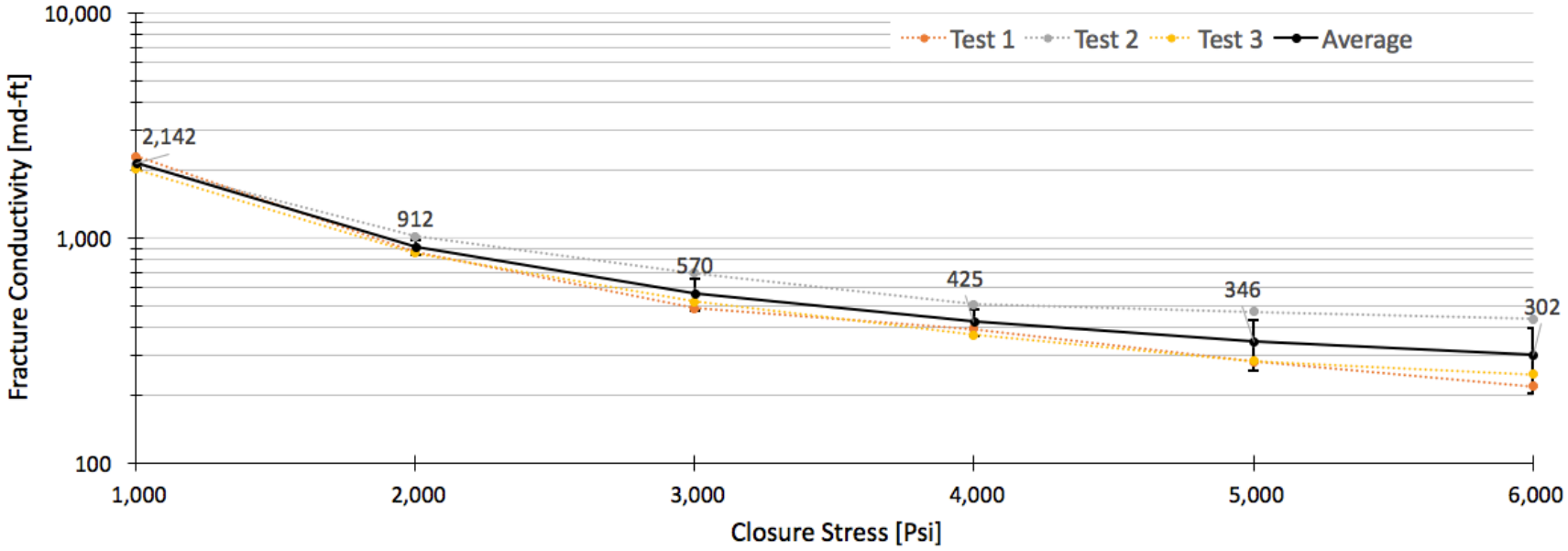

Figure B.5 20/40 glass individual test conductivity results.

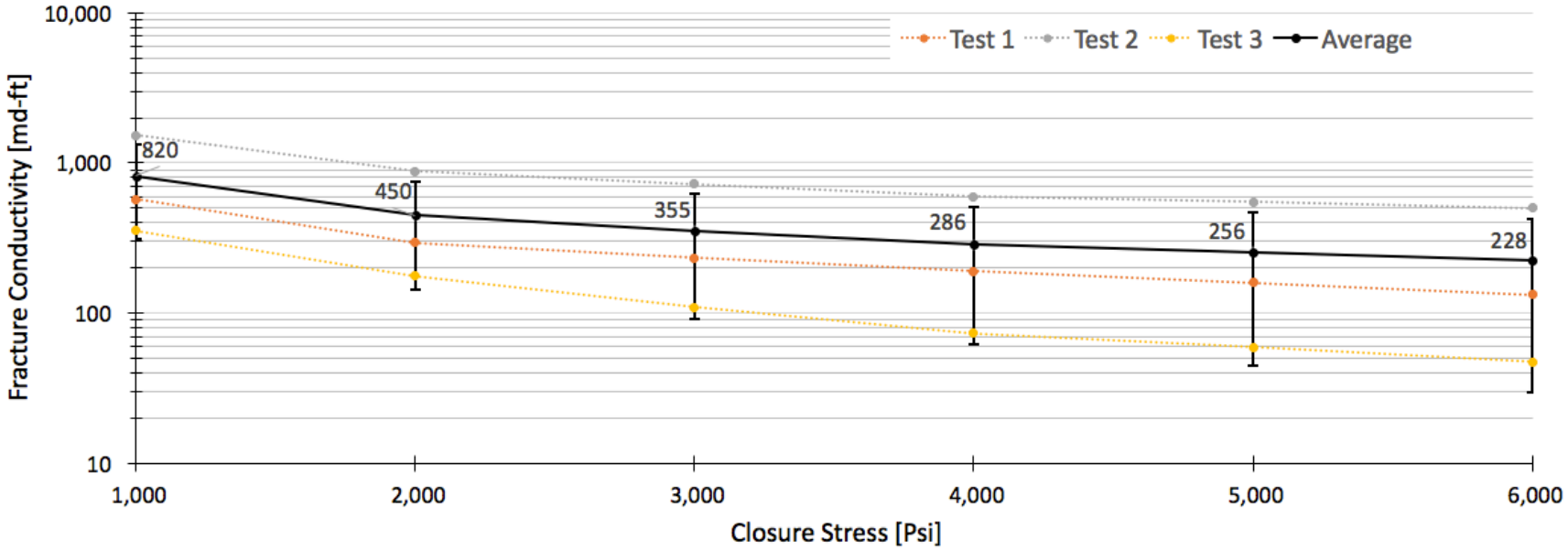

Figure B.6 40/70 glass individual test conductivity results.

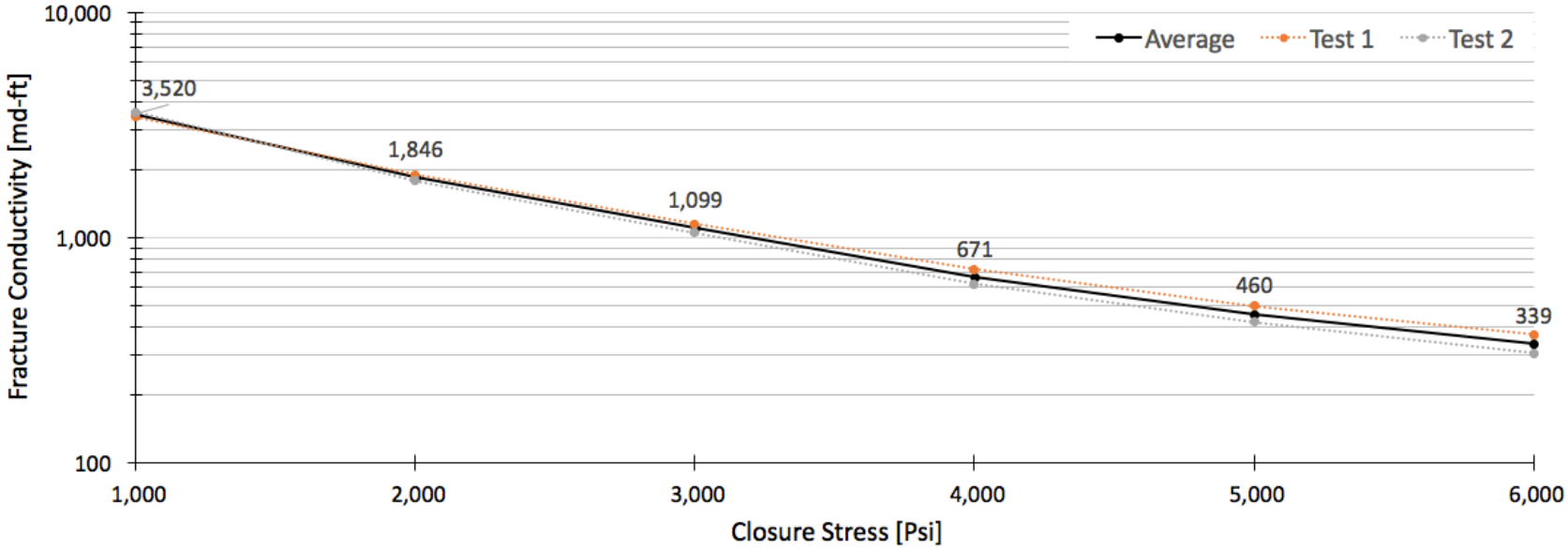

Figure B.7 20/40 taconite individual test conductivity results.

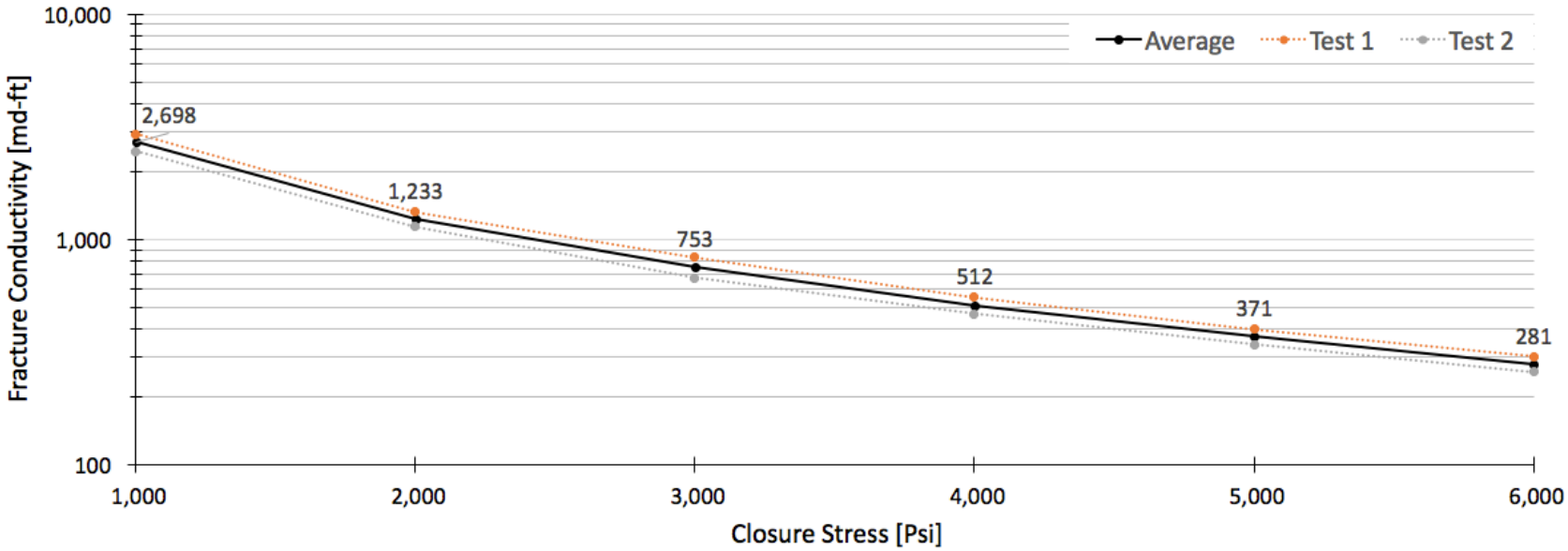

Figure B.8 30/50 taconite individual test conductivity results.

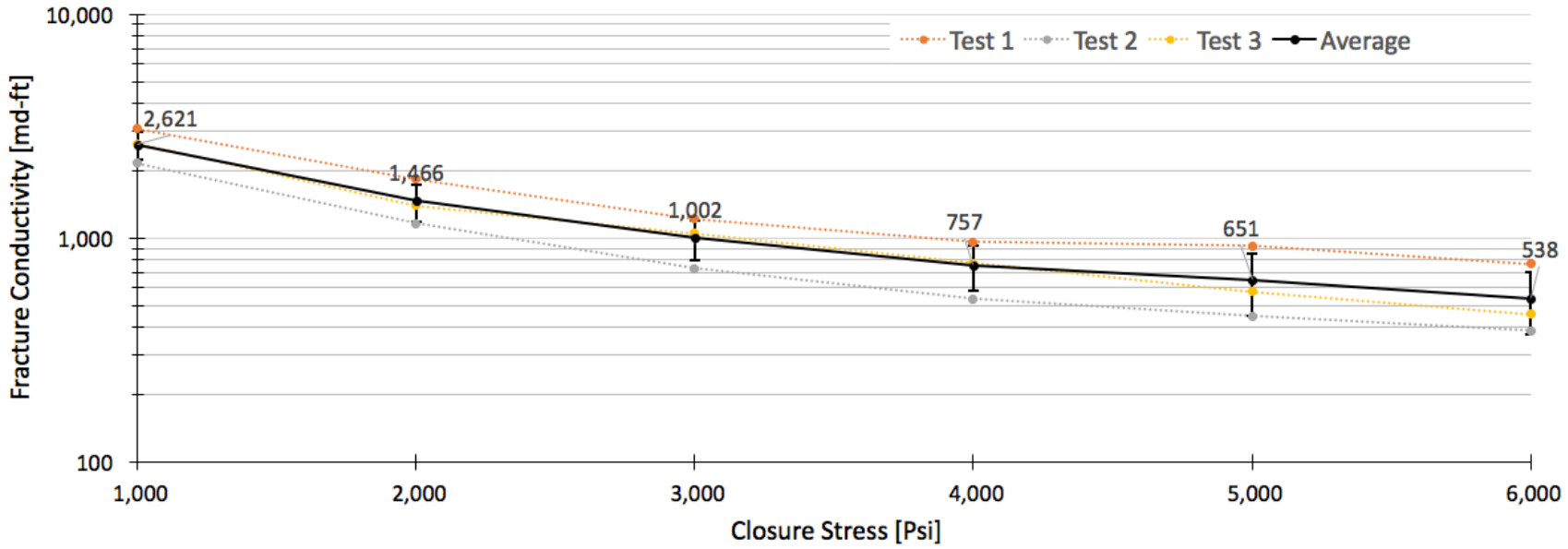

Figure B.9 40/70 taconite individual test conductivity results.

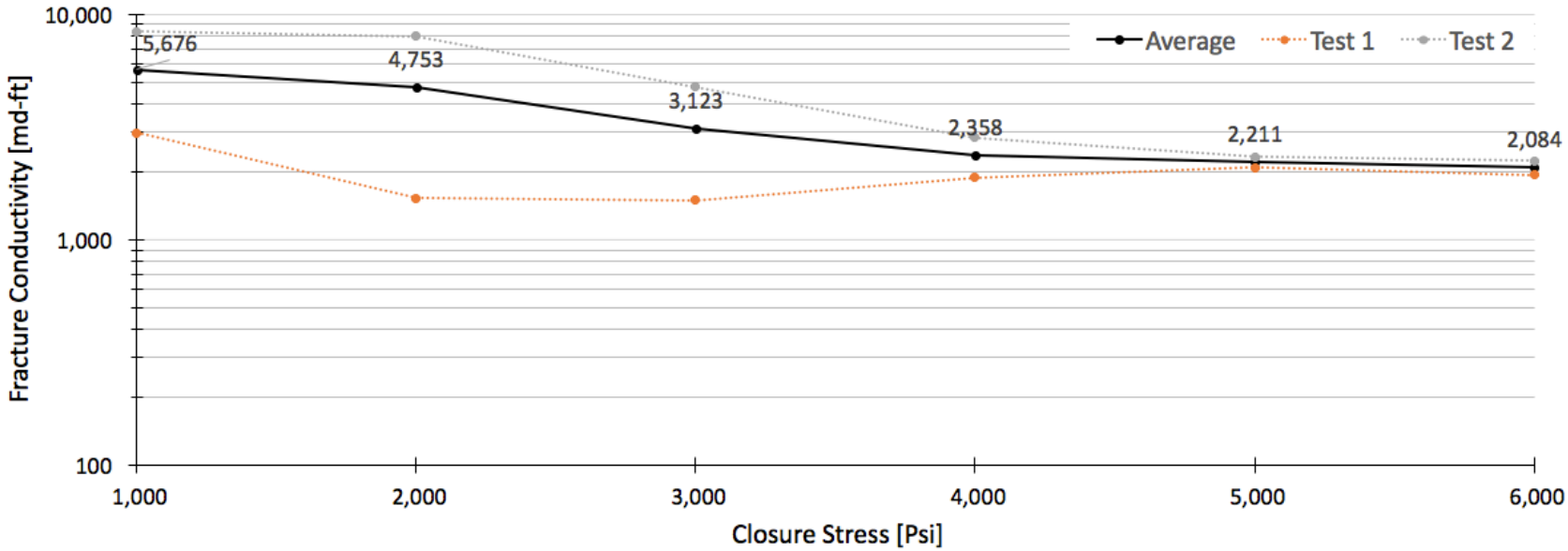

Figure B.10 80/100 coal individual test conductivity results.

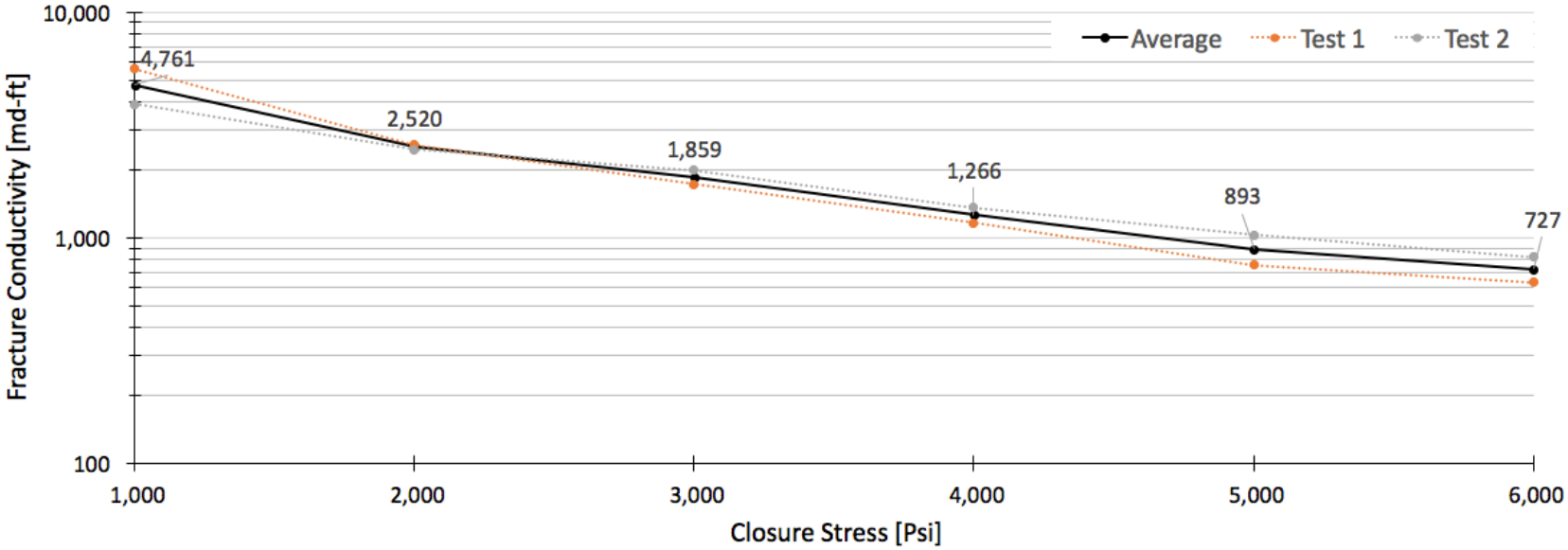

Figure B.11 20/40 sand and glass mixture individual test conductivity results.

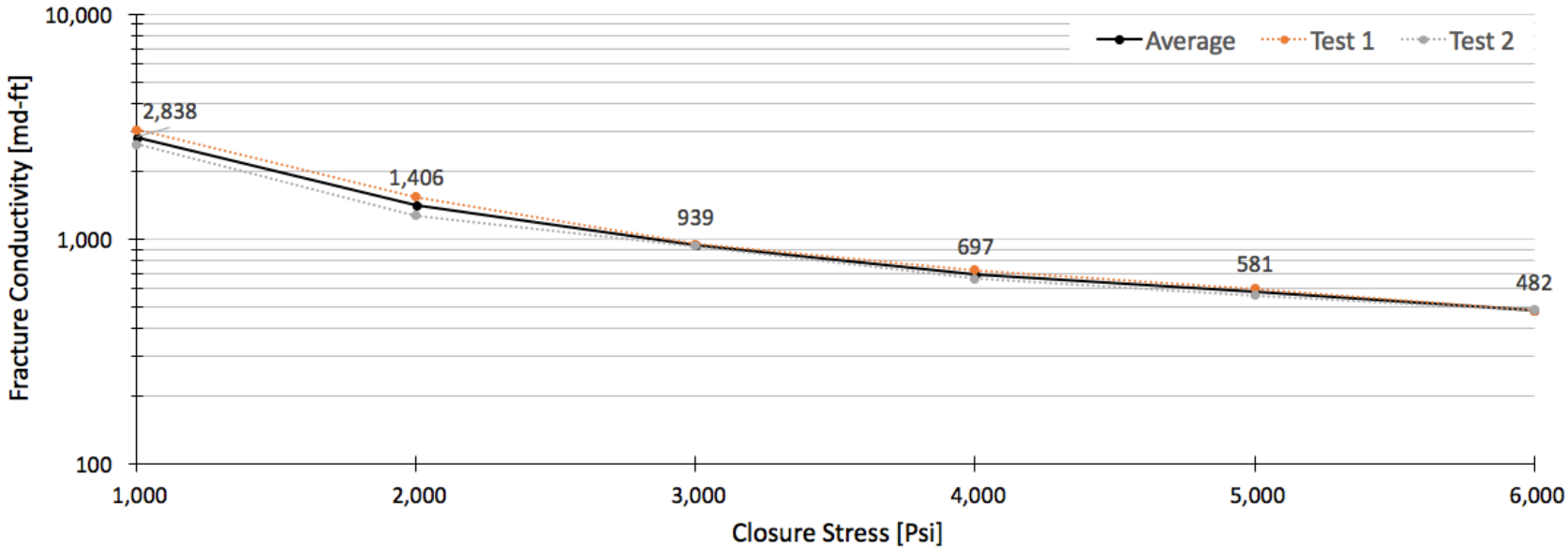

Figure B.12 40/70 sand and taconite mixture individual test conductivity results.

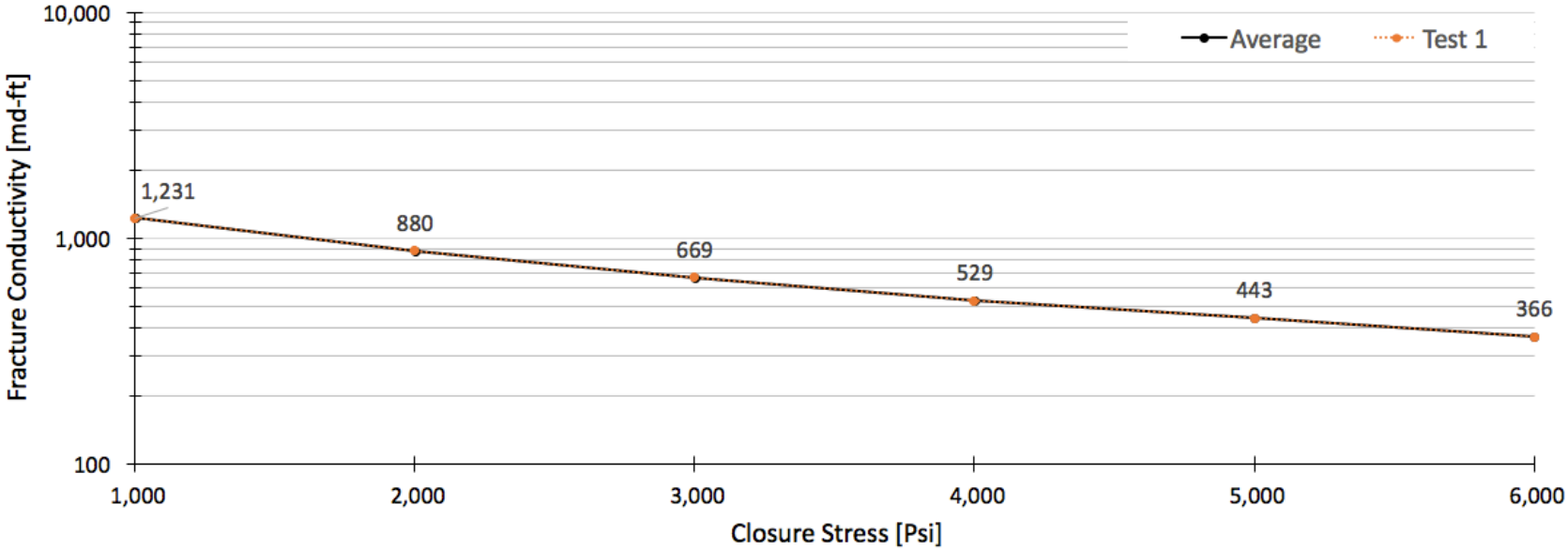

Figure B.13 40/70 sand and glass mixture individual test conductivity results.